REGULATION OF METABOLISM BY FIBROBLAST GROWTH FACTOR 21

APPROVED BY SUPERVISORY COMMITTEE

_____

Steven A. Kliewer, Ph.D.

_____

David J. Mangelsdorf, Ph.D.

_____

Joel K. Elmquist, D.V.M., Ph.D.

_____

Jay D. Horton, M.D.

_____

Joyce J. Repa, Ph.D.

To My Family - Past and Present -

For giving me the strength, courage and reason to search for a cure.

REGULATION OF METABOLISM BY FIBROBLAST GROWTH FACTOR 21

by

PAUL ANTHONY DUTCHAK

DISSERTATION

Presented to the Faculty of the Graduate School of Biomedical Sciences

The University of Texas Southwestern Medical Center at Dallas

In Partial Fulfillment of the Requirements

For the Degree of

DOCTOR OF PHILOSOPHY

The University of Texas Southwestern Medical Center at Dallas

Dallas, Texas

December, 2010

ACKNOWLEDGEMENTS

I would like to begin by acknowledging and thanking my mentors Drs. Steven Kliewer and David Mangesldorf. In their individual ways, they have been very gracious and supportive in helping me develop as a scientist during my time in their lab. I will always appreciate Steven for having his "open-door policy" and willingness to discuss data/experiments/models at any time. I will always appreciate David/Davo/Mango/Davo-Mango for his ability to keep science fun and instill confidence to go after the next "big thing". I am very fortunate to have had my Ph.D. training experience with these two outstanding scientists. Their encouragement to "follow the data" has been very helpful for the progress that I have made in my thesis work and has taught me to follow my own path in science and not to succumb on a path that others are following.

I would also like that thank my committee members: Dr. Joyce Repa, Dr. Joel Elmquist and Dr. Jay Horton. Their support and perspectives during my committee meeting were always refreshing. I am very thankful to each of them for their willingness to share reagents, wisdom, and experiences with me. It has been a privilege to have them as my committee.

I am very grateful to all my friends, class-mates, and lab-mates that I have had the pleasure of getting to know during my graduate student life at UTSW. Particularly, I would like to thank all my 'first-year' friends for helping me adjust in my life in the U.S.A. Without the help of my big-sib James Deng, classmates:

Gregory Kunkel, Scott Younger, Nate DeCarolis, Stephen Helms, Calli Merkel and Jon Self, I would have surely died in Dallas had it not been for their help with frequent late-night trips to the grocery store. I would like to thank all my lab-mates from the Mango/Kliewer lab for providing a fun and energizing environment to work in. Particularly, I would like to thank my bench-mates and friends Drs. Sam Holmstrom, Takeshi Inagaki, and the late addition Takeshi Katafuchi, for having provided the "best" space in the lab to do our research in. I would also like to thank Angie Bookout for her help in the lab, openness to discuss experiments and awesome ability to fix the PCR machines when they were not working. I would also like to thank Gail Wright for all her help over the years, all the great discussions, and always having a full jar of candy.

I would especially like to thank my beautiful fiancée Dr. Chantelle Sephton, who has been with me from the start. I am forever grateful for having you in my life and having your support. I love you and look forward to August 7, 2011.

Finally, I would like express my appreciation and love to my parents, Irene and Tony Dutchak, for helping me pursue my love of science. I am so fortunate to have them in my life, to share in my successes, and lift my spirits when things get tough. Their strong convictions in a good education have helped me strive to keep learning and growing as an individual.

METABOLIC REGULATION BY FIBROBLAST GROWTH FACTOR 21

Paul Anthony Dutchak

The University of Texas Southwestern Medical Center at Dallas, 2010.

Supervising Professors: **Steven A. Kliewer, Ph.D.**

David J. Mangelsdorf, Ph.D.

Fibroblast growth factor 21 (FGF21) is a secreted hormone that can beneficially regulate glucose and lipid homeostasis. Through a reverse endocrinology approach, we uncovered that FGF21 expression is transcriptionally regulated by the peroxisome proliferator activated-receptor alpha (PPARα) in liver. PPARα is a member of the nuclear hormone receptor superfamily that is physiologically activated by increased fatty acid mobilization to liver during fasting, and regulates the genetic program whereby lipids are converted to ketone bodies through a process known as ketogenesis. Here, I show the effects of FGF21 as a fasting hormone that is expressed in liver and contributes to the regulation of adipose tissue and hepatic ketogenesis during the fasted state. Using *in vitro* and *in vivo* methods to investigate the effects of FGF21, a model whereby FGF21 stimulates lipolysis in adipose tissue was generated. Intriguingly, using our FGF21 transgenic mice, I observed the expression of many genes involved in lipogenesis was highly induced in adipose tissue in an FGF21-dependent manner. Moreover, many of these lipogenic genes were found to be down-regulated in adipose of the FGF21 knockout mouse. The inhibition of lipogenic genes in adipose tissue was associated with increased SUMOylation of PPARγ protein in this tissue. Using a feeding-fasting paradigm, I

found that FGF21 expression in the liver and adipose tissue was rhythmic, peaking in liver prior to feeding and peaking in the adipose after feeding. Furthermore, the induction of FGF21 by PPARγ ligands suggested a unique function for this protein in adipose, independent from its role in the fasted state. To assess the contribution of FGF21 to the anti-diabetic properties of PPARγ agonists (ie. thiazolidinediones), diet-induced obese wild type and *Fgf21*$^{-/-}$ mice were treated with the TZD rosiglitazone. Rosiglitazone produced a significant increase in adipose FGF21 expression, but decreased hepatic FGF21 mRNA and circulating FGF21 protein. These data suggest that FGF21 functions as an autocrine factor within adipose tissue. Moreover, the therapeutic effects of rosiglitazone as an insulin sensitizer were lost in the *Fgf21*$^{-/-}$ mouse, as assessed by glucose and insulin tolerance tests. Several other effects of rosiglitazone were lost in the *Fgf21*$^{-/-}$ mice, including increased adipose mass, edema, and PPARγ target gene expression in the adipose. These data indicated that PPARγ can control the expression of FGF21, which functions as a feed-forward mechanism to stimulate PPARγ target genes and PPARγ dependent physiology. Since PPARγ can be modified by SUMO on two different sites on the protein, *in vitro* experiments were performed to show that PPARγ is SUMOylated at Lysine-107, a previously identified negative regulator of its transcriptional activity. Importantly, I found that treatment of *Fgf21*$^{-/-}$ adipocytes with FGF21 reduced the amount of SUMOylated PPARγ, thereby allowing it to be it an active state. Collectively, these data reveal that FGF21 has two independent roles in regulating metabolism *in vivo*: as a hepatic endocrine hormone that is induced during the fasting response through PPARα, and as an adipose autocrine/paracrine factor that is induced in a feed-forward loop to stimulate PPARγ activity.

TABLE OF CONTENTS

PRIOR PUBLICATIONS

Dutchak, P.A., Katafuchi, T., Bookout, A.L., Mangelsdorf, D.J., Kliewer, S.A. Fibroblast Growth Factor-21 Regulates PPARγ Activity and the Antidiabetic Action of Thiazolidinediones. (Manuscript *Submitted*)

Wei. W., Dutchak, P.A., Ding, X., Wang, X., Bookout, A.L., Zhang, Y., Dechow, P.C. Mangelsdorf, D.J., Kliewer, S.A., Wan, Y. FGF21 Inhibits Bone Formation by Potentiating PPARγ-Induced Marrow Adipogenesis (Manuscript *In Preparation*)

Inagaki, T., Dutchak, P.A., Guixiang, Z., Ding, X., Gautron, L., Parameswara, V., Li, Y., Goetz, R., Mohammadi, M., Esser, V., Elmquist, J. K., Gerard, R. D., Burgess, S.C., Hammer, R.E., Mangelsdorf, D.J., Kliewer, S.A. (2007) Endocrine Regulation of the Fasting Response by PPARα-Mediated Induction of Fibroblast Growth Factor 21. Cell Metabolism *5*, 415-425.

LIST OF FIGURES AND TABLES

LIST OF ABBREVIATIONS

ACACA	Acetyl-Coenzyme A Carboxylase
ACLY	ATP-Citrate Lyase
AF	Activation Function
AMPK	Adenosine Monophosphate-activated Protein Kinase
aP2	Adipocyte Fatty Acid Binding Protein
ATGL	Adipose Triglyceride Lipase
ATP	Adenosine Triphosphate
AUC	Area Under Curve
BAT	Brown Adipose Tissue
CEL	Carboxyl Ester Lipase
C/EBP	CCAAT/Enhancer Binding Protein
ChIP	Chromatin Immunoprecipitation
CLPS	Colipase, Pancreatic
CPT1a	Carnitine Palmitoyltransferase 1a
CYP7A1	Cytochrome P450 7 alpha Hydroxylase A1
DGAT	Diacylglycerol Acyltransferase
DMEM	Dulbuccco's Modified Eagle Medium
DMSO	Dimethysulfoxide
DNA	Deoxyribonucleic Acid
DR	Direct Repeat
ECL	Enhanced Chemiluminescence
EDTA	Ethylene Diamine Tetraacetic Acid

ELISA	Enzyme-linked immunosorbent assay
ELOVL	Elongation of Very Long Chain Fatty Acids Protein
ER	Endoplasmic Reticulum
eWAT	Epididymal White Adipose Tissue
FASN	Fatty Acid Synthase
FBS	Fetal Bovine Serum
FFA	Free Fatty Acid
FGF	Fibroblast Growth Factor
FGFR	Fibroblast Growth Factor Receptor
FOXO	Forkhead Box
FXR	Farnesoid X Receptor
GFP	Green Fluorescent Protein
GTT	Glucose Tolerance Test
GLUT	Glucose Transporter
HEK	Human Embryonic Kidney Cells
HDS	Hydroxysteroid Dehydrogenase
HMGCS	3-Hydroxy-3-Methylglutaryl-CoA Synthase
HSL	Hormone-Sensitive Lipase
IBMX	3-Isobutyl-1-Methylxanthine
IGF	Insulin-like Growth Factor
IL	Interleukin
IP	Immunoprecipitation
ITT	Insulin Tolerance Test
Jak/STAT	Janus Kinase-Signal Transducer and Activator of Transcription

KL	Klotho
KLB	Beta Klotho
LXR	Liver X Receptor
ME1	Malic Enzyme
OB-R	Leptin (Obesity) Receptor, Short Form
OB-Rb	Leptin (Obesity) Receptor, Long Form
PBS	Phosphate Buffered Saline
PCK1	Phosphoenolpyruvate Carboxykinase 1 (soluble)
PCR	Polymerase Chain Reaction
PCX	Pyruvate Carboxylase
PDX	Pancreatic Duodenum Homeobox
PNLIP	Pancreatic Lipase
PNLIPRP	Pancreatic Lipase-Related Protein
PPAR	Peroxisome Proliferator Activated Receptor
PPRE	Peroxisome Proliferator Response Element
RT-qPCR	Reverse Transcription Quantitative Polymerase Chain Reaction
RXR	Retinoid X Receptor
SLC	Solute Carrier Family
SMRT	Silencing Mediator of Retinoic Acid and Thyroid Hormone Receptor
SREBP	Sterol Regulatory Element Binding Protein
SUMO	Small Ubiquitin-Like Modifier
TAG	Triglyceride
TG	Transgenic
TNFa	Tumor Necrosis Factor Alpha

TZD	Thiazolidinediones
WAT	White Adipose Tissue
WB	Western Blot
WT	Wild Type

CHAPTER 1

INTRODUCTION

Mammalian systems have developed highly integrated response mechanisms to maintain homeostasis when challenged by physiological and environmental stress. The homeostatic mechanisms that respond to energy deprivation or nutrient availability represent a diverse set of biochemical reactions that influence the metabolism of cells within an organism to sustain life. The ability to regulate metabolic fuel consumption and storage is a fundamental connection between the genes of an organism and its environment. Over the last century, alterations in human lifestyles have led to an unprecedented shift in the balance between our genes and the natural environment, as individuals become accustomed to sedentary lifestyles with easy access to high-calorie, low-nutrient food sources. This shift is apparent in the human population, illustrated by the rapid increase in obesity and increased diagnosis of subsequent disease including type 2 diabetes, high blood pressure and heart disease (Grundy, 2004).

Nuclear hormone-receptor transcription factors (NHR) represent an intriguing means whereby gene expression can be manipulated. NHRs can directly influence gene expression by binding small lipophilic ligands and transcriptional modulators to alter the expression of diverse genetic programs that regulate growth, development, reproduction and metabolism (Bookout et al., 2006). Therefore, understanding the

physiological contribution of NHRs is critical to our fundamental knowledge of biology and expands our rationale to pharmacologically target NHR to modulate gene expression for the treatment of disease.

Fibroblast growth factor 21 (FGF21) is a novel hormone that can beneficially regulate metabolism and is transcriptionally regulated by a subclass of NHRs called peroxisome proliferator activated receptors (PPARs). The work in this thesis characterizes the pharmacological and physiological regulation of FGF21 in mice, and describes the function of FGF21 in both the fed and fasted state. In Chapter 2 of this thesis I show that the NHR called PPARα controls the hepatic production of FGF21 as part of the fasting response. In this context, FGF21 regulates the adaptive response to nutrient deprivation by increasing hepatic production of ketone bodies from fatty acids, stimulating glycerol release from white adipose tissue and sensitizing mice to a state of energy-conservation called torpor. In Chapter 3 of this thesis, I demonstrate that FGF21 is induced in the adipose tissue of mice when the NHR called PPARγ is activated, either by after feeding or by treatment with a PPARγ specific ligand called rosiglitazone. In addition, Chapter 3 describes my observations that FGF21 functions as an autocrine/paracrine factor within the adipose tissue to enhance the transcriptional activity of PPARγ by altering its post-translational modifications. The works presented in this thesis elucidate diverse biological functions of FGF21 in the fed and fasted states, which have not previously been addressed.

1.1 Overview of Metabolic Homeostasis

Metabolic homeostasis is mediated through a series of complex biochemical events that can impact every characteristic of a living organism. In general, physiological regulation of metabolism can be mediated through hormonal, intracellular signaling and transcriptional events to mediate rapid or prolonged changes within the organism. Hormonal regulation can be viewed to impact tissue specific metabolic changes, whereas signaling and transcriptional events mediate cell autonomous changes within the tissue of an organism. These various levels of regulation occur in a precise and highly regulated manner, ensuring the well-being of the organism during periods of stress. Importantly, proper metabolic regulation is necessary for the overt characteristics of organisms including: growth, reproduction, digestion, mineral and fluid balance, and basic organ function.

1.1.1 Hormonal Regulation of Metabolism

Hormones are generally classified in three main categories: peptide or protein (e.g. growth hormone, IGF-1, FGF21), steroid (e.g. cortisol and testosterone), and amino acid derivatives (e.g. epinephrine and thyroxine). Hormones are produced within the cells of organs or ductless (endocrine) glands and initiate changes in cells that express their receptor. Hormones can act within the cell of their origin (autocrine action), adjacent cells (paracrine action) or on cells of distal tissues (endocrine action), to integrate and amplify a biological change. Semantically, secreted factors

that are produced in a cell and act in an autocrine or paracrine manner have been termed cytokines, or more generally "factors", but this terminology is not strictly adhered to since several of these biomolecules can act through a variety of these mechanisms (Vona-Davis and Rose, 2007). For the purpose of this thesis, I will focus on the biological role of major peptide hormones that originate from hepatic and adipose tissues.

The liver synthesizes and secretes several important hormones that influence metabolic homeostasis; discovering how these hormones function constitutes a major area of current endocrinology research. Important hepatic hormones include: insulin-like growth factor-1 (IGF-1) and FGF21 (Refer to Chapter 2). These hormones illustrate a unique way that hepatic hormones can regulate biological outcomes through their expression patterns. IGF-1 is a classic example of a nutritionally regulated peptide hormone that controls body growth, where hepatic IGF-1 contributes to 30% of an adult's size (Le Roith et al., 2001; Stratikopoulos et al., 2008). IGF-1 expression is regulated by growth hormone and nutritional status such that malnutrition reduces IGF-1 expression to slow growth rates and conserve energy (Thissen et al., 1994). In contrast to IGF-1, FGF21 is a hormone that is highly expressed in the liver by fasting conditions where its expression is regulated by PPARα. Intriguingly, our group has found that overexpressing FGF21 in mice impairs their growth by inhibiting growth hormone dependent IGF-1 expression in the liver (Inagaki et al., 2008). This type of functional interplay between hormonal

pathways resonates in homeostatic pathways, and remains an important area for metabolic exploration.

The adipose tissue secretes hormones called adipokines. In general, the term adipokine is applied to a biologically active substance that is produced by the adipocyte and acts on distal tissues or the adipocyte itself. Importantly, their syntheses may also occur at sites outside this tissue (e.g. Angiopoietin-like protein 4). Adipokines are considered a major link between obesity-related exogenous factors (lifestyle and nutrition) and molecular events that lead to metabolic syndrome (Deng and Scherer, 2010). Well characterized adipokines include: leptin, adiponectin, FGF21 (Refer to Chapter 3), as well as proteins involved in mediating the inflammatory response, such as TNFα and IL-6. Leptin was the first described adipokine that is highly expressed after eating and negatively regulates food intake (Frederich et al., 1995; Zhang et al., 1994). The initial characterization of leptin suggested that adipose tissue can regulate energy homeostasis by altering behavior, therefore having a function beyond its previously recognized role in lipid storage, and led to the Lasker Award being granted to Dr. Jeffery Friedman in 2010. Leptin functions in tissues that express the leptin receptor (OB-Rb), and activate the Janus kinase-signal transducer and activator of transcription (Jak/Stat) signaling pathway (Vaisse et al., 1996). Circulating leptin levels reflect the energy status of adipose tissue and regulate feeding behavior accordingly through direct signaling in the hypothalamus (Elmquist et al., 1997). The short OB-R form is highly expressed in the brain microvessels in mice, whereas a longer OB-RB form is highly expressed in

the hypothalamus, and several peripheral tissues (Hileman et al., 2002; Tartaglia et al., 1995). The adipokine called adiponectin is a 30kDa protein that has structural homology with collagens VIII and X and complement factor C1q and circulates in the plasma in different molecular weight complexes (Pajvani et al., 2003; Scherer et al., 1995). Adiponectin increases fatty acid oxidation and decreases gluconeogenesis, while sensitizing hepatocytes to the effects of insulin (Berg et al., 2001). Importantly, decreased adiponectin levels are associated with obesity and insulin resistance (Weyer et al., 2001), whereas anti-diabetic PPARγ ligands increase adiponectin levels (Yu et al., 2002) contributing to the insulin-sensitizing effects of this drug class (Nawrocki et al., 2006; Pajvani et al., 2004). Adiponectin stimulates a signal transduction pathway in tissues that express the AdipoR1 and AdipoR2 receptors, but may also activate the T-cadherin receptor in endothelial and muscle cells (Hug et al., 2004). Signal transduction from adiponectin receptor stimulates the phosphorylation and activation of the 5'-AMP protein kinase to enhance insulin sensitivity and glucose metabolism (Yamauchi et al., 2002). Recently, studies of adipose tissue from obese individuals have found elevated levels of pro-inflammatory peptides cytokines, including TNFα and IL-6. Although these inflammatory cytokines can modulate lipid accumulation (Grohmann et al., 2005; Wallenius et al., 2002), further studies are required to fully elucidate the mechanism whereby they influence metabolic homeostasis.

Pertaining to this thesis, the results presented in the following chapters demonstrate that FGF21 is an atypical hormone with unique endocrine and

autocrine/paracrine functions. The hormonal effects of FGF21 are not only via an endocrine pathway that stems from the liver, where its expression is induced in the liver by fasting, ketogenic diets (Badman et al., 2007) and carbohydrate-rich diets (Iizuka et al., 2009), but also through an autocrine/paracrine pathway in adipose tissue where FGF21 is expressed during the fed state. The data presented in this thesis provide one of the first descriptions of a metabolically active secreted factor having the properties of both a fasting-state hepatic endocrine hormone and a fed-state adipocyte autocrine factor.

1.1.2 Signal Transduction Regulation of Metabolism

Many homeostatic responses to physiological and environmental change primarily rely on signal transduction pathways as a rapid way to alter intracellular function. The classical signal transduction response originates from a transmembrane receptor (e.g. FGF receptor tyrosine kinase) binding a ligand, to stimulate an intracellular series of events. Typically these signals are amplified by one or more enzymatic steps, leading to altered gene expression through changes in the post-translational modifications in enzymes, transcription factors, cofactors or histones. (Pires-daSilva and Sommer, 2003) These modifications can include proteolytic cleavage, phosphorylation, glycosylation, SUMOylation, and acetylation, which may shift the equilibrium between inactive and active forms, or alter protein stability. Importantly, post-translational modifications can have opposing effects on different

transcription factors. For instance, downstream of the phosphotidylinositol 3-kinase pathway, PDX1 (pancreatic duodenum homeobox) phosphorylation induces its nuclear translocation and increases insulin gene expression (MacFarlane et al., 1994; Rafiq et al., 1998); whereas phosphorylation of FOXO (forkead box o) factors targets them for export from the nucleus, preventing their transcriptional activity (Tran et al., 2003). Crosstalk between signal transduction cascades can make it challenging to distinguish noise from the true events that elicit cellular changes, highlighting the comprehensive circuitry that is required to generate an integrative cellular response.

1.1.3 Transcriptional Regulation of Metabolism

Transcriptional regulation of metabolic homeostasis is a highly orchestrated process that represents a fundamental connection between our genes and the environment. At the molecular level, the link between transcription and metabolic regulation can be observed when alterations in transcription factor function elicit metabolic disturbances. By altering the expression of major enzymes, transcription factors can stimulate long-term changes in a metabolic pathway within a cell. Although by virtue of their nature, all transcription factors influence metabolism in one way or another, certain factors have a clearly dominant and dedicated role in metabolism.

Several mechanisms have been identified to alter transcription of metabolic genes. These include: the NHRs that act as "sensors" (e.g. PPARs, FXR, LXR), the

transcriptional effectors of signal transduction pathways (ex. FOXO), and the constitutive regulators that are modified by differential expression of their binding partners (ex. C/EBPs). Additionally, gene expression can be regulated by various cellular organelles, where changes in the organellar compartments can initiate a transcriptional response. A classical example of transcriptional regulation by organellar sensing is represented by the sterol regulatory element-binding protein transcription factors (SREBPs). These transcription factors reside in the endoplasmic reticulum, but are released when low cholesterol levels are sensed, translocate to the nucleus and regulate the expression of lipid and cholesterol synthesizing enzymes (Horton et al., 2002; Wang et al., 1994). It is beyond the scope of this thesis to fully discuss all the transcription factors and cofactors that mediate metabolic regulation; readers are referred to several reviews that are devoted to this subject (Desvergne et al., 2006; Glass and Rosenfeld, 2000; Naar et al., 2001).

1.2 Liver Metabolism

The liver plays a central role in the regulation of whole body energy homeostasis with its ability to orchestrate carbohydrate, lipid, and amino acid metabolism during periods of nutrient availability and deprivation. The liver functions as the body's main glucose "buffer", providing glucose through gluconeogenesis (with a contribution from the kidney and small intestine) when nutrients are scarce, and storing glucose in the form of glycogen when food is abundant. Additionally, hepatic regulation of lipid metabolism comprises three major

facets: lipogenesis, secretion of lipids in the form of lipoprotein complexes and fatty acid oxidation. These mechanisms are influenced by nutritional status and regulated by numerous hormonal, cell signaling and transcriptional events within the liver. For the purpose of this thesis, the main opposing situations in liver metabolism are considered here: the fed state and the fasted state.

1.2.1 Liver and the Fed State

Upon feeding, nutrients are absorbed along the digestive tract and are shunted to the liver. Along with absorbed metabolites, hormones produced by digestive organs, including FGF15 from the intestine and insulin from the pancreas, circulate back to the liver and regulate biosynthetic pathways within the liver (Inagaki et al., 2005; Schmidt et al., 2010). Absorbed metabolites are either stored directly in the liver (i.e. glycogen), or are packaged and secreted into circulation where they are taken up by peripheral tissues and immediately used, or stored for periods of nutritional shortage.

In conditions of dyslipidemia, the liver can function as reserve for excess storage of fats, a condition termed non-alcoholic fatty liver disease (Reddy and Rao, 2006). Hepatic steatosis can result from increased circulating fatty acids and decreased β-oxidation in the mitochondria (Malhi and Gores, 2008). It has been determined that patients with NAFLD accumulate 59% of liver triglycerides from fatty acids derived from adipose lipolysis, 26% from *de novo* lipogenesis and 15%

from the dietary non-esterfied fatty acid pool (Donnelly et al., 2005). Future research to investigate the molecular mechanisms that govern the partitioning of free fatty acids (FFA) in the initiation of fatty liver will provide new insights to target metabolic homeostasis in pathological conditions.

1.2.2 Liver and the Fasted State

The liver has evolved as a major regulator of the fasting response, as highlighted in Chapter 2. The hepatic fasting response can be viewed as a progressive response that is composed of distinct metabolic changes. Brief periods of fasting cause the liver to mobilize glucose from its glycogen stores; a process that is stimulated by elevated glucagon and reduced insulin. As the glycogen depot is depleted, triglyceride catabolism begins to supply substrates for gluconeogenesis from glycerol, and ketogenesis from free fatty acids. In addition, gluconeogenic and ketogenic amino acids are converted by anaplerotic reactions that feed substrates into the metabolic cycle for energy production. During prolonged fasts, ketone bodies provide nearly half of the body's energy requirements and 70% of the energy requirement for the brain (Cahill, 2006).

During starvation, hepatic fatty acid oxidation in the mitochondria, peroxisomes and microsomes functions as the primary source for catabolic energy. These processes are all activated by PPARα (Reddy and Hashimoto, 2001). Mitochondrial β-oxidation primarily uses short ($<C_6$), medium (C_8-C_{12}) and long

(C_{12}-C_{20}) chain fatty acids to produce acetyl-CoA subunits that can be condensed into ketone bodies that are used as oxidizable substrates in extrahepatic tissues. Peroxisomal β-oxidation uses very long straight-chain fatty acids (>C_{20}), 2-methyl branched fatty acids, prostanoids, dicarboxylic acids, and the C_{27} bile acid intermediates di- and trihydroxyprostanoic acids to generate acetyl-CoA (Ferdinandusse et al., 2009; Jia et al., 2003). Microsomal ω-oxidation, which differs from β-oxidation by its use of the distal carboxyl group of fatty acids, is carried out in the endoplasmic reticulum by CYP4As (Reddy and Hashimoto, 2001). This catabolic process is a minor pathway for breaking down medium chain fatty acids, but becomes more important if β-oxidation is defective. PPARα regulates all three fatty acid oxidation systems, and therefore represents a major regulator of the catabolism of lipids in the liver.

1.3 White Adipose Tissue Metabolism

As a storage tissue, white adipose tissue constitutes a multi-depot organ that is innervated and rich in blood vessels. Several distinguishable cell types comprise the adipose tissue including: lipid-laden mature adipocytes, adipocyte precursors (preadipocytes), immunological cell types, and the stromal vascular fraction that consists of endothelial cells, and macrophages. During development, mature adipocytes acquire the enzymatic machinery to carry out and regulate lipogenic and lipolytic functions (Cornelius et al., 1994). Expansion of the adipose mass is frequently associated with proinflammatory states, hypertension, dyslipidemia,

hyperglycemia, insulin resistance, cancer and some degenerative diseases (McMillan et al., 2006). Adipose tissue has a remarkable ability to expand during excess nutrient availability, by increasing both the size and number of adipocytes through a process of proliferation and differentiation of preadipocytes. Importantly, proper regulation of adipose tissue mass is necessary since either too little (lipodystrophy) or too much (obesity) adipose tissue contributes to metabolic abnormalities including: hyperlipidemia, insulin resistance and type 2 diabetes (Chehab, 2008).

1.3.1 White Adipose Tissue and the Fed State

During periods of nutrient availability adipose tissue functions as a storage site for energy in the form of triglycerides, which helps to supply whole body energy when nutrients are in shortage. Although originally thought of as an inert tissue mass that stores excess energy and provides insulation and padding for the body, the discovery that adipose functions as a secretory tissue has enlightened researchers and spawned intense investigation to explore this tissue. In the fed state, normal adipose tissue has the remarkable capacity to increase the number of adipocytes through the process of differentiation.

Early adipocyte differentiation studies using *in vitro* approaches have yielded valuable information about the pathways that are utilized for this process. Hormonally, the induction of preadipocyte differentiation has been shown to require high doses of insulin and growth hormone (Nixon and Green, 1984; Student et al.,

1980; Zezulak and Green, 1986); but it was later discovered that both hormones exerted their effects though the IGF-1 receptor (Smith et al., 1988), and could be replaced by physiological doses of IGF-1. The discovery that IGF-1 functioned as a stimulant for adipocyte differentiation highlighted the involvement of tyrosine kinase-mediated signaling pathways since the IGF-1 receptor is a tyrosine kinase. Pertaining to Chapter 3, other groups have shown the importance of FGF-receptor tyrosine kinase signaling event as regulators of the differentiation process where inhibiting FGF10 signaling by anti-FGF10 antibodies or overexpression of a dominant negative FGFR1 prevents differentiation and lipid accumulation. In this respect, my observations that FGF10 is most abundantly expressed at day 2 and day 4 of differentiation, whereas FGF21 and βklotho are expressed from day 4, suggesting that FGF-dependent activation of this receptor tyrosine signaling pathway is required throughout the differentiation process. Intriguingly, insulin and FGF21 both share the ability to stimulate glucose transport into adipocytes (Kharitonenkov et al., 2005; Moyers et al., 2007), suggesting that FGF21 regulates the late phase of adipocyte maturation. Differentiation can also be initiated in preadipocytes grown in serum-free media that is supplemented with transferrin, fetuin, growth hormone, triiodothyronine, and high concentrations of insulin (or IGF-1), where this cocktail activates the expression of early adipocyte markers such as lipoprotein lipase. However, additional adipogenic agents such as glucocorticoids, arachidonic acid or prostacyclin are required for the terminal differentiation of these cells (Catalioto et al., 1991; Gaillard et al., 1989; Gaillard et al., 1991; Negrel et al., 1989)

demonstrating that adipocyte differentiation progresses through a series of regulated events. Regarding adipocyte differentiation, hormones affect both the signal transduction and transcriptional regulation of adipocyte differentiation.

The transcriptional regulation of adipocyte differentiation is mediated though a several transcription factors that regulate distinct processes from progression of preadipocyte to mature adipocyte. The time windows of each of these factors are rigidly controlled to facilitate an orderly progression through the differentiation process, and involves both transcriptional activators (C/EBPα, C/EBPβ, PPARγ), and repressors (CHOP/gadd153, C/EBPβ/LIP, CUP, PRE). As discussed in Section 1.4.2, PPARγ is a master regulator of adipocyte differentiation (van Beekum et al., 2009). PPARγ is both necessary and sufficient to cause mouse fibroblasts to differentiate into white adipocytes. PPARγ cooperates with the CCAAT/enhancer-binding protein (C/EBP) family of transcription factors to regulate adipogenesis (Wu et al., 1999). C/EBPβ and C/EBPδ are present early during adipogenesis and induce PPARγ expression (Wu et al., 1996). C/EBPα is expressed later to enhance the expression of PPARγ and cooperate in inducing the adipocyte-specific pattern of gene expression (Rosen et al., 2002).

1.3.2 White Adipose Tissue and the Fasted State

During fasting conditions, the adipose tissue switches its role as a storage site of triglycerides, to a contributor of metabolites for use in other tissues. In the fasting

state hormone sensitive lipase (HSL) and adipose specific triglyceride lipase (ATGL) are activated in adipose tissue to provide glycerol and fatty acid substrates for metabolism in other tissues. The glycerol released from adipose is primarily used as a gluconeogenic substrate whereas fatty acids are shunted toward the synthesis of ketone bodies in the liver. Lipid metabolism in the adipose tissue is controlled at three levels: fatty acid uptake, lipogenesis, and lipolysis. These processes are all hormonally regulated by factors such as insulin, corticoids, catecholamines, and various cytokines (Anghel and Wahli, 2007).

Adipokines stimulate an integrated response by acting on various organs in the body where there expression is influenced by the integrity and physiological status of the adipose tissues. The mechanism by which nutrient availability influences leptin expression remains poorly defined, but PPARγ agoinsts including thiazolidinediones have been shown to repress leptin in a manner that is consistent with a role of PPARγ function in the fed state (Kallen and Lazar, 1996). In addition, treatment of adipocytes with catecholamines or dexamethasone represses leptin gene transcription in a manner that is dependent on the production of the intracellular signaling molecule cAMP (Rentsch and Chiesi, 1996).

1.4 Overview of the PPAR Nuclear Hormone Receptors

Peroxisome proliferator-activated receptors (PPARs) are members of the nuclear receptor family of ligand-activated transcription factors. The human genome

codes for 48 nuclear hormone receptors that can be assigned to one of four groups: steroid hormone receptors, retinoid x receptors (RXR) heterodimers, dimeric orphan receptors, and monomeric orphan receptors. Additionally, NHRs can be classified into three groups: endocrine, adopted orphan, and orphan receptors according to the source and type of their ligand (Chawla et al., 2001) (Figure 1.1A). There are three homologs of the PPAR gene family all belonging to the adopted orphan receptor group, termed PPARα (NR1C1), PPARβ/δ (NR1C2), and PPARγ (NR1C3). PPAR members share similar structural characteristics in that they have distinct functional domains, including the N-terminal transactivation domain (AF1), a highly conserved and centrally located DNA-binding domain (DBD) composed of two zinc fingers, a hinge region that binds corepressor proteins, and a C-terminal ligand binding domain (LBD) (Figure 1.1B) (Desvergne and Wahli, 1999). The unique LBD of these receptors confers ligand-binding specificity and ligand-dependent transactivation function (AF2).

The PPAR subfamily of NHRs was originally described in the 1990's from work exploring the mechanism of action of peroxisome proliferator small molecules. Peroxisome proliferators are a group of structurally diverse compounds that lower serum lipids by stimulating the transcription of fatty acid oxidation genes and proliferation of peroxisomes in the liver (Reddy et al., 1980; Reddy et al., 1986; Reddy et al., 1976). Cloning of the first PPAR, PPARα, was completed in 1990 (Issemann and Green, 1990) and subsequent studies identified the two additional members PPARβ/δ and PPARγ (Dreyer et al., 1992). Further characterization of each PPAR highlighted their unique biological functions, where PPARα and PPARβ stimulate energy consumption and PPARγ stimulates energy storage in adipose tissue.

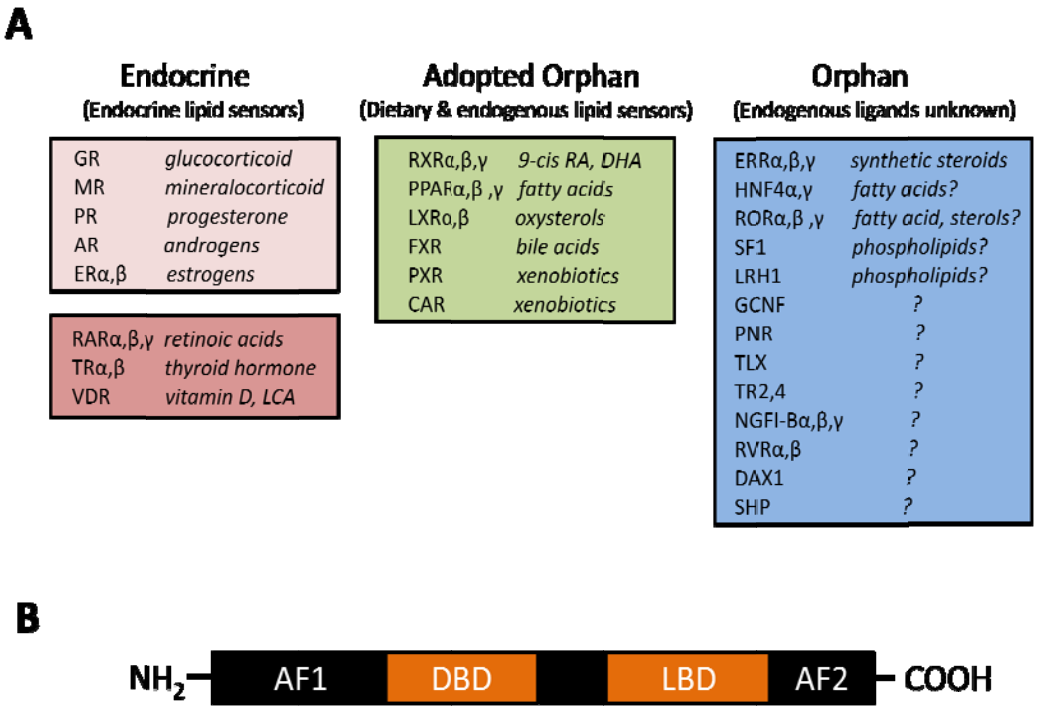

Figure 1.1 The nuclear hormone receptor superfamily (A). General structure of nuclear hormone receptor transcription factors (B).

The LBD pocket of PPARs is larger than most NHRs, with a total volume ranging from 1300 to 1400Å (Desvergne and Wahli, 1999; Xu et al., 2001). PPARs function as "lipid sensors", binding fatty acid metabolites and regulating the transcription of an array of genes involved in lipid homeostasis (Evans et al., 2004). Ligand binding to the LBD of PPARs results in a conformational change in the protein structure that permits the recruitment of coactivator proteins, such as SRC1/CBP and TRAP/DRIP/ARC, and activates the expression of genes with peroxisome proliferator response element (PPRE) in their promoters (Nolte et al., 1998; Perissi and Rosenfeld, 2005). In contrast, unliganded PPARs can be bound to promoters and recruit corepressor proteins such as SMRT and N-CoR, to deacetylate histones, resulting in transcriptional repression (Guan et al., 2005). In addition to the distinct PPAR LBDs, the unique AF1 regions of the PPARs confer specificity of gene transcription between the isoforms (Hummasti and Tontonoz, 2006). Through a series of mutational analysis, Hummasti *et al.* (2006) demonstrated the modular functions of the PPAR AF1 regions by creating chimeric proteins at the N-terminus of each PPAR, and illustrating their unique ability to regulate selective gene expression programs.

In addition to ligand dependent activation, PPAR members also require an obligate heterodimers partner, the retinoic acid X receptor (RXR), to effectively bind DNA and stimulate maximal gene expression (Kliewer et al., 1992; Mangelsdorf and Evans, 1995). PPARs can be activated by their own PPAR ligand or RXR ligands, such as 9-cis retinoic acid (Heyman et al., 1992; Mangelsdorf et al., 1990). RXR

functions as an accessory factor that is required for optimal binding of several NHRs. RXR and PPARs function as permissive heterodimeric partners where ligand binding to either RXR or its partner leads to receptor activation, while the presence of both ligands stimulates a synergistic activation of transcription. Alternatively, conditional partners of RXR exist, where ligand binding to RXR can activate transcription only in the presence of the partner ligand; and non-permissive partners of RXR exist, where its ligand is not sufficient to induce activation of the heterodimers (ex. VDR, TR) (Shulman et al., 2004). The PPAR:RXR complex binds directly to the PPAR response element (PPRE) in the promoter region of genes.

The PPRE is a direct repeat (DR1) motif with a hexanucleotide sequence of AGGTCA, separated by one nucleotide (Kliewer et al., 1992). Importantly, the unique 5'-region of the PPRE DR1 motif imposes a polarity to the DNA such that PPARγ interacts with the upstream extended core hexamer, and RXR interacts with the downstream sequence (Juge-Aubry et al., 1997; Mangelsdorf and Evans, 1995). This binding arrangement is unique from other heterodimers of RXR, where RXR typically occupies the upstream core of the hexanucleotide motif.

The major physiological differences between the PPARs are believed to occur from their specific activation by different ligand affinities, protein structure, and unique expression pattern among different tissues. The expression profiles of the PPARs, along with all other NHRs, illustrate the potential ability of this gene family to coordinate transcriptional programs and regulate distinct physiological changes.

Collectively, the NHR transcriptional networks have been divided into two major physiological paradigms consisting of 1) reproduction, development and growth, and 2) nutrient uptake, metabolism and excretion (Bookout et al., 2006), where PPARs can regulate both.

1.4.1 PPARα Overview

PPARα was the first identified member of the peroxisome proliferator activated-receptor family. The human PPARα gene spans ~93.2 kb and is located on chromosome 22 at position 22q12-q13.1 (Sher et al., 1993), whereas the mouse gene is located on chromosome 15 at position E2 (Issemann and Green, 1990). PPARα is highly expressed in tissues with active fatty acid catabolism such as the liver, heart, kidney, brown adipose tissue, muscle, small intestine and large intestine (Bookout et al., 2006).

Expression and activity of PPARα is increased in the liver during periods of starvation, resulting in increased expression of enzymes that catabolize fatty acids (Kersten et al., 1999; Rakhshandehroo et al., 2007). During fasting conditions, fatty acids are mobilized from peripheral stores and are sent back to the liver to be converted to ketone bodies. These fatty acids act as ligands for PPARα-dependent transcriptional activation to increase the expression of genes involved in lipid catabolism and ketogenesis. PPARα is hormonally regulated by various factors including: growth hormone, glucocorticoids, insulin and leptin. In humans, PPARα

has been shown to be transcriptionally regulated by the nuclear receptors hepatocyte nuclear factor 4 (HNF4), and chicken ovalbumin upstream promoter-transcription factor II (COUP-TFII) (Pineda Torra et al., 2002).

The LBD of PPARα is comprised of amino acids 280-468 and forms two α-helices flanking a four-stranded β-sheet. Lipid metabolites, including polyunsaturated fatty acids eicosapentaenoic acid (C20:5n-3), docosahexaenoic acid (C22:6n-3) and long chain fatty acids can bind to and activate PPARα to stimulate its target genes (Desvergne, 2007). Following ligand binding, the AF2 undergoes a conformational change, allowing the formation of hydrogen bonds between Tyr-314 and Tyr-464 and a charge clamp between Glu-462 and Lys-292, which directs the LXXLL motif to a hydrophobic cleft on the surface on the receptor (Xu et al., 2001). This LXXLL motif participates in protein-protein interactions with additional transcription regulators (Heery et al., 1997).

PPARα activity is also regulated by various post-translational modifications. PPARα can be phosphorylated in an insulin-dependent manner at Ser12 and Ser21 (Juge-Aubry et al., 1999), by p38 MAPK at Ser6, Ser12, and Ser21 (Barger et al., 2001), and by PKC at Ser179 and Ser230 (Blanquart et al., 2004). Recently, PPARα has been found to be modified by the small ubiquitin-like modifier protein (SUMO) in a sexually dimorphic manner that mediates female-dependent repression of PPARα target genes in the liver (Leuenberger et al., 2009). These studies suggested that SUMO:PPARα leads to DNA methylation by recruiting Dnmt3. In male mice, this

effect is mimicked by synthetic ligands for PPARα suggesting a ligand-dependent SUMOylation event, similar to the AF2 SUMOylation of PPARγ in macrophages, as discussed below (Pascual et al., 2005). Future studies of sex-dependent regulation of gene expression will be necessary to characterize the molecular mechanisms by which phenotypic anomalies occur between male and females, such as inflammation and hepatocellular carcinoma (Crockett et al., 2006; Naugler et al., 2007).

The significance of PPARα in the regulation of lipid metabolism was first demonstrated *in vivo* using *Pparα*$^{-/-}$ mice, which were generated over 15 years ago (Lee et al., 1995). These mice were created by disrupting the LBD of PPARα through homologous recombination. Although *Pparα*$^{-/-}$ mice are viable and fertile, with no detectable gross phenotypic defects, they do not produce peroxisome proliferator-induced liver tumors with chronic treatment and suffer from severe hepatic steatosis upon fasting or high fat diets (Hays et al., 2005; Kersten et al., 1999). This phenotype was associated with defective activation of the fatty acid oxidation system (Hashimoto et al., 2000).

In vivo, hepatic PPARα activity is also influenced by peripheral energy homeostasis through leptin, where leptin treatment was found to cause a 55% decline in epididymal fat pad weight of wild-type mice and only 6% decrease in *Pparα*$^{-/-}$ mice; additionally, liver triglycerides are decreased by 39% in leptin treated wild-type mice but are unaffected in *Pparα*$^{-/-}$, suggesting a defect in hepatic lipid oxidation (Lee

et al., 2002). Therefore, it is possible that PPARα regulated genes in the liver may affect adipose tissue mass through a hormone mediated event (Potthoff et al., 2009).

1.4.2 PPARγ Overview

PPARγ is a member of the peroxisome proliferator activated-receptor subfamily. The human PPARγ gene is located on chromosome 3p25 (Beamer et al., 1997), whereas the mouse PPARγ gene is located on chromosome 6 at position E3 (Zhu et al., 1995). Both human and mouse genes express two distinct protein isoforms of PPARγ (PPARγ1, PPARγ2) through differential promoter usage and alternative splicing. PPARγ is considered the master regulator of adipocyte differentiation as it is both necessary and sufficient to induce differentiation into mature adipocytes (Hamm et al., 1999; Rosen et al., 1999). Given its important role in lipid storage, PPARγ is most abundantly expressed in the white adipose, brown adipose (Bookout et al., 2006; Tontonoz et al., 1994a). Low levels of PPARγ expression can be observed in the colon, bone, heart, testis, brain, lung and skeletal muscle (Bookout et al., 2006).

The differential expression profiles of PPARγ isoforms suggest tissue specific functions of the receptor. For instance, PPARγ2 is the most abundant form in adipose tissue of rodents, whereas PPARγ1 is the most abundant isoforms in other tissues (Desvergne and Wahli, 1999). The unique function of PPARγ2 has been ascribed to its extra 30 amino acid extension at the N-terminal domain, which displays a 30-fold

greater activation function than the AF1 of PPARγ1 when measured by cell reporter assays (Werman et al., 1997). This functional difference is observed in mice that have a selective knockout of the PPARγ2, leading to impaired development of adipose tissue and decreased insulin sensitivity (Zhang et al., 2004).

The identification of PPARγ as the therapeutic target of the anti-diabetic compounds, called thiazolidinediones spawned an enormous amount of interest and research in this receptor (Lehmann et al., 1995). This discovery gave researchers a tool to study the effects of PPARγ using *in vitro* and *in vivo* models, which helped to characterize PPARγ as the master regulator of adipogenesis.

In addition to ligand-dependent regulation of PPARγ transcriptional activation, post-translational modifications of the protein have been found to play important functions in modulating its activity (van Beekum et al., 2009). Initial studies of mouse PPARγ protein identified a conserved phosphorylation site at Ser112 of PPARγ2 (Ser82 of PPARγ1) (Hu et al., 1996). Phosphorylation of this site occurs through a mitogen activated protein kinase (MAPK) signal transduction mechanism. Subsequent studies described phosphorylation at this site by JNK1/2 and p38 (Adams et al., 1997; Camp et al., 1999). Functional studies have illustrated that phosphorylation at this residue represses PPARγ function (Hu et al., 1996), whereas hypophosphorylation at this site has been suggested to regulate its ubiquitination and degradation by the proteasome (Floyd and Stephens, 2002; Hauser et al., 2000). More recently, high expression of Dok1, a negative regulator of the MAPK signal

transduction pathway, was found to block the phosphorylation of PPARγ and permit its activity (Hosooka et al., 2008).

PPARγ can also be post-translationally modified by the small ubiquitin-like modifier (SUMO) at lysine residues. In mammals, three SUMO proteins exist. Biochemical approaches have shown that SUMO attachment involves an activation enzyme (SAE1/SAE2), a conjugation enzyme (Ubc9), and an E3 ligase that grants substrate specificity. Since no current biotechnique is available to specifically catalyze the ligation of SUMO1 to PPARγ in cells, all research to date has taken advantage of mutations in PPARγ that prevent its SUMOylation. PPARγ contains two consensus SUMOylation motifs of ψKxE/D where ψ represents a large hydrophobic residue and x may be any residue. These motifs reside at Lys107 and Lys395 in PPARγ2 (Lys77 and Lys365 in PPARγ1). Conjugation of SUMO-1 to Lys107 by the E3 SUMO ligases PIAS1 or PIASχβ negatively modulate PPARγ function. Intriguingly, the Lys107 SUMOylation of PPARγ is linked to some extent, with the phosphorylation at Ser112 (Yang and Gregoire, 2006). This represents a phosphorylation-dependent SUMOylation motif with a consensus site of ψKxExxSP where ψ is a hydrophobic residue, K is the SUMO acceptor lysine, x is any amino acid and SP forms part of the downstream phosphorylation site. This motif is unique to the γ subtype of PPARs, although it is also present in other transcription factors. Interestingly, a heterozygous mutation of Pro115Gln was found in a small population of Germans that displayed severe obesity (BMI 37.9-47.3), suggesting that this motif may be required for SUMOylation dependent silencing of PPARγ activity (Ristow et al., 1998). The potential contribution of Lys107 was alluded to in studies where this region of the PPARγ protein had been truncated, showing enhanced PPARγ activity

and increased ability to stimulate lipid accumulation *in vitro* (Ohshima et al., 2004; Tontonoz et al., 1994b). Lys395 SUMOylation of PPAR is not involved in the regulation of direct PPARγ target genes, but in the transrepression of inflammatory genes by PPARγ in macrophages (Pascual et al., 2005). Treatment of macrophages with PPARγ ligand stimulates Lys395 SUMOylation, which in turn targets PPARγ2 to NCoR corepressor and binds to NF-κB target genes. Identifying cellular events that control PPARγ post-translational modification will clearly enhance our understanding of PPARγ biology.

The role of PPARγ has been extensively studied *in vitro*, but there is a paucity of data from *in vivo* studies since the classic knockout mouse studies have proven difficult because the homozygous null mice do not survive past the midembryonic stage (Miles et al., 1999). In order to circumvent this problem, chimeric mice were created and demonstrated that PPARγ is essential for adipose and sebaceous gland development (Rosen et al., 1999). Selectively knocking out PPARγ from mature adipocytes, using the Cre-*loxP* system, mice develop increased plasma free fatty acids, triglyceride, decreased leptin, and adiponectin, fatty liver and enhanced hepatic gluconeogenesis (He et al., 2003). Importantly, all mouse strains that express defective PPARγ result in mice with mild to severe lipodystrophy (Gray et al., 2005). Aside from PPARγ association with adipogenesis, when floxed animals were crossed to Tie2-cre expressing cells to knockout expression in endothelial cells and hematopoietic lineages, the data showed that osteoclastogenesis was regulated by PPARγ, resulting in osteopetrosis (Wan et al., 2007). Collectively these data indicate a broad role for PPARγ beyond its function in adipogenesis.

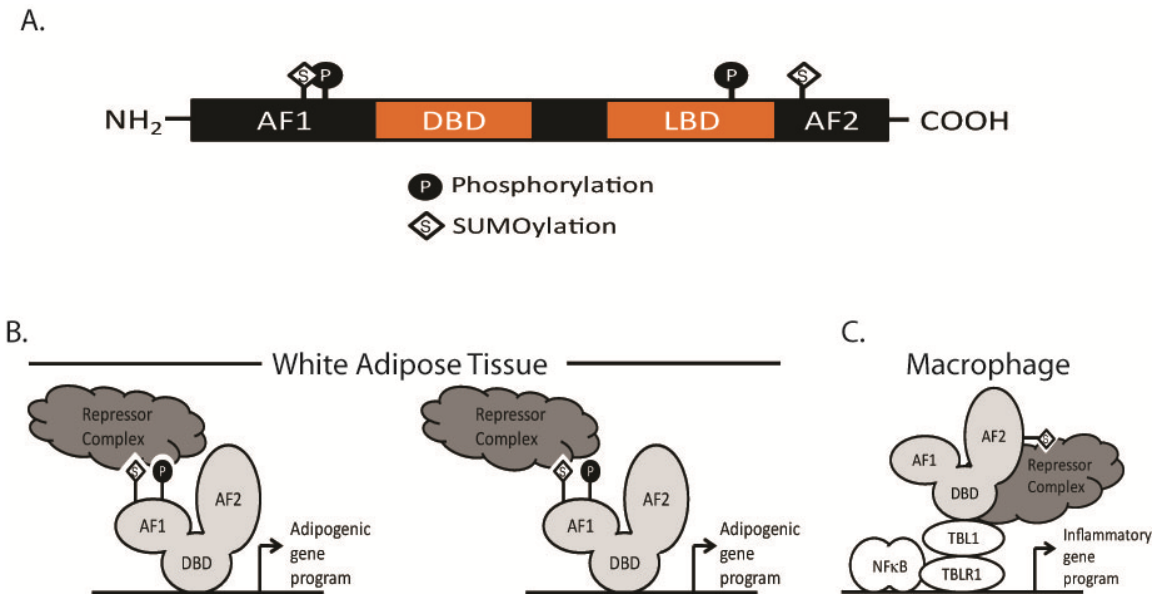

Figure 1.2 Post-translational modifications of PPARγ (A). Diagram of PPARγ dependent transcriptional repression in WAT (B) and macrophage (C); adapted from (van Beekum et al., 2009)

1.3 The FGF Superfamily

Fibroblast growth factors are a large group of structurally related proteins that control a wide range of biological functions, including: cell proliferation, survival, migration and differentiation (Itoh and Ornitz, 2008). The prototypical FGFs, FGF1 (acidic FGF) and FGF2 (basic FGF), were originally identified as mitogens for fibroblasts from the brain and pituitary. An increase in the number of FGFs is believed to have occurred partly by gene duplications early in metazoan evolution, but mainly through two large-scale genome duplication events early in vertebrate evolution (Itoh and Ornitz, 2004). The structure of canonical FGFs contain a heparin-binding site that is necessary for stable binding to FGFRs and enhanced signal transduction. Classical FGFs are readily sequestered by the extracellular matrix and are released by heparinases, proteases, or specific FGF-binding proteins. In contrast to classical FGFs, the endocrine-like FGFs have acquired endocrine functions by reducing their heparin-binding capacity, allowing them to escape the extracellular matrix of the tissues of their origin.

The *FGF* family consists of 22 members and can be divided into seven subfamilies as illustrated in Figure 1.3. These subfamilies can be further grouped into three classes through their mechanism of action: the intracellular *FGF11/12/13/14* subfamily, the hormone-like (endocrine) *FGF19/21/23* subfamily, and the canonical *FGF* subfamily of *FGF1/2/5*, *FGF3/4/6*, *FGF7/10/22*, *FGF8/17/18*, and *FGF9/16/20* (Itoh and Ornitz, 2004, 2008). Canonical FGFs act as autocrine/paracrine factors that bind to and activate cell surface tyrosine kinase FGFRs with heparin/heparin sulfate

as a cofactor. In contrast to the secreted FGFs, intracellular FGFs act as signaling molecules within the cell in an FGFR-independent manner. They can interact with intracellular domains of voltage-gate sodium channels and neuronal mitogen-activated protein kinase scaffold proteins, islet-brain-2, and regulate neuronal function at postnatal stages (Goldfarb, 2005; Goldfarb et al., 2007).

Secreted FGFs function as ligands to extracellular receptor tyrosine kinases. Five distinct subfamilies of the FGF receptors (FGFRs) exist: FGFR1, -2, -3 and -4 possess intrinsic tyrosine kinase activity (Powers et al., 2000); whereas FGFR-5 does not have any intracellular kinase domain (Kim et al., 2001; Sleeman et al., 2001). FGFRs are expressed in many different cell types and regulate major cell functions, such as proliferation, differentiation and survival (Fon Tacer et al., 2010). Importantly, specific cellular responses to FGFs are established by the expression profile of their FGFRs and the specific affinities of these receptors for each FGF. There is growing evidence that FGFRs also traffic to the nucleus where they may regulate cellular functions independently from their receptor tyrosine kinase signaling pathways (Beenken and Mohammadi, 2009), but more work is needed to define these mechanisms.

The discovery of the *klotho* family members (klotho, βklotho) demonstrated a further degree of FGF/FGFR regulation. Klotho family members are single pass transmembrane proteins that are obligate co-receptors for FGF21, FGF23 and FGF15/19 (Kurosu and Kuro-o, 2008). The *klotho* gene was originally identified as

an aging suppressor gene that extends life span when overexpressed and accelerates aging-like phenotypes when disrupted (Kuro-o et al., 1997). Phenotypic similarities between the Klotho-deficient and FGF23-deficient mice including hyperphosphatemia, hypervitaminosis D, and multiple age-like symptoms suggested an intimate relationship between the functions of these genes and helped to identify their functional connection (Razzaque et al., 2006; Shimada et al., 2004).

Binding of FGFs to their FGFRs stimulates a ligand-dependent dimerization, leading to a conformational change in the receptor structure, activation of the intracellular kinase domain, and intermolecular transphosphorylation of the tyrosine kinase domains. These phosphorylated residues function as docking sites for adaptor proteins, and may themselves be targeted for phosphorylation by the FGFR (Eswarakumar et al., 2005). Following activation of the FGFRs, negative feedback mechanisms are quickly induced to inhibit signaling through the receptor. The components of the negative feedback mechanism are only partially known, but include several protein phosphatases (DUSP4/6, Sprouty) and ubiquitin ligases (CBL) (Turner and Grose, 2010).

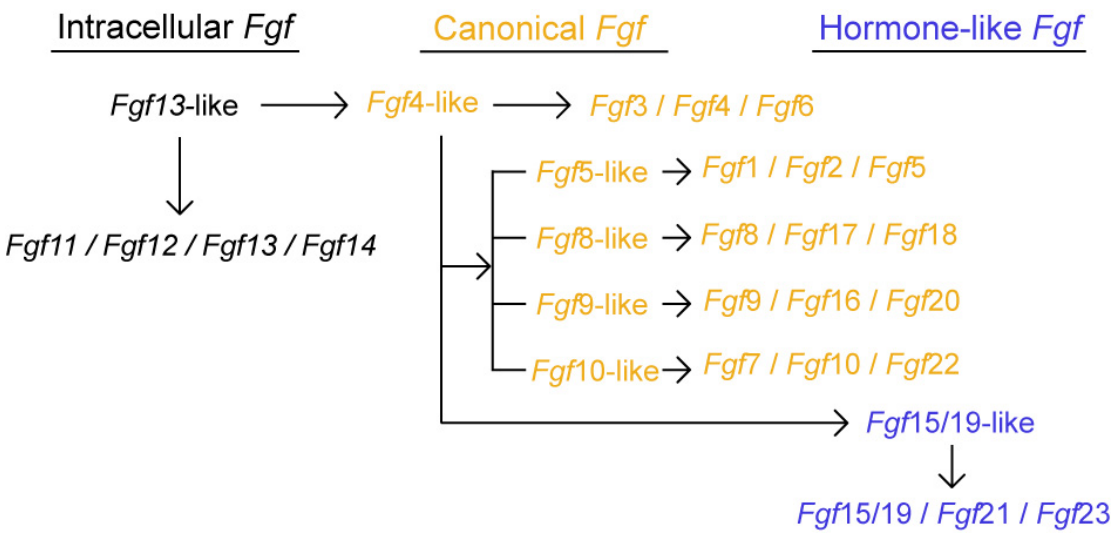

Figure 1.3 The FGF Superfamily. Evolutionary history of the Fgf gene family. Fgf13-like is an ancestral gene of the Fgf family. Fgf4-like is an ancestral gene of the canonical Fgf family. Fgf4-like was generated from Fgf13-like by gene duplication. Fgf15/19-like, an ancestral gene of the hormone-like Fgf subfamily, was generated from Fgf4-like by local gene duplication early in vertebrate evolution. Adapted from (Itoh, 2010)

1.5.1 FGF21 Signal Transduction

FGF21 is a secreted member of the FGF family that functions as a ligand for FGFR1c and βklotho coreceptor. As previously mentioned, structural and phylogenetic analysis of the FGF21 protein have placed it in the FGF19 subfamily of FGFs. This family of proteins consists of FGF15, which is the mouse ortholog of human FGF19, FGF23 and FGF21 (Itoh and Ornitz, 2004). FGF21 was originally identified in a screen using degenerate primers to human FGF19 in mouse embryos and determined to be expressed in the liver and the thymus (Nishimura et al., 2000). 5 years later, the ability of FGF21 to regulate metabolism was uncovered in a screen to find new molecules that simulated glucose uptake into adipocytes (Kharitonenkov et al., 2005). As a member of the FGF19-family, FGF21 shares the similar requirement with FGF19 and FGF23 for signal transduction in cells that express both the FGFR and the co-receptor βKlotho (Ogawa et al., 2007). Specifically, FGF21 signal transduction requires the expression of βKlotho (Ogawa et al., 2007), which is abundantly expressed with the FGFR1c on adipocytes (Kharitonenkov et al., 2005). βKlotho is a single-pass membrane-spanning protein with 2 glycosidase domains.

A breakthrough in understanding of the FGF19-family signal transduction regulation was made when it was identified that Klotho was an essential cofactor for FGF23 to activate downstream signaling (Urakawa et al., 2006). This discovery led investigators to examine why FGF21 could not signal in tissues that expressed various FGFRs and it was quickly discovered that another member of the Klotho family called βKlotho, with 41% amino acid identity, was required for FGF21

signaling (Kurosu et al., 2007; Ogawa et al., 2007). These observations suggested that the specific tissue distribution of FGFR isoforms and Klotho isoforms mediate the precise biological effects of the FGF19 subfamily.

Crystallographic studies of the FGF19 subfamily show the structural divergence from canonical paracrine FGFs (Goetz et al., 2007; Harmer et al., 2004), particularly, a reduced affinity for heparin/heparin sulfate. The effect of weak heparin binding affinity enables the FGF subfamily to escape the extracellular matrix from cells that produce them, allowing them to function as endocrine factors. However, the general structure of FGF21 is similar to other FGFs in that has as a β-trefoil-like core region, comprised of 12 anti-parallel β-strands, with disordered N- and C-termini. The particular function FGF21 N- and C-termini was examined by surface plasma resonance and demonstrates that the ends of this protein are necessary for recognition and binding to either FGFR or βKlotho, respectively (Micanovic et al., 2009; Yie et al., 2009).

1.5.2 Downstream Signaling of FGF21

Investigations of FGF21 signal transduction have primarily focused on adipose, liver and pancreatic cells. These cell types have been the focus for FGF21 signaling research as they express the necessary βKlotho and FGFR proteins. Binding of FGF21 to its receptor complex stimulates divergent downstream signaling

pathways mediated by FRS2, MAPK, SHP-2, PI3K, Raf, STAT, $p70^{S6K}$ and other signaling molecules (Moyers et al., 2007). Using 3T3-L1 adipocytes, Moyers *et al.* (2007), demonstrated the ability of FGF21 stimulate rapid and acute signaling events and prolonged effects of altered gene expression. Moreover, these researchers showed that FGF21 is able to act synergistically with PPARγ signaling to enhance the expression of GLUT1 mRNA. The synergistic effect of FGF21 and rosiglitazone treatment on glucose uptake was observable 6 hours after treatment, implying that transcriptional activation was involved with this response. In addition, intracellular Ca^{+2} was increased within 2 minutes of FGF21 treatment of 3T3-L1 adipocytes suggesting a role for calcium-dependent kinases in FGF21 signaling.

Recently, FGF21 administration was observed to induce the expression of the peroxisome proliferator-activated receptor γ coactivator protein-1α (PGC1α) in the liver (Potthoff et al., 2009). Increased PGC1α stimulated the transcription of genes in the liver involved in gluconeogenesis, fatty acid oxidation and ketogenesis, discussed in Section 1.3.4 (Potthoff et al., 2009; Rhee et al., 2003; Yoon et al., 2001). More work is required to distinguish what each component of FGF21 signaling does within the cell to regulate physiologic changes

1.5.3 Regulation of FGF21 Expression

The distinct tissue expression profile of FGF21 in various metabolic and pharmacological states illustrates a complex transcriptional regulatory mechanism.

Various ligands of nuclear hormone receptors including those for PPARα, PPARγ, ROR and TR have been shown to effect FGF21 expression at the transcriptional level (Adams et al., 2010; Inagaki et al., 2007; Muise et al., 2008; Wang et al., 2008; Wang et al., 2010). In addition, carbohydrate-rich diets have been described to stimulate FGF21 induction in the liver though ChREBP activation (Iizuka et al., 2009; Sanchez et al., 2009) Therefore, the ability of distinct transcription factors to induce the expression of FGF21 implies a complex function for the protein.

Several studies have examined FGF21 expression in humans. Circulating concentrations of FGF21 vary over a 250-fold range and do not correlate to age, sex, body mass index, serum lipids, or plasma glucose (Galman et al., 2008). However, FGF21 is increased in humans over a 7-day fast and hypertriglyceridemic patients express a 2-fold increase, which were further increased by treatment with PPARα agonist fenofibrate. Recent reports show that FGF21 is increased in subjects that are overweight, type 2 diabetic, have impaired glucose tolerance or NAFLD (Chen et al., 2008; Li et al., 2010; Li et al., 2008; Zhang et al., 2008). Additionally, FGF21 levels were significantly reduced in subjects with anorexia nervosa (Dostalova et al., 2008). Similarly, circulating FGF21 protein and FGF21 mRNA in liver and WAT are increased in *db/db* mice (Zhang et al., 2008). Paradoxically, serum FGF21 levels are elevated in patients with obesity and were independently associated with metabolic syndrome in humans (Zhang et al., 2008).

Initial studies of FGF21 expression in mice focused on the liver where its expression was found to be induced under the fasted state (Inagaki et al., 2007). The expression of FGF21 in the liver during the fasted state requires the expression of PPARα, since PPARα knockout mice do not induce expression, whereas treatment of wild-type mice with PPARα ligand, GW-7647 can stimulate a robust ~ 25-fold increase. In reporter assays, using the FGF21 promoter linked to luciferase, the transcriptional response was mapped to 2 regions within 1.5kb up-stream of the transcriptional start site that contain PPAR binding sites. In addition, ketogenic diets stimulate FGF21 in a PPARα dependent manner, producing a similar effect to fasting (Badman et al., 2007). These data strongly supported the concept that FGF21 is an important mediator of the physiological response to fasting.

Regulation of FGF21 by PPARγ ligands and various metabolic conditions in adipose suggested a role for FGF21 beyond that of a typical fasting hormone (Muise et al., 2008; Wang et al., 2008). Mutational analysis of PPARγ illustrated that helix-7 of the protein was important for the induction of FGF21 by the ligand troglitazone (Wang et al., 2008) although ligand GW1929 could still function. A comprehensive analysis of secreted proteins in adipose was performed by Muise, *et al.* (2008) who found that FGF21, along with 33 other genes, was upregulated by PPARγ ligand treatment in the adipose. Using adipose tissue of diabetic *db/db* mice treated with vehicle or one of two structurally different PPARγ ligand, rosiglitazone or COOH, FGF21 was found to be induced both at the mRNA level, and protein level in plasma (Muise et al., 2008). Treating *db/db* mice, C57BL/6 and lean CD1 mice with PPARγ

ligands increased FGF21 mRNA over 2-fold in adipose tissue, but had no significant effect on FGF21 expression in the liver (Muise et al., 2008). In addition, PPARα ligands, fenofibrate or WY14643, induced FGF21 mRNA in a PPARα dependent manner in the liver, but only induced FGF21 in adipose tissue of lean C57BL/6 mice, not CD1 mice or 3T3-L1 adipocytes in culture. Importantly, FGF21 was also found to be upregulated by high fat diet feeding in adipose or TZD treatment in adipocyte cultures, suggesting a role of FGF21 in lipid metabolism, beyond that of the fasted state (Muise et al., 2008; Wang et al., 2008). The regulation of FGF21 by PPARγ ligands in lean C57BL/6 mice indicated that FGF21 was not regulated by glucose or other metabolites that are altered by PPARγ agonists in lean animals. These observations suggest the intriguing possibility that FGF21 contributes to the therapeutic actions of thiazolidinediones, as discussed in Chapter 4.

1.6 FGF21 and Metabolism

Basic metabolic alterations elicited by FGF21 were first characterized by Kharitonenkov *et al.* (2005). These initial experiments demonstrated that FGF21 can potently activate glucose uptake in 3T3-L1 and human adipocytes, protect animals from diet-induced obesity, and lower blood glucose and triglyceride levels when therapeutically administered to diabetic rodents. Induction of glucose uptake in adipocytes was correlated with the induction of glucose transporter, GLUT1, likely mediated through a transcriptional event since long term treatments were required to

stimulate glucose uptake. Pharmacological administration of recombinant FGF21 to obese, insulin-resistant *ob/ob*, or *db/db* mice or Zucker diabetic fatty rats reduced plasma glucose and insulin concentrations, indicating that FGF21 may represent a novel treatment for type 2 diabetes (Kharitonenkov et al., 2005)

Subsequent studies showed that administration of FGF21 to high fat diet-induced obese mice increased fat utilization and energy expenditure and reduced plasma glucose, insulin and lipid and hepatic triglyceride concentrations (Coskun et al., 2008; Xu et al., 2009). FGF21 also improved hepatic and peripheral insulin sensitivity in both high fat diet-induced obese and lean mice. Studies of FGF21 in diabetic rhesus monkeys showed similar effects with mouse studies. FGF21 decreased fasting plasma glucose, insulin and triglycerides (Kharitonenkov et al., 2007). FGF21 also decreased LDL cholesterol, increased HDL cholesterol and caused modest weight loss without hypoglycemia.

Some of the metabolic effects of FGF21 may be directly through the endocrine pancreas. Overexpression of a dominant negative FGFR-1 in β-cells leads to diabetes in mice, implying that proper FGF signaling is required for normal β-cell function and glycemic maintenance (Hart et al., 2000). Also, short-term treatment of wild-type and *db/db* mice with FGF21 lowered plasma insulin concentrations but increased both the number of islets and the amount of insulin per islet (Wente et al., 2006).

In liver, FGF21 induces a metabolic profile characteristic of fasting. FGF21 stimulates hepatic gluconeogenesis, fatty acid oxidation, and ketogenesis through a PGC-1α dependent mechanism (Badman et al., 2007; Inagaki et al., 2007; Potthoff et al., 2009). However, FGF21 does not stimulate glycogenolysis, and FGF21-transgenic mice accumulate significantly more hepatic glycogen than do their wild-type controls when fed ad libitum (Potthoff et al., 2009). These observations suggest that in the liver FGF21 does not play an immediate role in the early stages of fasting, when glucagon is a dominant regulator of metabolism, but rather that FGF21 stimulates gluconeogenesis and ketogenesis as part of the long term fasting and starvation response when glycogen stores are already depleted. This is consistent with human studies that found increased concentrations of circulating FGF21 only after prolonged fasting (Galman et al., 2008). In contrast, *Fgf21*$^{-/-}$ mice were found to have elevated plasma ketone bodies in the fasted state, significantly greater than wild-type fasted mice indicating the FGF21 is not required for ketogenesis during fasting (Hotta et al., 2009). More research is required to determine if FGF21 alters the livers substrate preference for ketogenesis since fatty acids and amino acids can be used in this process.

As shown in Chapter 2, FGF21 induces a variety of pancreatic lipases in the liver, which include pancreatic lipase, pancreatic lipase-related protein 2, and carboxyl ester lipase (Inagaki et al., 2008). These lipases are not typically expressed in the liver, but are found to be induced in hibernating ground squirrels (Andrews et al., 1998). Since pancreatic lipases efficiently hydrolyze triglycerides over a broad

range of temperatures, it was proposed that their induction is necessary for providing fatty acid substrates under stressful environmental conditions. Particularly, these enzymes are induced during torpor in mice, the equivalent of hibernation (Zhang et al., 2006). These data suggest that FGF21 may sensitize mice to torpor and elicit hallmarks of the torpor response, including changes in lipase gene expression and metabolism. Characterizing the physiological and pharmacological aspects of FGF21 treatment will benefit from tissue-specific deletion of the FGF21 signaling components in mice.

CHAPTER 2

FGF21 as an Endocrine Hormone in the Fasted State

2.0 Introduction

A reverse endocrinology approach was successfully used by our lab to identify FGF15 as an enterohepatic signal that decreases the first and rate-limiting step of the classical bile synthesis pathway, cholesterol 7 alpha-hydroxylase (Inagaki et al., 2005). This study was expanded to determine the tissue specific expression profile of all members of the FGF family and characterize their transcriptional response to various well-defined nuclear receptor ligands. Using this approach, our lab identified a robust regulation of FGF21 by PPARα ligands. As discussed in Chapter 1, the similar protein identity between FGF15/19 and FGF21 (Nishimura et al., 2000) suggested that the endocrine capabilities of FGF15 might be maintained with FGF21. During this time, studies were also being conducted in the lab of Dr. Makoto Kuro-o (University of Texas Southwestern Medical Center at Dallas) that helped characterize the FGF21 receptor as a protein complex consisting of the FGFR1c and βklotho, as well as a general tissue distribution profile of these complexes that indicated a specificity for the FGF signal transduction system (Kurosu et al., 2007; Ogawa et al., 2007). Since FGF21 was expressed in the liver and its receptors were found to be abundantly expressed in the adipose tissue, a model that described FGF21 as a novel endocrine factor was developed through the following studies.

2.1 FGF21 mRNA is Induced During Fasting by PPARα.

By taking a systematic approach to determine if nuclear receptors could regulate FGFs, we found that PPARα regulates *Fgf21* in the liver. Using RT-qPCR, *Fgf21* mRNA was induced ~25-fold in the liver of wild-type mice in response to GW7647, a selective PPARα agonist (Brown et al., 2001). Moreover, in *Pparα*$^{-/-}$ mice, the basal expression of *Fgf21* mRNA was reduced ~5-fold and GW7647 treatment did not increase its expression (Figure 2.1A). FGF21 was also regulated in a similar PPARα-dependent manner in human liver since primary hepatocyte cultures treated with GW7647 for 12 hours also showed an increase in *Fgf21* mRNA (Figure 2.1B). These data demonstrated that *Fgf21* mRNA is regulated by PPARα in the liver.

Since PPARα activation plays an important role in transcriptional regulation during the fasted response in the liver, we investigated if *Fgf21* is regulated by fasting. *Fgf21* mRNA increased ~28-fold after fasting for 12 hr, while re-feeding for 12 hr reduced *Fgf21* mRNA to pre-fasting levels (Figure 2.1C). Although the induction of *Fgf21* by fasting was significantly reduced in the *Pparα*$^{-/-}$ mice, a 5-fold induction of *Fgf21* mRNA was detectable (Figure 2.1C). This increase may be explained by additional transcription factors contributing to the regulation at the *Fgf21* promoter. These data demonstrated that *Fgf21* is induced in the liver during fasting by a mechanism that is largely attributed to PPARα.

To determine if *Fgf21* is directly regulated by PPARα a *Fgf21* promoter fragment from -1497 to +5 was used to generate the FGF21 -1497/+5-luciferase reporter construct. Transfection assays were performed in CV-1 cells, and showed a 5-fold induction of the *Fgf21* promoter by PPARα in the presence of GW7647 (Figure 2.1D). Mutational analysis showed that a truncation of the *Fgf21* promoter to -977 resulted in a loss of most of the PPARα response, whereas deletion to -66 eliminated it entirely (Figure 2.1E). To determine whether PPARα bound to the *Fgf21* promoter in liver, chromatic immunoprecipitation assays were performed using mouse liver. PPARα was detected using primers extending from -1119 to -1044 (Figure 2.1F). Thus, PPARα directly regulates *Fgf21* expression in the liver.

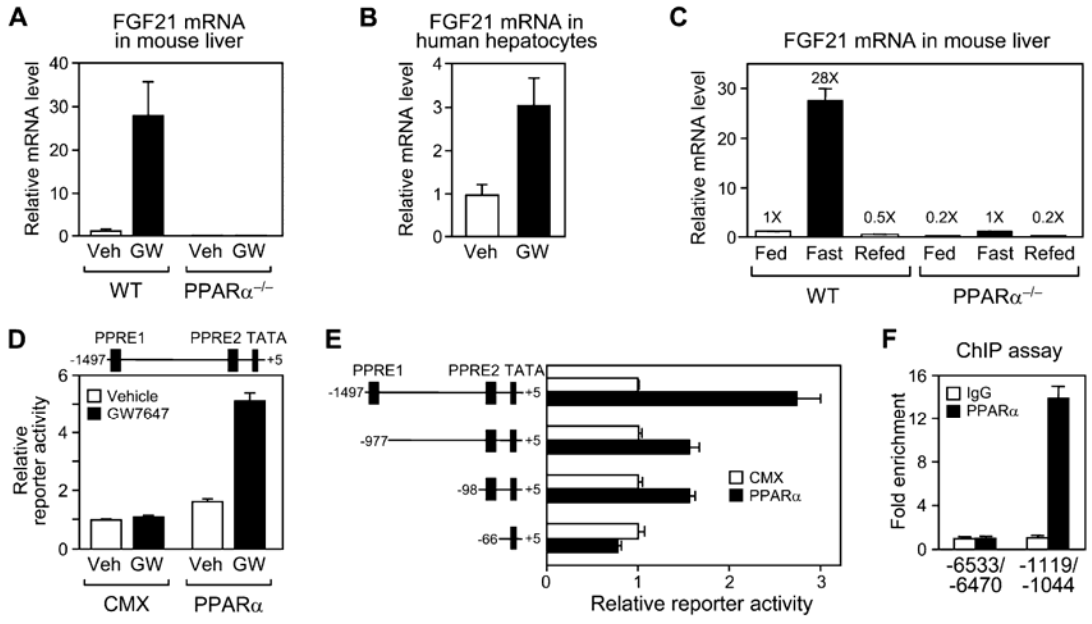

Figure 2.1. FGF21 mRNA Levels are Induced During Fasting by PPARα.

A) WT and *Pparα*$^{-/-}$ mice were administered GW7647 (GW; 5 mg/kg by oral gavage) or vehicle (Veh) and killed 14 hr later. FGF21mRNA levels were measured by RT-qPCR. (n = 5 mice per group.)

B) Primary cultures of human hepatocytes were treated for 12 hr with GW7647 (GW; 1 μM) or vehicle (Veh). FGF21 mRNA levels were measured by RT-qPCR.

C) WT and *Pparα*$^{-/-}$ mice were killed in the fed state, after a 12 hr fast, or after 12 hr refeeding. FGF21 mRNA levels were measured by RT-qPCR. (n=4 mice/group) The fold induction relative to WT mice is shown above each bar.

D) Cell-based reporter assays were performed in CV-1 cells cotransfected with *Fgf21* -1497/+5-luciferase reporter and the PPARα expression plasmid or control plasmid (CMX). Cells were treated with either vehicle (white bars) or 100 nM GW7647 (black bars).

E) Cell-based reporter assays were performed in CV-1 cells cotransfected with the indicated *Fgf21*-luciferase reporter vector in the presence of control plasmid (CMV; white bars) or PPARα expression plasmid (black bars). Cells were treated with 100 nM GW7647.

F) Chromatin immunoprecipitation assays were performed using liver and either PPARα antibodies (black bars) or control IgG (white bars) and primers to the proximal PPARα binding site (-1119 to -1044) or a control region (-6533 to -6470).

(A-C performed by T. Inagaki; D-F performed by X. Ding)

2.2. FGF21 induces Ketogenesis in the Liver

To study the effect of elevated FGF21 expression, transgenic mice were generated to express the FGF21 coding region under the control of the apolipoprotein E (*ApoE*) promoter and drive chronic expression of the transgene in liver (Simonet et al., 1993). As measured by RT-qPCR, *Fgf21* mRNA was expressed at ~50-fold higher concentrations in *Fgf21* transgenic mice than in fasted wild-type mice.

Since *Pparα*$^{-/-}$ mice have impaired ketogenesis and hepatic steatosis during fasting (Hashimoto et al., 2000; Kersten et al., 1999; Leone et al., 1999), we measured serum β-hydroxybutyrate, triglyceride and hepatic triglyceride concentrations in wild-type and *Fgf21* transgenic mice under the fed and fasted condition. In the fed state, serum concentrations of β-hydroxybutyrate were increased by ~5-fold in the *Fgf21* transgenic mice compared to wild-type (Figure 2.2A). The increase in ketone bodies was accompanied by significant decreases in serum and hepatic triglyceride concentrations (Figure 2.2B-C). Under the fasted state, when endogenous hepatic FGF21 expression is elevated, only serum triglyceride concentrations were significantly lower in transgenic mice compared to wild-type mice (Figure 2.2B).

The increase in β-hydroxybutyrate in the fed *Fgf21* transgenic mice suggested that FGF21 induces ketogenesis. To examine this possibility, total ketone body production was measured in isolated perfused livers from wild-type and *Fgf21* transgenic mice. Ketogenesis was increased ~30% in the livers from *Fgf21* transgenic mice (Figure 2.2D).

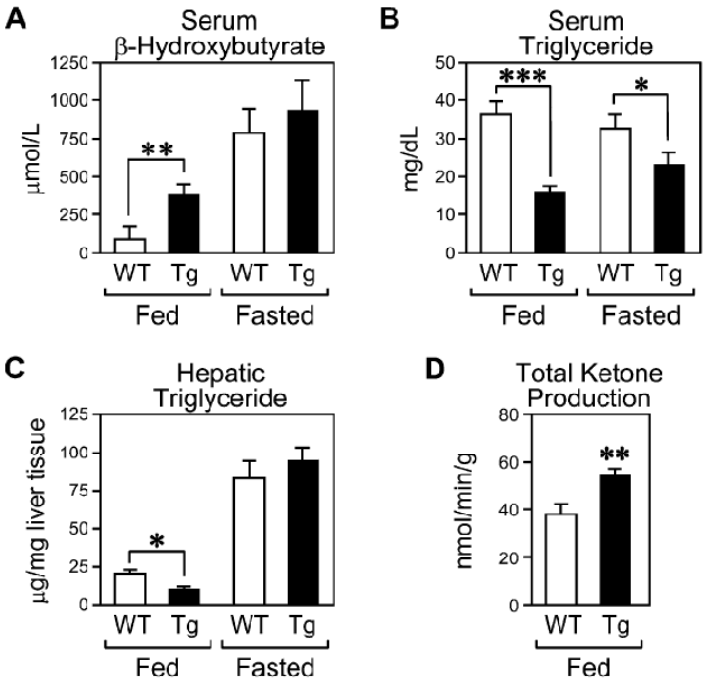

Figure 2.2. ***Fgf21*** **Transgenic Mice Exhibit Increased Ketogenesis.**

A-C.) Serum β-hydroxybutyrate (A) and triglyceride (B) concentrations and hepatic triglyceride concentrations (C) were measured in WT and *Fgf21* transgenic mice either in the fed state or after a 24 hr fast. (n=4 per group)
D.) Total ketone body production was measured using perfused livers from WT and Tg mice. (n=4-5 mice per group) *p<0.05; **p<0.001; ***p<0.001
(Serum measurements by T. Inagaki; Total Ketone Body Production by Burgess Lab)

To determine if short-term administration of recombinant FGF21 recapitulated the effects seen in *Fgf21* transgenic mice, wild-type and *Pparα*$^{-/-}$ mice were injected with recombinant FGF21 or control (saline) for 3 days, and β-hydroxybutyrate and triglyceride concentrations were measured in the fed state and after a subsequent 24 hr fast. In the fed state, FGF21 increased serum β-hydroxybutyrate over 2-fold in both wild-type and *PPARα*$^{-/-}$ mice and caused a decrease in serum triglyceride concentrations (Figure 2.3A-B). As expected, fasting induced serum β-hydroxybutyrate in wild-type mice but had no effect in *PPARα* $^{-/-}$ mice (Figure 2.3A). FGF21 had no effect on the already high levels of serum β-hydroxybutyrate in fasted wild-type mice, but increased concentrations ~3-fold in fasted *Pparα*$^{-/-}$ mice (Figure 2.3A) and reduced triglyceride abundance in the livers of fasted *Pparα*$^{-/-}$ mice (Figure 2.3C). These data suggest that FGF21 can partially rescue the hypoketonemia and hepatic steatosis that occur during fasting in the *Pparα*$^{-/-}$ mice.

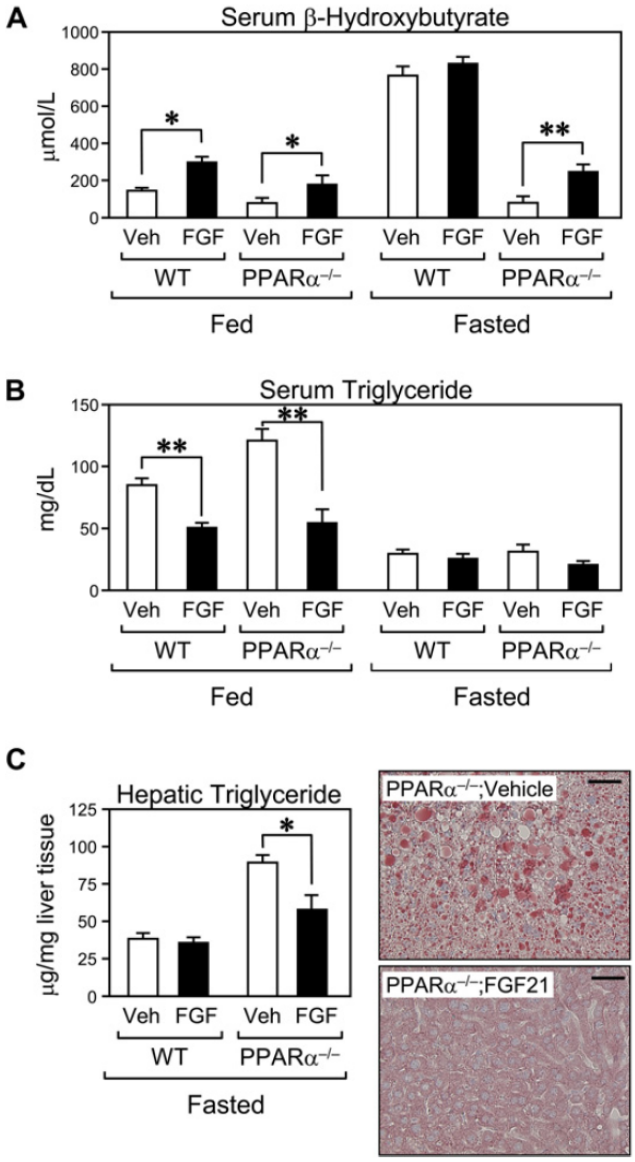

Figure 2.3. Recombinant FGF21 Injection Induces Ketogenesis.

A-C.) Serum β-hydroxybutryate (A), triglyceride (B) and hepatic triglyceride (C) concentrations were measured in WT and *Pparα*$^{-/-}$ mice administered either FGF21 (0.75mg/kg/day, subcutaneous) or vehicle (Veh) for 3 days. Serum was taken from mice in the fed state or after a 24 hr fast as indicated. (n=4 mice per group) *p<0.05; **p<0.01. Oil Red-O stained liver sections (C) from fasted *Pparα*$^{-/-}$ mice administered either FGF21 or vehicle is shown. Scale bar = 40µm. (Measurements made by T. Inagaki; Histology by UTSW Histology Core)

2.3 FGF21 induces Lipolysis

Carnitine palmitoyltransferase 1a (CPT1a) and 3-hydroxy-3-methyglutaryl-CoA synthase 2 (HMGCS2) mediate important steps in ketogenesis and are transcriptionally regulated by PPARα in the starvation response. Although CPT1a and HMGCS2 mRNA levels were not changed in the *Fgf21* transgenic, their protein concentrations were found to be increased in the liver (Figure 2.4A). These data suggest that FGF21 may regulate the protein levels of these proteins by modification of their posttranslational regulatory mechanism to enhance ketogenesis. To gain insight into how FGF21 regulates ketogenesis, microarray experiments were performed using mRNA from livers of wild-type and *Fgf21* transgenic mice. No increase in typical PPARα target genes was observed, but increases in mRNAs encoding several pancreatic lipases, including pancreatic lipase (*Pnlip*), pancreatic lipase-related protein 2 (*Pnliprp2*), carboxy ester lipase (*Cel*), and pancreatic co-lipase (*Clps*). The expression of these genes is typically found at very low levels in the liver. RT-qPCR confirmed these genes were induced in *FGF21* transgenic mice, *Pparα*$^{-/-}$ mice infected with FGF21 expressing adenovirus, 12 hr fasted wild-type mice, and wild-type mice administered the PPARα ligand Wy14,643 for 5 days (Figure 2.4B-E).

Histology of the *Fgf21* transgenic adipose tissue showed smaller adipocytes compared to wild-type mice (Kharitonenkov et al., 2005) (Figure 2.5A), suggesting that FGF21 may regulate lipase expression in the WAT. Although *Pnlip*, *Pnliprp2*, *Cel* and *Clps* mRNAs were modestly upregulated in the WAT from *Fgf21* transgenic mice, no increase was observed in the WAT from *Pparα*$^{-/-}$ mice infected

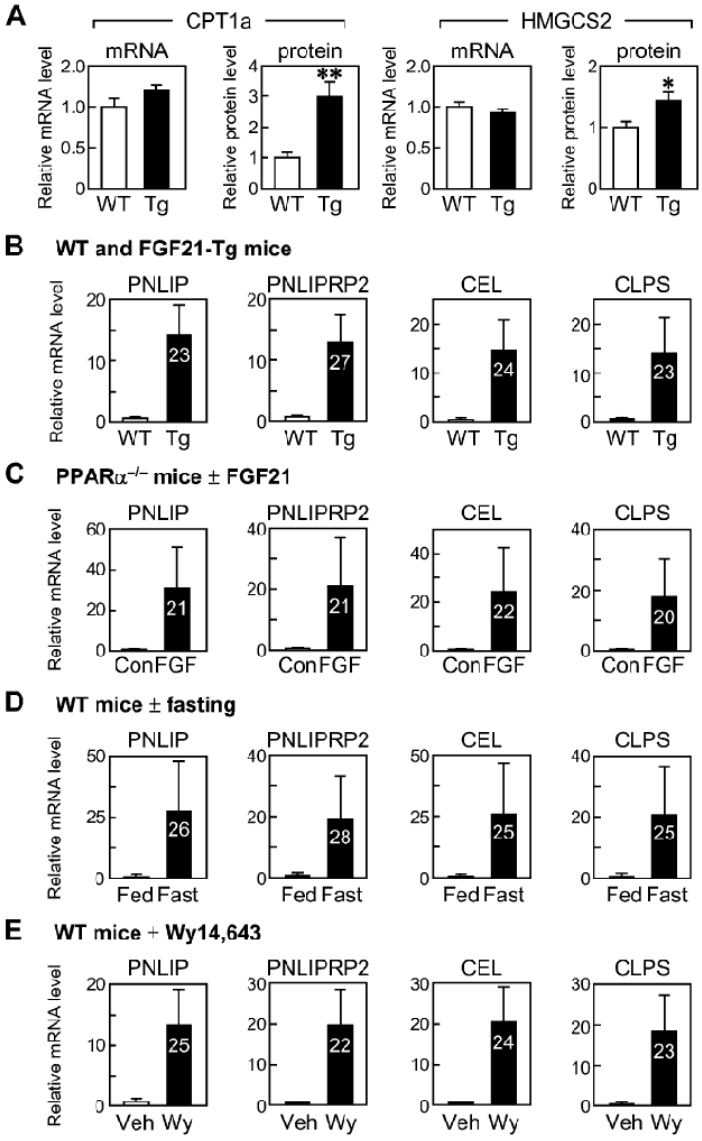

Figure 2.4 FGF21 Induces Ketogenic Enzymes and Lipases in Liver

(A) CPT1a and HMGCS2 mRNA and protein concentrations in livers from fed wild-type (WT) and *Fgf21* transgenic (Tg) mice were measured by RT-qPCR and western blot analysis, respectively. Western data for individual mice are shown in Figure S2. (n = 4 mice per group.) *p < 0.05; **p < 0.01. (B–E) Pancreatic lipase (PNLIP), pancreatic lipase-related protein 2 (PNLIPRP2), carboxyl ester lipase (CEL), and pancreatic colipase (CLPS) mRNA levels were measured by RT-qPCR in livers from WT and Tg mice (B), *Pparα*$^{-/-}$ mice infected with either control (Con) or FGF21-expressing (FGF) adenoviruses for 5 days (C), WT mice either fed ad libitum or after a 12 hr fast (D), and WT mice administered vehicle (Veh) or the PPARa agonist Wy14,643 (Wy; 0.1% in chow) for 5 days (E). (n = 4–5 mice per group.) Average Ct values are indicated on the bars. (Lipase Analysis by T.Inagaki)

with FGF21-expressing adenovirus. However, levels of mRNAs encoding hormone sensitive lipase (*Hsl*) and adipose triglyceride lipase (*Atgl*) were increased in *Fgf21* transgenic mice, *Pparα*$^{-/-}$ mice infected with FGF21-expressing adenovirus, and wild-type mice administered Wy14,643 (Figure 2.5B). A corresponding increase in HSL and ATGL protein was also observed in the *Fgf21* transgenic (Figure 2.5B). The increased lipase expression, smaller adipocytes and elevated serum free fatty acid concentrations were consistent with increased lipase activity.

To examine whether FGF21 induces lipolysis directly, glycerol release was measured in differentiated 3T3L1 adipocytes treated with either FGF21 or the β-adrenergic receptor agonist isoproterenol. As expected, isoproterenol caused a time-dependent increase in glycerol release into the media (Figure 2.5F). Importantly, FGF21 also stimulated glycerol release, albeit at reduced efficacy compared to isoproterenol (Figure 2.5F). The 0.5 nM concentration of FGF21 used in the assays were saturating for lipolysis as determined by dose-response analysis. Thus, FGF21 can stimulate lipolysis in adipocytes as determined by glycerol release assays. Western blot analysis was used to examine the effect of FGF21 and isoproterenol on known post-translational modifications of HSL in a time course study using differentiated 3T3L1 adipocytes. FGF21 treatment caused a slight phosphorylation at Ser563 of HSL in a similar time dependent manner as isoproterenol, albeit to a significantly lesser extent (Figure 2.6A). In contrast, FGF21 did not increase Ser660 phosphorylation, whereas isoproterenol stimulated a robust phosphorylation at this residue. Phosphorylation at Ser565 was unchanged in either treatment group.

Therefore, the slight increase in phosphorylation at Ser563 may enhance the activity of the enzyme to increase basal lipolytic rates, *in vitro* (Stralfors and Belfrage, 1983). Cotreatment of 0.5 nM FGF21 and 5 nM isoproterenol did not result in any additional stimulation of lipolysis above isoproterenol treatment alone (Figure 2.6B), suggesting the compounds may act though a common pathway, such as HSL. No increase in HSL or ATGL mRNA levels was observed in the short term (4 hour) FGF21 treatment studies *in vitro*, suggesting that *in vivo* results may be part of an adaptive response to longer-term FGF21 exposure, or subsequent metabolic or hormonal changes that occur in the context of a whole animal may originate from other FGF21 target tissues, including the brain and brown adipose tissue. In the context of Chapter 3, the increased expression of HSL and ATGL may result from enhanced differentiation of the adipocytes within the transgenic tissue since mature adipocytes acquire an enhanced capacity to both store and breakdown triglycerides (Kershaw et al., 2007).

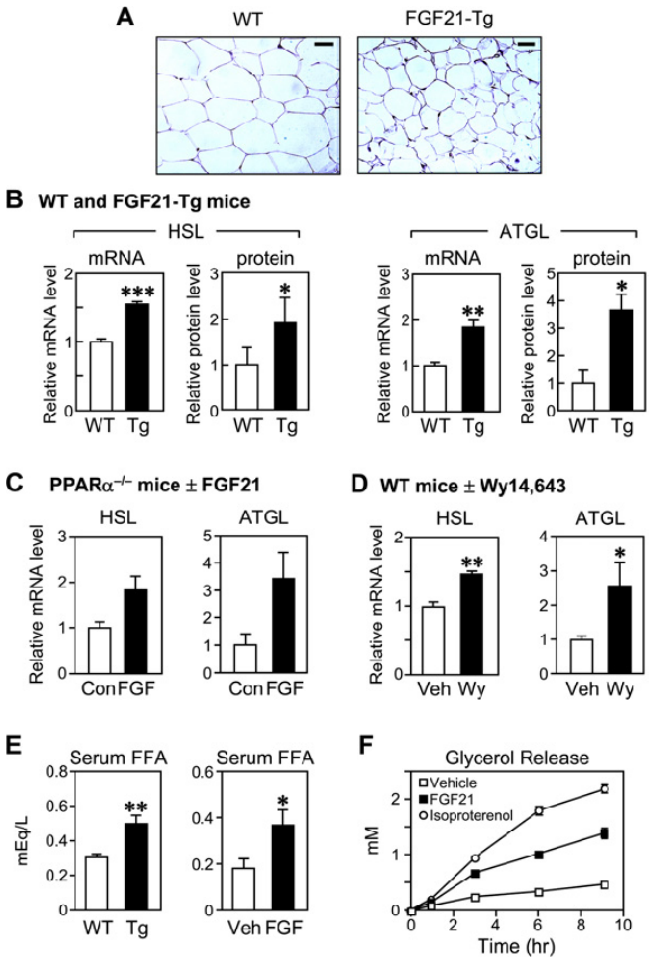

Figure 2.5 FGF21 Induces Lipolysis in White Adipose Tissue.

A) Hematoxylin and eosin-stained sections of epididymal white adipose tissue (WAT) from wild-type (WT) and *Fgf21* transgenic (Tg) mice. Scale bars = 40 mm.
B) Hormone-sensitive lipase (HSL) and adipose triglyceride lipase (ATGL) mRNA and protein concentrations in epididymal WAT from fed WT and Tg mice were measured by RT-qPCR and western blot analysis. (n = 4 mice per group.) *p < 0.05; **p < 0.01; ***p < 0.001.
C-D.) HSL and ATGL mRNAs were measured by RT-qPCR in epididymal WAT from *Ppara*$^{-/-}$ mice infected with either control (Con) or FGF21-expressing (FGF) adenovirus for 5 days (C) and WT mice administered vehicle (Veh) or the PPARa agonist Wy14,643 (Wy; 0.1% in chow) for 5 days (D). (n = 4 mice per group.) *p < 0.05; **p < 0.01.
E) Serum free fatty acid concentrations were measured in fed WT and Tg mice (left panel) or WT mice injected with FGF21 (FGF; 0.75 mg/kg/day, subcutaneous) or vehicle alone (Veh) for 3 days (right panel). (n = 4mice per group.) *p < 0.05; **p < 0.01. Measurement by T. Inagaki.
F) Glycerol release was measured from 3T3L1 adipocytes treated with vehicle, 0.5nM FGF21, or 5nM isoproterenol for the indicated times. Assays were performed in triplicate.

A

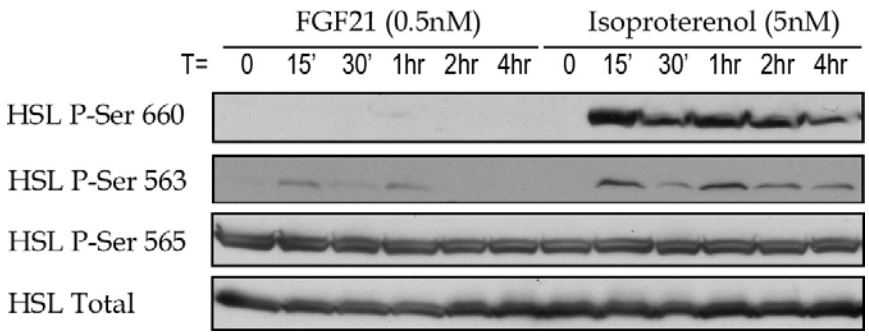

B

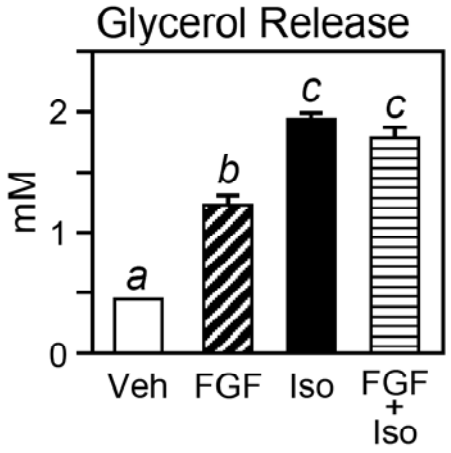

Figure 2.6 Activation of HSL in 3T3L1 Adipocytes.

A) 3T3L1 adipocytes were serum starved and treated with FGF21 (0.5nM) or Isoproterenol (5nM) over a 4 hours time course. Western blots were performed against HSL P-Ser660, HSL P-Ser563, HSL P-Ser565 and total HSL.
B) Glycerol release was measured in media from 3T3L1 adipocytes treated for 6 hours with FGF21, isoproterenol or both. Data are the mean and S.E. of assays performed in triplicate. Different lowercase letters indicate statistical significance ($p<0.05$) as determined by one-way ANOVA.

2.4 FGF21 enhances Torpor

Since FGF21 induced the expression of lipase genes that are associated with torpor (Zhang et al., 2006), telemeters were implanted into wild-type and *Fgf21* transgenic mice to determine the effect of elevated FGF21 expression on body temperature. Basal core body temperature of the *Fgf21* transgenic mice was consistently 1˚C to 2˚C lower that the wild-type mice (Figure 2.7A). Importantly, during a 24 hr fast, *Fgf21* transgenic mice entered a state of torpor, the rodent equivalent of hibernation, by reducing their body temperature and decreasing their locomotion (Figure 2.7A). A similar effect was observed in wild-type mice infected with the FGF21-expressing adenovirus compared to a control adenovirus (Figure 2.7B). To determine if conditions that induce the expression of endogenous FGF21 effected core body temperature, wild-type mice were treated with PPARα agonist Wy14,643 or vehicle. PPARα agonist reduced both basal and fasting-body temperature, but also reduced food intake, complicating the interpretation of the results (Figure 2.7C).

Decreased leptin expression or function has been associated with torpor phenotype in rodents (Gavrilova et al., 1999). Serum leptin concentrations were determined to be significantly lower in 6 month old *Fgf21* transgenic mice compared with wild-type mice, both male and female (Kharitonenkov et al., 2005) (Figure 2.8A). RT-qPCR confirmed leptin mRNA is reduced in the WAT of fed *Fgf21* transgenic mice compared to wild-type (Figure 2.8B). This is consistent with my observation that 3T3L1 adipocytes treated with 5nM FGF21 caused a >2-fold repression of *Leptin* mRNA within a 2 hour period, suggesting that leptin is regulated

in an FGF21-dependent manner. To determine if leptin replacement in the *Fgf21* transgenic mice is able to prevent the fasting induced reduction in body temperature as a result of starvation, Alzet® osmotic pumps were used to deliver a continuous dose of leptin in *Fgf21* transgenic and wild-type mice that were implanted with telemeters. Intriguingly, exogenous leptin raised fed-state body temperature of the *Fgf21* transgenic mice by 1-2˚C. Unexpectedly, leptin treatment exacerbated the torpor response in *Fgf21* transgenic mice, producing a 4-5˚C further decrease in body temperature in the *Fgf21* transgenic mice (Figure 2.8C-D). At the endpoint of the experiment, leptin concentration in the *Fgf21* transgenic mice was slightly lower compared to wild-type mice in spite of exogenous dosing with the mini-pump (Figure 2.8E). *Fgf21* transgenic mice may have enhanced leptin clearance rates since they have significantly elevated expression of Ob-Rb, the leptin receptor, in the liver. Collectively, these data suggest that *FGF21* sensitizes mice to the fasting induced torpor by a leptin-independent mechanism. The dramatic drop in body temperature in the fasted *Fgf21* transgenic mice may be due to a lack physical activity, lack of nutrient availability for non-shivering-dependent thermogenesis, or the smaller size of these animals compared to age matched wild-type mice. It is worth noting that treatment of wild-type mice by intraperitoneal injection of FGF21 was found to decrease plasma leptin levels in an inconsistent manner. As discussed in Chapter 3, the dynamic regulation of FGF21 expression in the liver and WAT may confound the pharmacological results since injections may not have been given at the optimal time of the day to observe a consistent effect. As such, FGF21 may only impact leptin expression *in vivo* at a specific period of the day or a particular nutritional state of the mouse. This remains to be characterized.

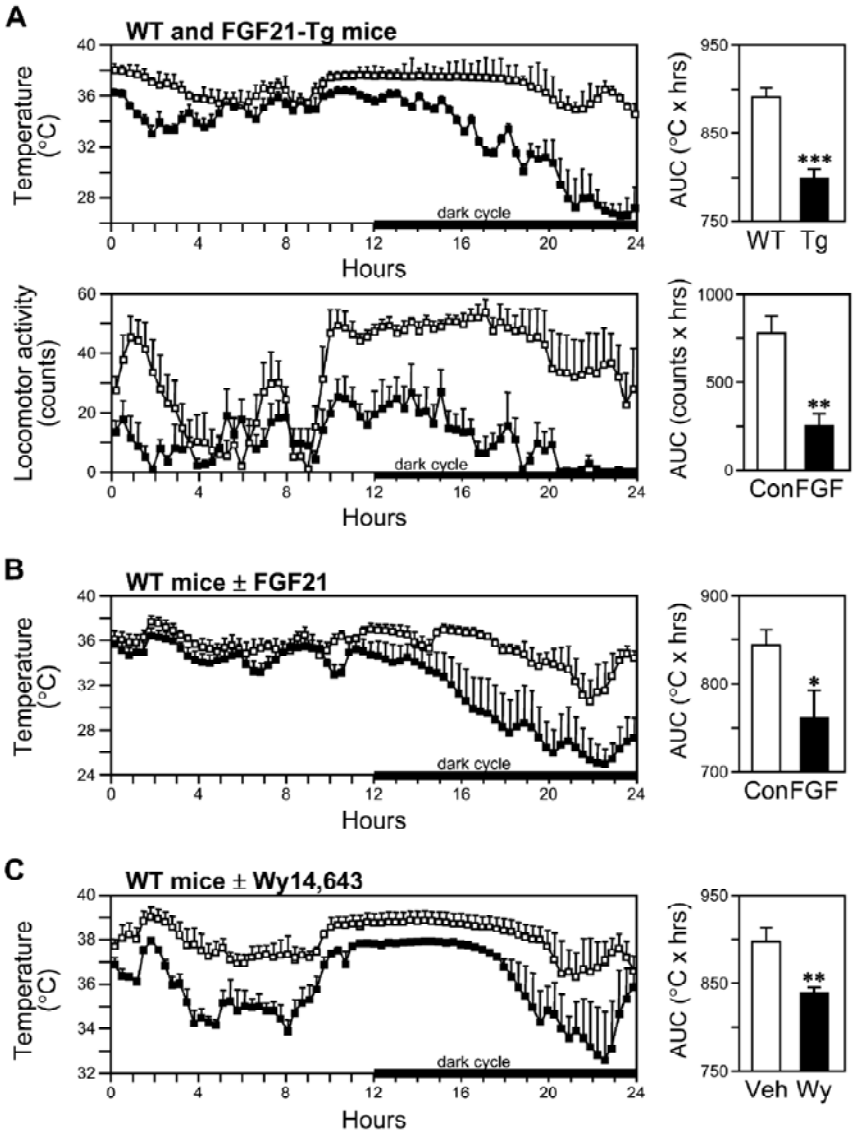

Figure 2.7 FGF21 Stimulates Torpor

Core body temperature was measured by telemetry in wild-type (WT) mice (open symbols) and *Fgf21* transgenic (Tg) mice (closed symbols) fasted for 24 hr ([A], top panel), WT mice infected with a control adenovirus (open syrmbols) or an FGF21-expressing adenovirus (closed symbols) for 5 days (B), and WT mice treated with vehicle (open symbols) or Wy14,643 (0.1% in chow; closed symbols) for 5 days prior to initiating a 24 h fast (C). In the bottom panel of (A), locomotor activity was measured during the 24 hr fast. (n = 4 miceper group.) For each experiment, the area under the curve (AUC) for body temperature or locomotor activity during the entire 24 hr period was calculated using GraphPad Prism software.*$p < 0.05$; **$p < 0.01$; ***$p < 0.001$. (Telemetry by T. Inagaki)

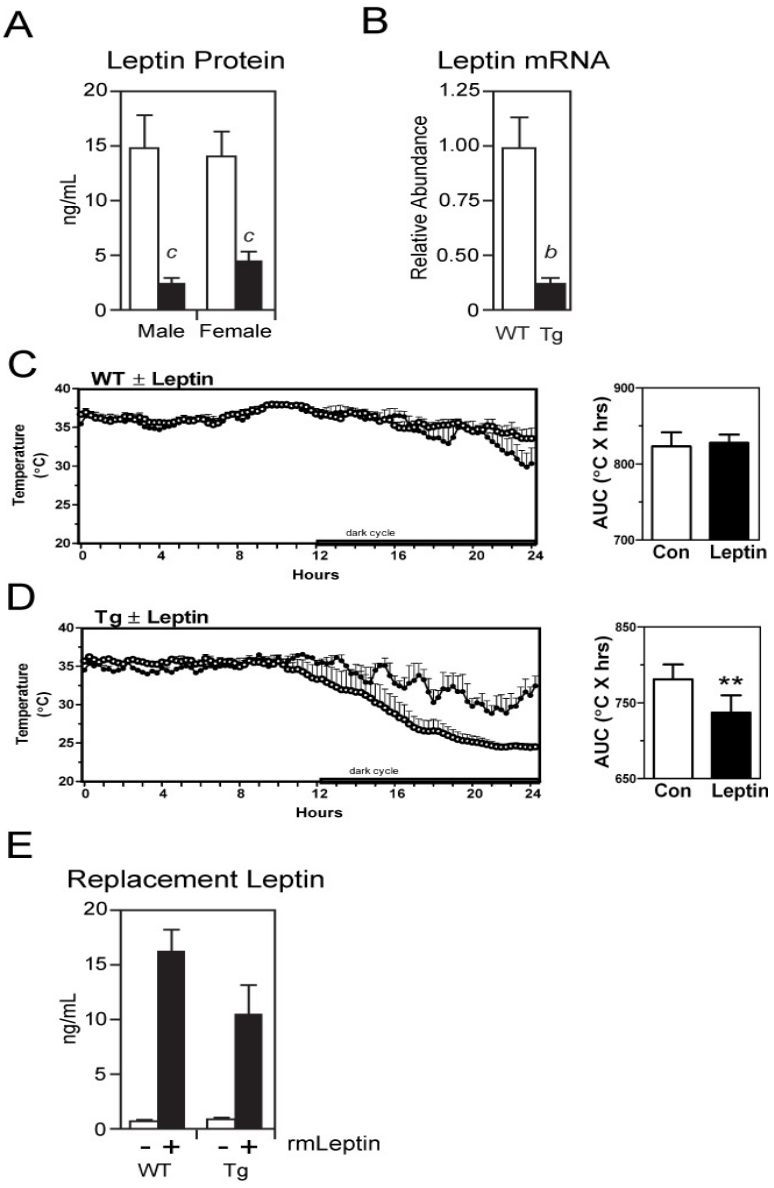

Figure 2.8 FGF21 Stimulated Torpor is Enhanced by Leptin

(A) Circulating leptin concentration was determined in fed 6-month old wild-type and *Fgf21* transgenic male and female by ELISA. (B) RT-qPCR was used to measure leptin mRNA in the WAT of male mice. (C) Core body temperature was measured by telemetry in vehicle treated (closed symbols) and leptin treated (open symbols) wild-type and *Fgf21* transgenic mice fasted for 24 hr. For each telemetry experiment, the area under the curve (AUC) for body temperature during the entire 24 hr period was calculated using GraphPad Prism software. $^{**}p<0.01$ (D) Circulating leptin concentration was measured in leptin and vehicle treated wild-type and *Fgf21* transgenic mice at the end of the 24-hour fast by ELISA.

CHAPTER 3

FGF21 as an Autocrine/Paracrine Factor in the Fed State

3.0 Introduction

Following the report that FGF21 is expressed in the liver in a PPARα dependent manner, several lines of evidence emerged to suggest that FGF21 had biological effects beyond hepatic ketogenesis and the fasting condition. The activation of FGF21 expression in cultured adipocytes and adipose tissue by PPARγ ligands suggested that FGF21 may be important in the fed state (Muise et al., 2008; Wang et al., 2008). As discussed in Chapter 1, several similar effects of pharmacological FGF21 and thiazolidinediones treatments indicated that FGF21 may contribute to the downstream effect of PPARγ activation. Initial characterization of the gene expression profile of our *Fgf21* transgenic mice revealed a robust increase in lipogenic gene expression in the white adipose tissue (WAT), a hallmark of PPARγ activation, but no change in the liver (Figure 3.1A-B). In addition, *Fgf21* transgenic mice expressed elevated levels of *11bHsd1* mRNA and reduced amounts of *11bHsd2* in the adipose indicating the higher localized production of corticosterone, a pro-adipogenic steroid (Figure 3.1C). Analysis of protein lysates from the *Fgf21* transgenic mice confirmed elevated expression of FASN, indicating an enhanced capacity for lipogenesis. My model that FGF21 is a fed state autocrine/paracrine factor that regulates PPARγ function in the adipose tissue is developed in the following studies.

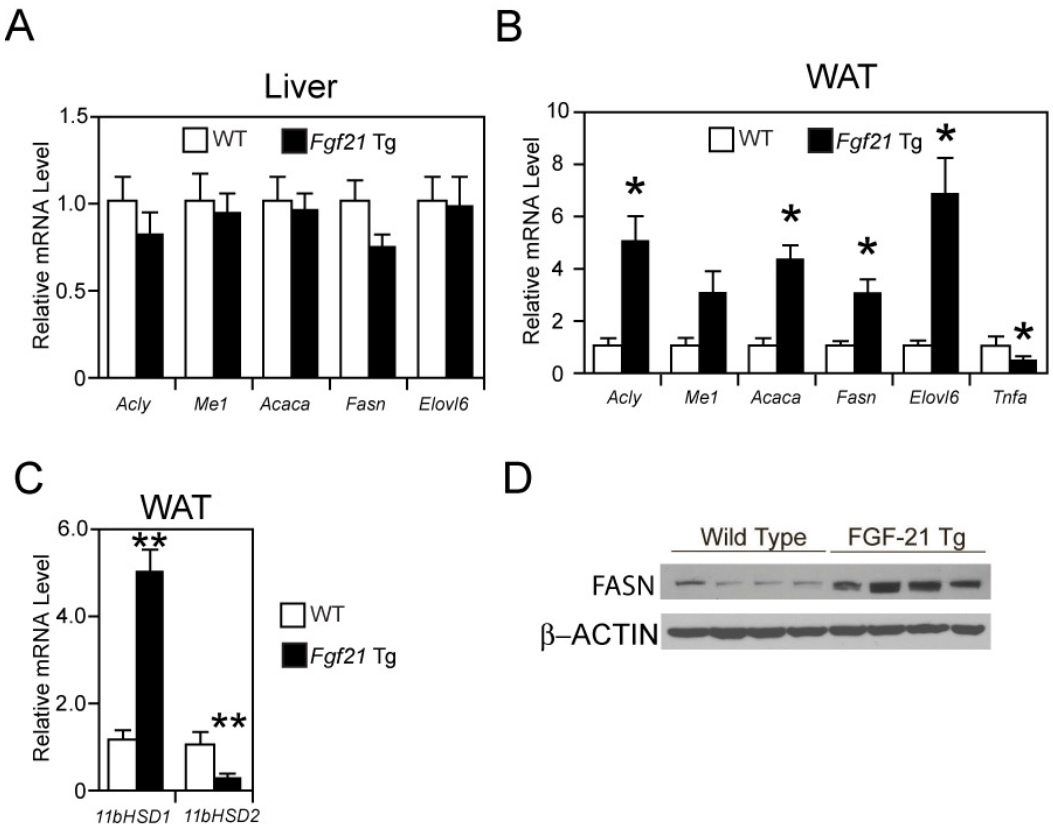

Figure 3.1 Lipogenic Gene Expression in *Fgf21* Transgenic Mice.

RT-qPCR was used to measure the expression of ATP citrate lyase (*Acly*), malic enzyme (*Me1),* acetyl-CoA carboxylase α (*Acaca*), fatty acid synthase (*Fasn*), and fatty acid elongase-6 (*Elovl6)* in the (A) liver and (B) WAT of wild-type and *Fgf21* transgenic mice. (C) Expression of *11bHSD1* and *11bHSD2* were measured by RT-qPCR in the WAT of wild-type and *Fgf21* transgenic mice. (D) FASN was measured in the WAT of wild-type and *Fgf21* transgenic mice by western blot, with β-ACTIN as a load control. *p0.05; **p<0.01

3.1 FGF21 Regulation in Adipose Tissues

Previous studies showed that FGF21 is induced by rosiglitazone in WAT of wild-type and *db/db* mice (Muise et al., 2008). Since PPARα was shown to regulate the expression of *Fgf21* mRNA in the liver as part of the fasting response, we tested the ability of PPAR ligands to regulate the expression of *Fgf21* in WAT and liver with a short term treatment of either PPARα agonist (GW7647), or PPARγ agonist (rosiglitazone) over one day. Consistent with previous observations, FGF21 is induced by rosiglitazone in WAT but not liver of wild-type mice (Figure 3.2A). Conversely, FGF21 was induced by the PPARα agonist, GW0742, in liver but not WAT (Figure 3.2B). Although rosiglitazone treatment increased FGF21 concentrations in WAT, it did not increase FGF21 levels in serum like PPARα ligand (Figure 3.2C-D). These data suggest that FGF21 produced in WAT functions in an autocrine or paracrine manner. To determine if FGF21 is induced in the WAT by diet, *Fgf21* mRNA levels were measured at 4 hour intervals in the epididymal WAT and liver from mice that were restricted to feeding during a 4 hour period in the middle of the dark cycle. As expected *Fgf21* mRNA expression was highest in the liver prior to feeding, when the mice were in the most fasted state (Figure 3.2E). In contrast, *Fgf21* mRNA expression was significantly induced 4 hours after eating to an absolute level that was comparable to that of the fasted liver (Figure 3.2E) and returned to basal levels 8 hours after food was removed from the cages. These data suggested a unique function for *Fgf21* within the adipose tissue, and indicated that FGF21 is part of the feeding response in the adipose tissue.

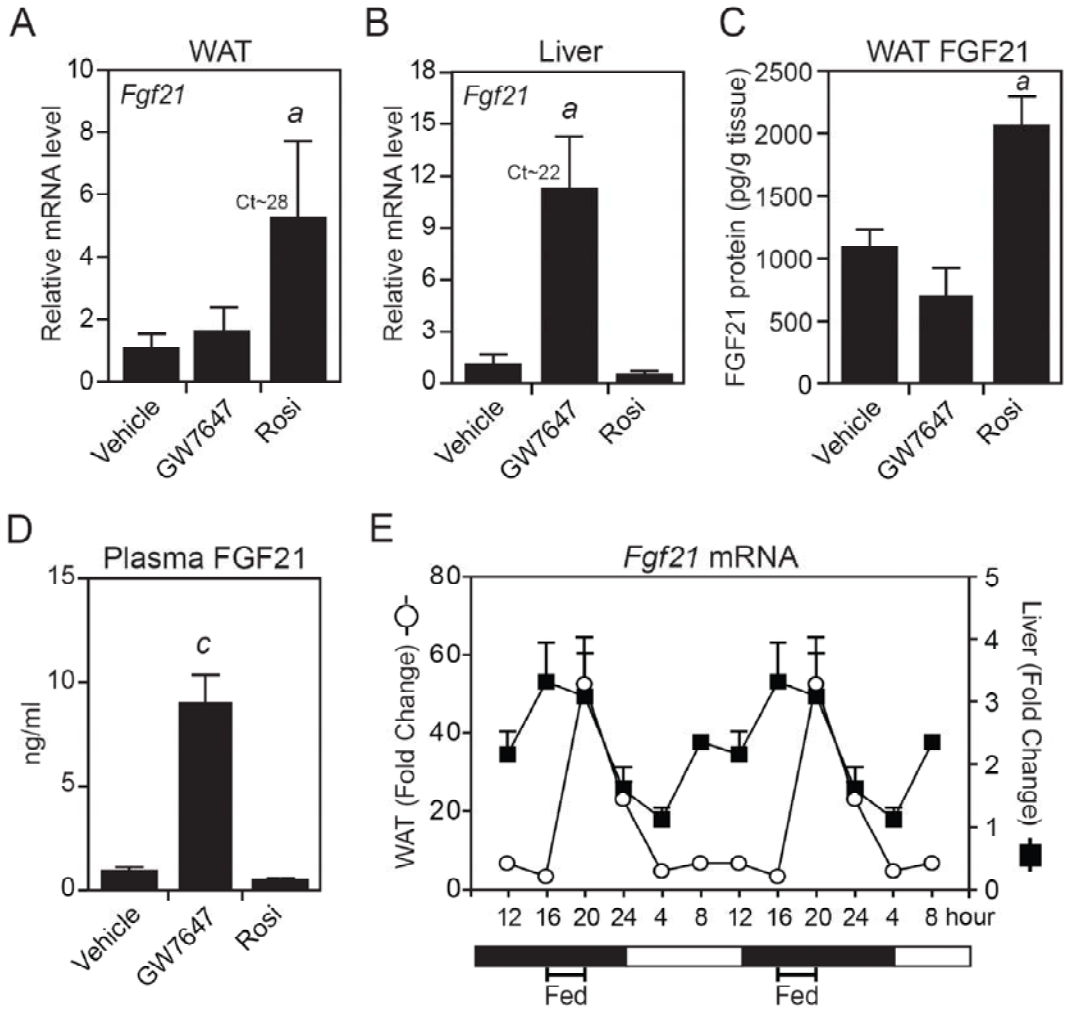

Figure 3.2 *In vivo* Regulation of FGF21 Expression.

(A-D) 2 month old mice were gavaged over one day with GW7647 (10 mg/kg), rosiglitazone (rosi; 10 mg/kg) or vehicle (1% methycellulose). FGF21 mRNA in epididymal WAT (A) and liver (B) was measured by RT-qPCR. FGF21 protein in WAT (C) and plasma (D) was measured by ELISA. n=4/group.
(E) Mice were food-entrained for 2 weeks by restricting their access to chow to a 4 hour period in the middle of the dark cycle. Tissues were collected at 4 hour intervals over a 24 hour period and FGF21 mRNA was analyzed by RT-qPCR. Data are double plotted (n=6/group).
Error bars represent the mean ± SEM. *a*, $P<0.05$ vs vehicle; *b*, $P<0.01$ vs vehicle

3.2 *Fgf21*$^{-/-}$ Mice Display Mild Lipodystrophy

The high level of FGF21 expression in the WAT during the fed state suggested that the *Fgf21*$^{-/-}$ mice might display an adipose phenotype. Body composition was analyzed in 2-month old wild-type and *Fgf21*$^{-/-}$ mice using the Bruker Minispec mq10. *Fgf21*$^{-/-}$ mice had a slight decreased in body mass, a statistically significant decrease in fat mass, a statistically significant increase in lean mass, and no change in fluid mass (Figure 3.3A-D). The difference in body fat and lean mass that was observed in 2-month old mice was found to be exaggerated in mice that were measured at 6-months of age. Consistent with these findings, *Fgf21*$^{-/-}$ mice had reduced eWAT:body mass ratio (Figure 3.3E), but no difference in the DNA content of the eWAT between the wild-type and *Fgf21*$^{-/-}$ mice (Figure 3.3F). These data suggest that decreased adiposity of the *Fgf21*$^{-/-}$ is a consequence of smaller adipocytes rather than a decrease in adipocyte number. This difference in adipocyte size was confirmed by histomorphometry (Figure 3.3G-H). Although it was previously reported by Hotta *et al.* (2009) that FGF21$^{-/-}$ mice had larger white adipocytes than wild-type mice, the reason for this discrepancy is unknown but might be a consequence of their different diet.

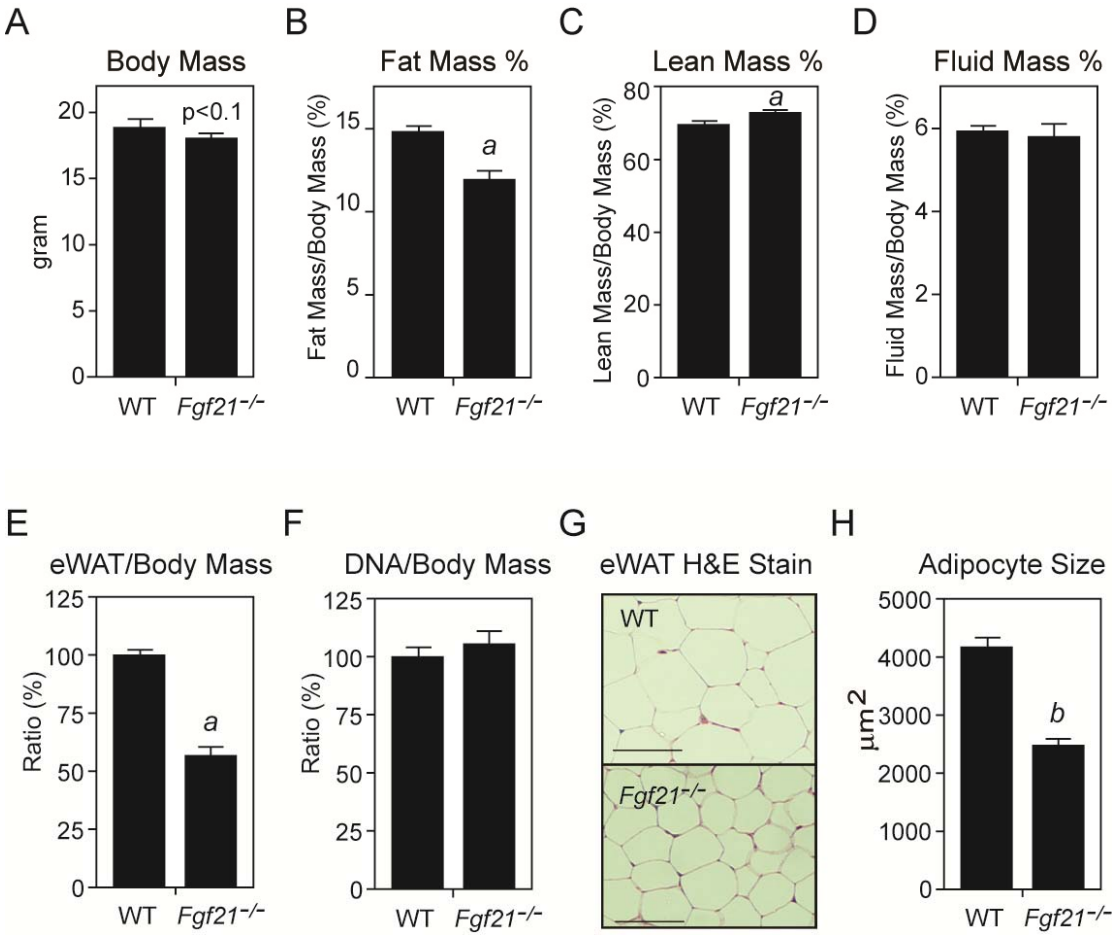

Figure 3.3 Phenotypic Analysis of the *Fgf21*$^{-/-}$ Mouse.

(A-D) Body mass, fluid, fat and lean composition of 2-month WT and *Fgf21*$^{-/-}$ mice was measured using the Bruker Minispec mq10 NMR (n=11-12, respectively). (E) eWAT pads were removed and weighted to determine the eWAT to body mass ratio and (F) DNA content of the eWAT pads were isolated, quantified by spectrometry (A_{260} O.D.), and used to calculate the DNA/body mass ratio (N=4 per group). (G-H) eWAT pads were sectioned, stained with hematoxylin and eosin, and a series of images were analyzed using ImageJ Version 1.44p software to determine the size of the adipocytes (scale bar = 100µm; n> 150 cells per group).
a p<0.01; *b* p<0.001.

3.3 FGF21 Stimulates Adipocyte Differentiation and Lipid Accumulation

To determine if FGF21 functioned in the adipose tissue in a cell autonomous manner, we examined the differentiation of preadipocytes derived from P4 wild-type and *Fgf21*$^{-/-}$ mice. Prior to differentiation, FGF21 mRNA levels were low but detectable in the wild-type cells (Figure 3.4A). *Fgf21* mRNA expression decreased after contact inhibition (day 0), but then increased steadily during the 8 day differentiation protocol. Importantly, the mRNA encoding βklotho (*Klb*), the essential cofactor for FGF21 signaling, was undetectable until day 4 of the differentiation protocol and increased throughout the differentiation period (Figure 3.4A). *Klb* mRNA expression was reduced in the *Fgf21*$^{-/-}$ along the time course, but was increased by the addition of recombinant FGF21 to the differentiation medium (Figure 3.4A). Expression of *Fgfr1c*, which encodes the other subunit of the FGF21 receptor, decreased during the early stages of differentiation and was unaffected by the absence of FGF21 (Figure 3.4A). These data suggest that autocrine effects of FGF21 signaling are established during the intermediate stage of adipocyte differentiation from days 2 to 4 and indicate that FGF21 could function to stimulate late stage development and establish the mature adipocyte.

We next examined a panel of genes that are temporally regulated along the process of adipocyte differentiation. The temporal pattern and absolute expression of C*ebpβ* and *Cebpδ*, which play important roles in the early stages of adipocyte differentiation, was similar between with wild-type and *Fgf21*$^{-/-}$ cells, and unaffected

by treatment with recombinant *Fgf21* (Figure 3.4A). In contrast the induction of *Cebpα* and *PPARγ* mRNA was delayed in the *Fgf21*$^{-/-}$ adipocytes but partially restored in the presence of recombinant FGF21. Additionally, the mRNAs encoding the fatty acid binding protein *(aP2*) and the lipogenic proteins solute carrier family 25, member 1 (*Slc25a1*), acetyl-CoA carboxylase α (*Acaca*), fatty acid synthase (*Fasn*), ATP citrate lyase (*Acly*), malic enzyme (*Me1*) and diacylglycerol-transferase 2 (*Dgat2*) had similar expression patterns: the level of each was reduced in *Fgf21*$^{-/-}$ adipocytes and either partially or fully restored by treatment with recombinant FGF21 (Fig. 3.4A). Remarkably, the expression of late genes was first found to be reduced in the *Fgf21*$^{-/-}$ cells at day 4 of differentiation, which is consistent with the time *Klb* expression first appears in wild-type adipocytes (Figure 3.4A). Phosphoenolpyruvate carboxykinase (*Pck1*) was induced only at day 8 of differentiation, and was expressed at ~50% the amount in *Fgf21*$^{-/-}$ adipocytes relative to wild-type, and partially restored by recombinant FGF21 (Figure 3.4.A). In agreement with the lipogenic gene expression data, lipid accumulation was reduced in the *Fgf21*$^{-/-}$ adipocytes and restored to wild-type levels in the presence of recombinant FGF21, as determined by Oil Red-O lipid stain (Figure 3.4B).

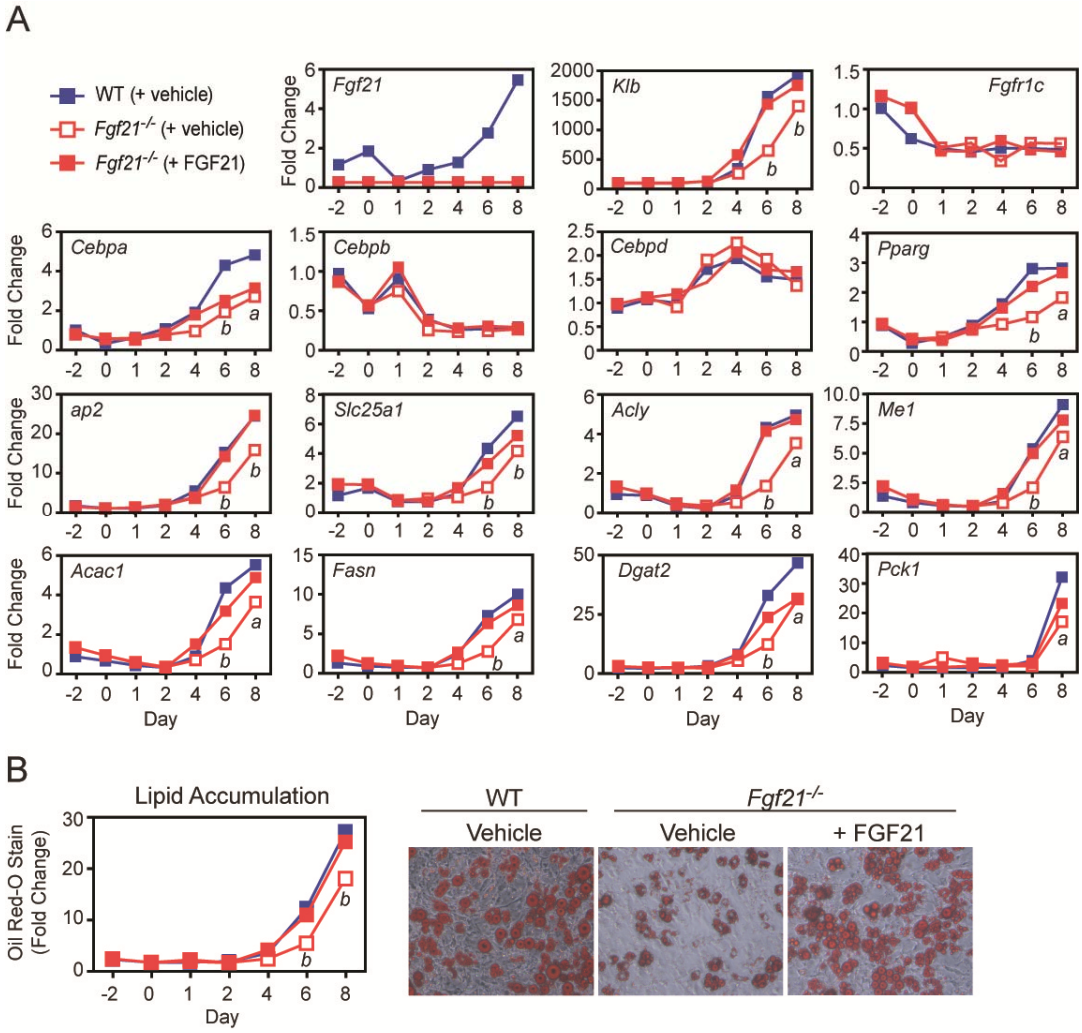

Figure 3.4 *Fgf21*$^{-/-}$ Adipocytes have Altered Gene Expression and Lipid Accumulation.

Primary preadipocytes were isolated from P4 WT and *Fgf21*$^{-/-}$ mice and differentiated *in vitro* over an 8-day period, in the presence of exogenous FGF21 (200ng/ml) or vehicle. (A)RT-qPCR was used to measure the expression of adipocyte markers and lipogenic genes over the differentiation period. (B) Lipid accumulation was monitored by Oil Red-O staining and a representative image of Oil Red-O stained WT and *Fgf21*$^{-/-}$ cells at day 8 is shown. Error bars represent the mean ± SEM. *a*, $P<0.05$ vs WT; *b*, $P<0.01$ vs WT.

3.4 FGF21 enhances PPARγ Transcriptional Activity.

The impaired differentiation and lipid accumulation of in the *Fgf21*$^{-/-}$ adipocytes suggested that FGF21 might be a regulator of PPARγ activity. My experiments to analyze the direct effect of FGF21 on PPAR response element driven luciferase expression demonstrated that standard luciferase reporter assays using HEK293 cells were not a viable option. HEK293 cells were transfected with *Klb*, to allow FGF21 signal transduction, and exogenous PPARγ. Using this approach, I found that FGF21 treatment stimulated the gene promoters of the transfected constructs, making valid comparison to vehicle treatment not feasible. Moreover, gene transfer into mature adipocytes for this purpose was not efficient by transfection or electroporation. Therefore, to examine the direct effect of FGF21 on PPARγ target genes expression *in vitro*, wild-type and *Fgf21*$^{-/-}$ cells were differentiated in the presence or absence of the PPARγ ligand, rosiglitazone. As expected, rosiglitazone markedly increased lipogenic gene expression and lipid accumulation in the wild-type adipocytes (Figure 3.5A-B). These effects were attenuated in the *Fgf21*$^{-/-}$ adipocytes, whereas the inclusion of recombinant FGF21 rescued the effect of rosiglitazone on gene expression and lipid accumulation (Figure3.5A-B).

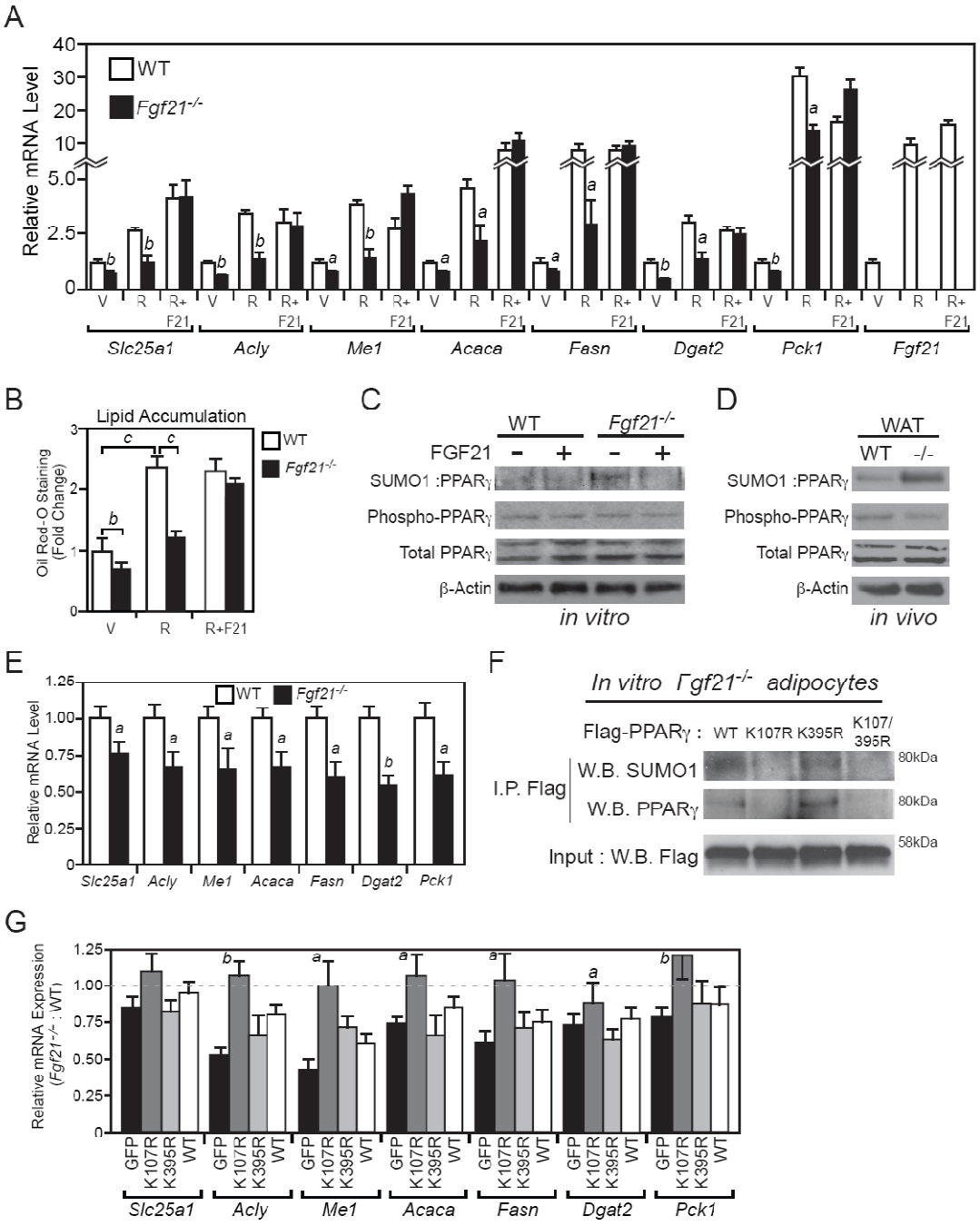

Figure 3.5. *Fgf21*$^{-/-}$ Adipocytes Have Defective PPARγ Function.

Figure 3.5. continued.

(A-B) Stromal vascular fraction preadipocytes from wild-type (WT) and *Fgf21*$^{-/-}$ mice were differentiated for 8 days in the presence of 0.5 μM rosiglitazone (R), 0.5 μM rosiglitazone + 100 ng/ml FGF21 (R+F21), or vehicle (V). Gene expression was measured by RT-qPCR (A). Lipid accumulation was measured by Oil Red O staining (B). Error bars represent the mean ± SEM. *a*, $P<0.05$; *b*, $P<0.01$; *c*, $P<0.005$.

(C) Sumoylated PPARγ, Ser-112 phosphorylated PPARγ and total PPARγ protein levels were measured in WT and *Fgf21*$^{-/-}$ adipocytes differentiated for 8 days and treated with vehicle or FGF21 (100 ng/ml) for 4 hour prior to harvest. Sumoylated PPARγ was detected by immunoprecipitation with a SUMO1 antibody followed by immunoblotting with a PPARγ antibody. Phosphorylated and total PPARγ and β-actin were detected by immunoblotting.

(D) Sumoylated PPARγ, Ser-112 phosphorylated PPARγ and total PPARγ protein levels were measured as in (C) in epididymal WAT from WT and *Fgf21*$^{-/-}$ mice killed in the fed state.

(E) Gene expression was measured by RT-qPCR in the epididymal WAT of WT and *Fgf21*$^{-/-}$ mice killed during the fed state (n=6-7/group). Error bars represent the mean ± SEM. *a*, $P<0.05$ vs WT; *b*, $P<0.01$ vs WT.

(F) FLAG-tagged PPARγ2, PPARγ2-K107R or PPARγ2-K395R were expressed in primary *Fgf21*$^{-/-}$ adipocytes and their sumoylation measured by immunoprecipitation with a Flag antibody followed by immunoblotting with either a SUMO1 or PPARγ antibody. Input levels of Flag-tagged PPARγ and the PPARγ mutants were determined by immunoblotting with a Flag antibody.

(G) Gene expression was measured by RT-qPCR in WT and *Fgf21*$^{-/-}$ in stromal vascular fraction preadipocytes transduced with lentiviruses expressing PPARγ2, PPARγ2-K107R, PPARγ2-K395R or GFP control and differentiated for 8 days. Data are plotted as relative mRNA expression in *Fgf21*$^{-/-}$ adipocytes compared to wild-type adipocytes. Error bars represent the mean ± SEM. *a*, $P<0.05$ vs GFP; *b*, $P<0.01$ vs GFP.

To investigate the mechanism by which FGF21 regulates PPARγ function, we sought to characterize the expression and post-translational modifications of the receptor in the wild-type and *Fgf21*$^{-/-}$ cells. Although FGF21 treatment had been shown to increase PPARγ concentrations in 3T3L1 adipocytes over a treatment period of 72 hours, the experiments in this reference did not have the necessary vehicle controls (Moyers et al., 2007). As PPARγ expression is known to increase over the differentiation course of preadipocytes into mature adipocytes, it was not surprising to see an increase in PPARγ in their study. My western blot analysis showed that PPARγ expression is similar between wild-type and *Fgf21*$^{-/-}$ cells at day 8 using a standard differentiation protocol. Likewise, there was no change in the level of phosphorylated PPARγ (Ser112) under these conditions (Figure 3.5C). Notably, there was an increase in the SUMOylation of PPARγ in the FGF21$^{-/-}$ adipocytes (Figure 3.5C). This increase in PPARγ SUMOylation was reversed by the addition of FGF21 to the *Fgf21*$^{-/-}$ cells (Figure 3.5C). Consistent with differentiated primary adipocytes, differentiated 3T3L1 adipocytes cultured in high glucose media in the presence of insulin and without fetal bovine serum, also showed reduced PPARγ SUMOylation when FGF21 was included in the media for 4 hours, yet no change in global SUMOylation status. Therefore, 3T3L1 cells may be a useful *in vitro* tool to characterize the signaling mechanism by which PPARγ SUMOylation is regulated. In agreement with these *in vitro* results, there was an increase in PPARγ SUMOylation and corresponding decrease in PPARγ target gene expression in WAT from *Fgf21*$^{-/-}$ mice, measured during the fed state when PPARγ is expected to be most

active (Figure 3.5D,E). Taken together, the *in vitro* and *in vivo* data suggest that FGF21 increases PPARγ transcriptional activity by decreasing its SUMOylation, in a feed forward autocrine loop.

PPARγ2 can be SUMOylated at Lys107 or Lys395 with different transcriptional outcomes. To determine at which position PPARγ2 is SUMOylated in *Fgf21*$^{-/-}$ adipocytes, the SUMOylation sites were mutated, either singly or together in the context of a tagged PPARγ2. Mutating Lys107 (Lys107Arg) but not Lys395 (Lys395Arg) blocked PPARγ2 SUMOylation in differentiated *Fgf21*$^{-/-}$ adipocytes (Fig. 3.5F). As discussed in Chapter 1, SUMOylation at Lys107 is associated with impaired PPARγ transcriptional activity (Yamashita et al., 2004); an FGF21-dependent decrease of SUMOylation at this site would be permissive for full PPARγ activation. These data suggest that in the absence of FGF21, PPARγ2 transcriptional activity is impaired by SUMOylation at Lys107 *in vitro* and *in vivo*.

We investigated whether introduction of the wild-type or mutant PPARγ2 would reverse the impaired differentiation of the *Fgf21*$^{-/-}$ preadipocytes. Preadipocytes derived from wild-type and *Fgf21*$^{-/-}$ mice were infected with lentivirus expressing wild-type PPARγ2, PPARγ2 (Lys107Arg) or PPARγ2 (Lys395Arg) or control (GFP). Cells were differentiation for 4 days, with only 0.5μM rosiglitazone in the media for the final 24 hours. Shortening the incubation time from 8 to 4 days was necessary since overexpression of PPARγ stimulated rapid lipid accumulation and led to cells bursting when differentiation was extended beyond 6 days. As expected,

adipocytes from *Fgf21*$^{-/-}$ mice infected with GFP-lentivirus showed decreased expression of *Slc25a1, Acly, Me1, Acaca, Fasn, Dgat2* and *Pepck* at the end of the differentiation period compared to adipocytes from wild-type mice (Figure 3.5G). Introduction of the Lys107Arg mutant increased expression of these genes in wild-type and *Fgf21*$^{-/-}$ adipocytes to similar levels (Figure 3.5G). Overexpression of wild-type PPARγ also increased adipogenic gene expression, although to a lesser extent than the Lys107Arg mutant (Figure 3.5G). In contrast, the K395R mutant generally had a similar effect as PPARγ on their expression in *Fgf21*$^{-/-}$ adipocytes (Figure 3.5G). These data suggest that increased SUMOylation of PPARγ in *Fgf21*$^{-/-}$ adipocytes is a major contributor to their impaired differentiation.

3.5 FGF21 is Required for the Anti-Diabetic Actions of Rosiglitazone.

To determine if FGF21 contributes to full PPARγ activity and the anti-diabetic effects of rosiglitazone, wild-type and FGF21$^{-/-}$ mice were given a high fat diet for 10 weeks to elicit insulin resistance and diet-induced obesity, and treated daily with rosiglitazone or vehicle (1% methylcellulose) for the final 2 weeks. As expected, rosiglitazone induced FGF21 mRNA and protein concentration in the WAT (Figure 3.6.A-B). Unexpectedly, rosiglitazone decreased FGF21 mRNA in the liver (Figure 3.6C) and circulating levels of FGF21 protein (Figure 3.6D). These data are consistent with the effects of rosiglitazone in lean mice (Figure 3.1A-D) and suggest

that circulating levels of FGF21 protein are derived from a hepatic origin, whereas FGF21 produced in the adipose tissue can function in an autocrine manner.

As expected, rosiglitazone treatment significantly reduced serum insulin and glucose concentrations in DIO wild-type mice (3.6E-F). While plasma insulin levels trended lower in the FGF21$^{-/-}$ mice this difference was not statistically significant. Glucose levels were lower in rosiglitazone treated FGF$^{-/-}$, but were not repressed to the extent of wild-type. Importantly, rosiglitazone treatment enhanced glucose disposal in a glucose tolerance test in wild-type mice, but had no effect in *Fgf21*$^{-/-}$ mice (Figure 3.6G). Additionally, insulin tolerance tests showed rosiglitazone enhanced insulin sensitivity in the wild-type mice, but were ineffective in the *Fgf21*$^{-/-}$ mice. Although serum and hepatic triglyceride concentrations and serum non-esterfied fatty acids were elevated in the DIO *Fgf21*$^{-/-}$ mice, they decreased in response to rosiglitazone (Table 3.1). These data suggest that carbohydrate metabolism is more sensitive to the absence of FGF21 that lipid metabolism.

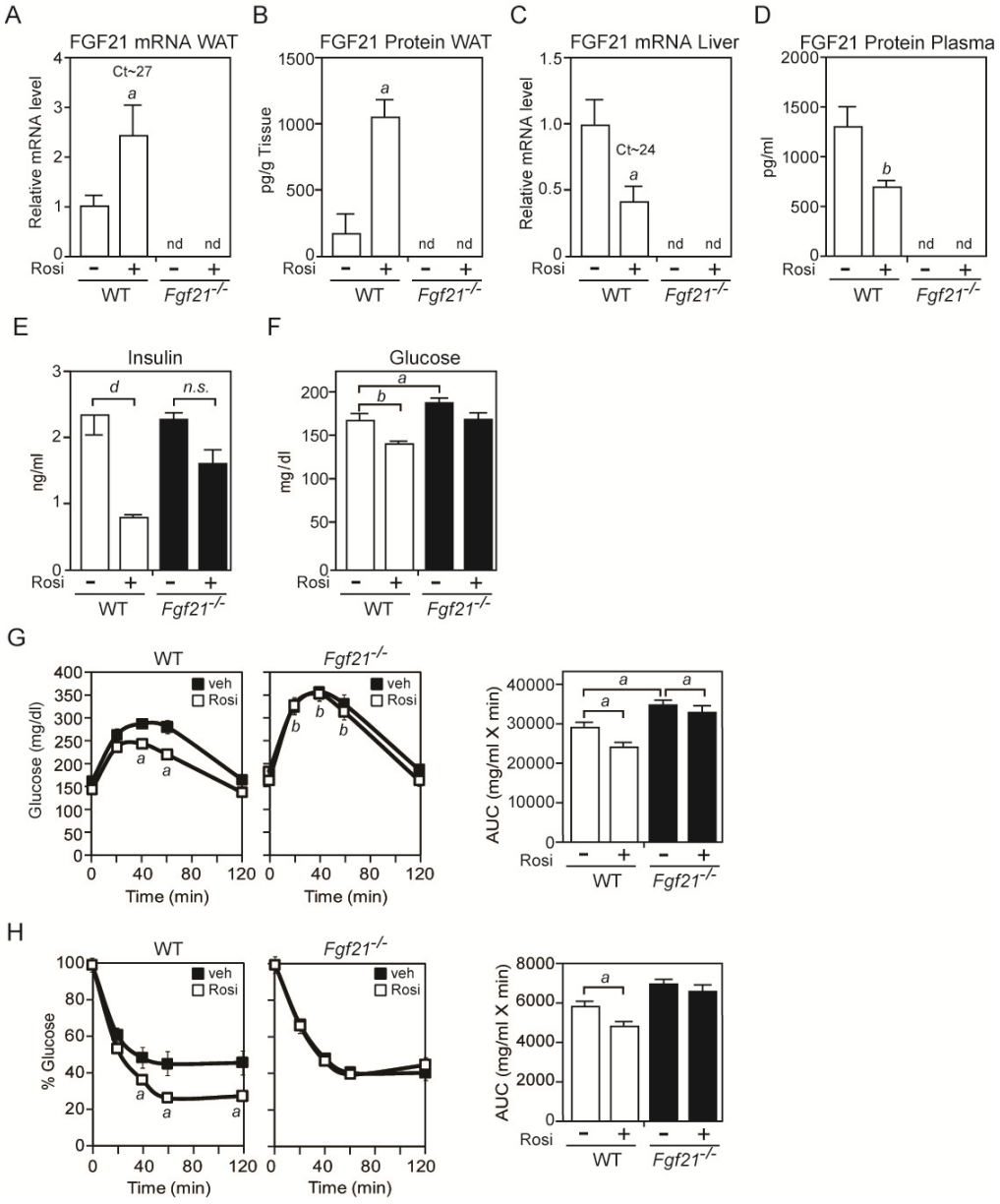

Figure 3.6 FGF21 is Required for the Insulin-Sensitizing Effects of TZDs.

Wild-type and *Fgf21*$^{-/-}$ mice were given a high fat diet for 10 weeks and treated with rosiglitazone (10mg/kg) or vehicle (1%methylcellulose) for the final 14 days. (A) WAT and (C) liver FGF21 mRNA expression was measured by RT-qPCR. (B) WAT FGF21, (D) plasma FGF21, and (E) plasma insulin concentrations were determined by ELISA. (F) Mice were fasted for 8 hours and subjected to a glucose tolerance test (2 g/kg D-glucose) or (G) fasted for 4 hours and subjected to an insulin tolerance test (0.75 U/kg). (n=13-16 per group) *a* $p<0.05$; *b* $p<0.01$ versus WT control.

3.6 FGF21 Is Required for PPARγ Target Gene Expression in WAT.

Morphometric analysis showed that DIO *Fgf21*$^{-/-}$ mice had larger eWAT adipocytes than DIO wild-type mice (Figure 3.7A). Rosiglitazone treatment caused a significant decrease in adipocyte size in both wild-type and *Fgf21*$^{-/-}$ mice. However, eWAT adipocytes remained larger in *Fgf21*$^{-/-}$ mice (Figure 3.7A), suggesting that their function is altered. As was observed in chow fed mice, SUMOylated PPARγ levels in WAT were markedly increased in DIO *Fgf21*$^{-/-}$ mice compared to DIO wild-type mice (Figure 3.6B). Consistent with these findings, rosiglitazone-mediated induction of PPARγ target genes was impaired in *Fgf21*$^{-/-}$ mice (Figure 3.6C). However, we note that basal expression of *Slc25a1* and *Fasn* was elevated in WAT of DIO *Fgf21*$^{-/-}$ mice (Figure 3.6C). Possible explanations for these findings are that the absence of FGF21 interferes with the ability of unliganded PPARγ to suppress basal expression of these genes, or there is compensation by other transcriptional regulators. *Pck1* expression was significantly reduced in *Fgf21*$^{-/-}$ WAT and unresponsive to rosiglitazone treatment (Figure 3.7C). Analysis of adipokines revealed the expected decrease in *Tnfa* expression in WAT of DIO wild-type mice treated with rosiglitazone (Figure 3.7D). This response was absent in *Fgf21*$^{-/-}$ mice (Figure 3.7D). Plasma adiponectin levels increased in response to rosiglitazone administration in both wild-type and *Fgf21*$^{-/-}$ mice, but the induction was significantly attenuated in *Fgf21*$^{-/-}$ mice (Figure 3.7E). Taken together, these data show that the actions of rosiglitazone are blunted in *Fgf21*$^{-/-}$ mice.

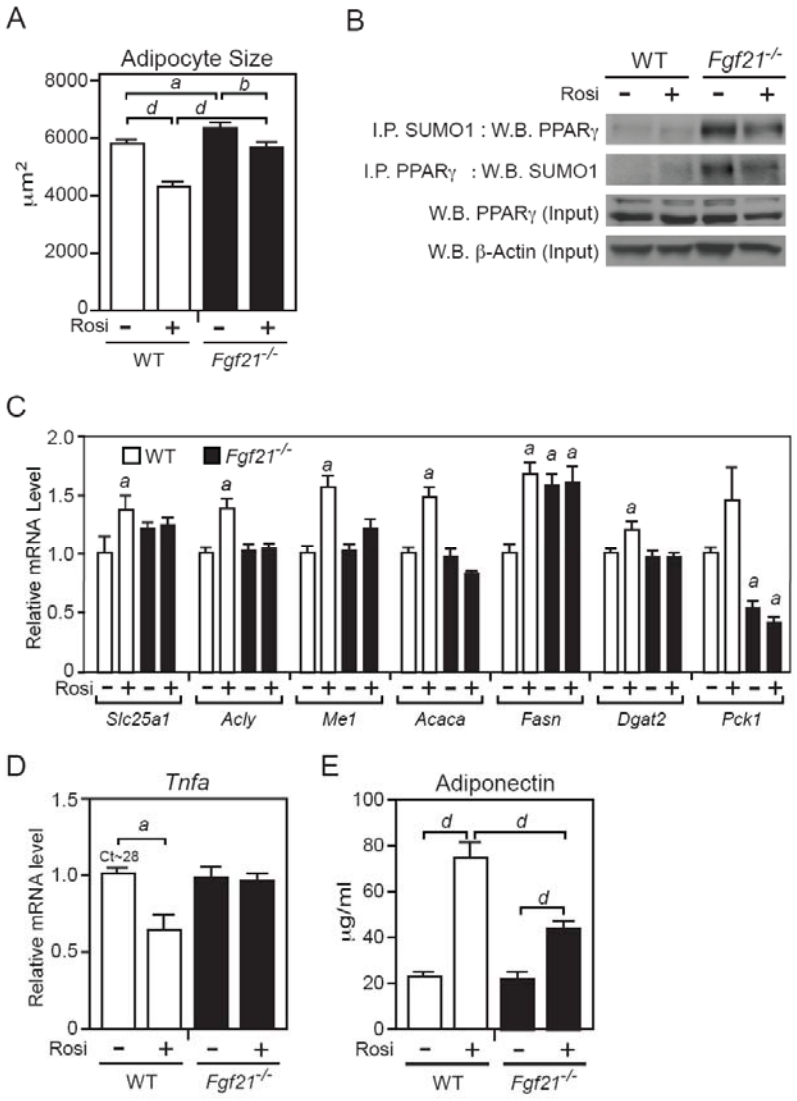

Figure 3.7 TZD Regulation of Adipose in DIO WT and *Fgf21*$^{-/-}$ mice.

Wild-type and *Fgf21*$^{-/-}$ mice were given a high fat diet for 10 weeks and treated with rosiglitazone (10mg/kg) or vehicle (1%methylcellulose) for the final 14 days. (A) eWAT was sectioned, stained with hematoxylin and eosin and a series of images were analyzed (n>250 cells per group; *a* $p<1x10^{-8}$, *b* $p<0.05$ versus WT control; *c* $p<0.01$ versus *Fgf21*$^{-/-}$ control; *d* $p<1x10^{-7}$ versus WT treated with rosiglitazone). (B) PPARγ SUMOylation was assessed in WAT by immunoprecipitation and western blotting and (C) Lipogenic gene expression and (D) TNF-α mRNA was measured in the WAT by RT-qPCR (C-D: *a* $p<0.05$ versus WT control). (E) Plasma adiponectin protein concentration was measured by ELISA. *d* $p<0.01$

To further characterize the role of FGF21 in mediating the actions of rosiglitazone in WAT, microarray analysis was performed (Ruth Yu, Salk Institute) on RNA isolated from DIO wild-type and *Fgf21*$^{-/-}$ mice that were treated with rosiglitazone, or vehicle, for 2 weeks. Microarray analysis showed over 300 gene targets that were uniquely induced by rosiglitazone in the wild-type mice but not in the *Fgf21*$^{-/-}$ mice (Figure 3.8). As expected, many genes involved in lipogenesis and fatty acid trafficking are induced by rosiglitazone treatment in eWAT of wild-type mice, but not in the *Fgf21*$^{-/-}$, as determined by DAVID v6.7 data analysis software (Dennis et al., 2003; Huang da et al., 2009). These data demonstrate that FGF21 plays an essential role in PPARγ-mediated induction of genes involved in lipogenesis and fatty acid metabolism. Collectively, these data suggest a broad role for FGF21 in regulating carbohydrate and lipid homeostasis in WAT in the fed state through a PPARγ dependent manner.

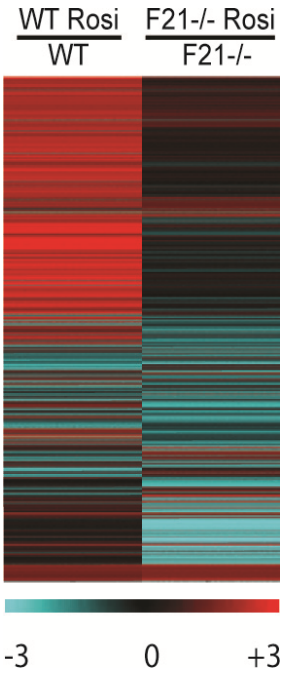

Figure 3.9 Microarray Heat Map of TZD Treated DIO WT and *Fgf21*$^{-/-}$ Adipose

Wild-type and FGF21$^{-/-}$ mice were given a high fat diet for 10 weeks and treated with rosiglitazone (10mg/kg) or vehicle (1%methylcellulose) for the final 14 days. RNA was isolated and used to probe the MouseRef-8 v2.0 expression array (Illumina, Inc.). Values indicate fold-change of samples treated with rosiglitazone versus control. (n=2 pools/2mice)

3.7 Side-Effects of Rosiglitazone in the *FGF21*$^{-/-}$ Mouse

Since beneficial effects of PPARγ ligand therapy were lost in the absence of FGF21, I sought to investigate the known side effects of rosiglitazone in the DIO mice. To investigate the detrimental changes in body mass composition elicited by rosiglitazone treatment wild-type and *Fgf21*$^{-/-}$ DIO mice were monitored after a 2 week rosiglitazone treatment using the Bruker Minispec mq10. While there was a trend toward increased body mass in DIO wild-type mice treated with rosiglitazone, there was no significant difference in body mass between wild-type and *Fgf21*$^{-/-}$ mice in response to either the high fat diet or rosiglitazone (Figure 3.9A). Although the fat mass trended lower and lean mass trended higher in DIO *Fgf21*$^{-/-}$ mice compared to wild-type mice, these changes were not statistically significant (Figure 3.9B, C). As expected, rosiglitazone treatment did increase fat and fluid mass and decrease lean mass in DIO wild-type mice (Figure 3.7B-D). Notably, these effects were absent in FGF21-KO mice (Fig. 7B-D). In a collaborative effort with Yihong Wan's lab at the University of Texas Southwestern Medical Center, the ability of thiazolidinediones to decrease bone density was also determined in the *Fgf21*$^{-/-}$ mice (Figure 3.7E). We found that rosiglitazone caused bone loss in an FGF21 dependent manner, such that *Fgf21*$^{-/-}$ had higher bone density than wild-type mice and rosiglitazone did not stimulate bone loss. These data indicated that FGF21 may have functions in tissues beyond the adipose pads, and may impact adipogenesis within the bone marrow to compromise the density of the bone itself. As such, FGF21 is a significant and novel regulator of the bone-loss associated with thiazolidinediones. The ability of rosiglitazone to increase in the heart to body mass was conserved in both wild-type and *Fgf21*$^{-/-}$ mice (Figure 3.7F). The heart remains a unique a target of rosiglitazone function in the *Fgf21*$^{-/-}$ *mice* since it expresses PPARγ, but does not express the FGF21 co-receptor βklotho**.** Thus, FGF21 is required for many clinically relevant side effects of rosiglitazone.

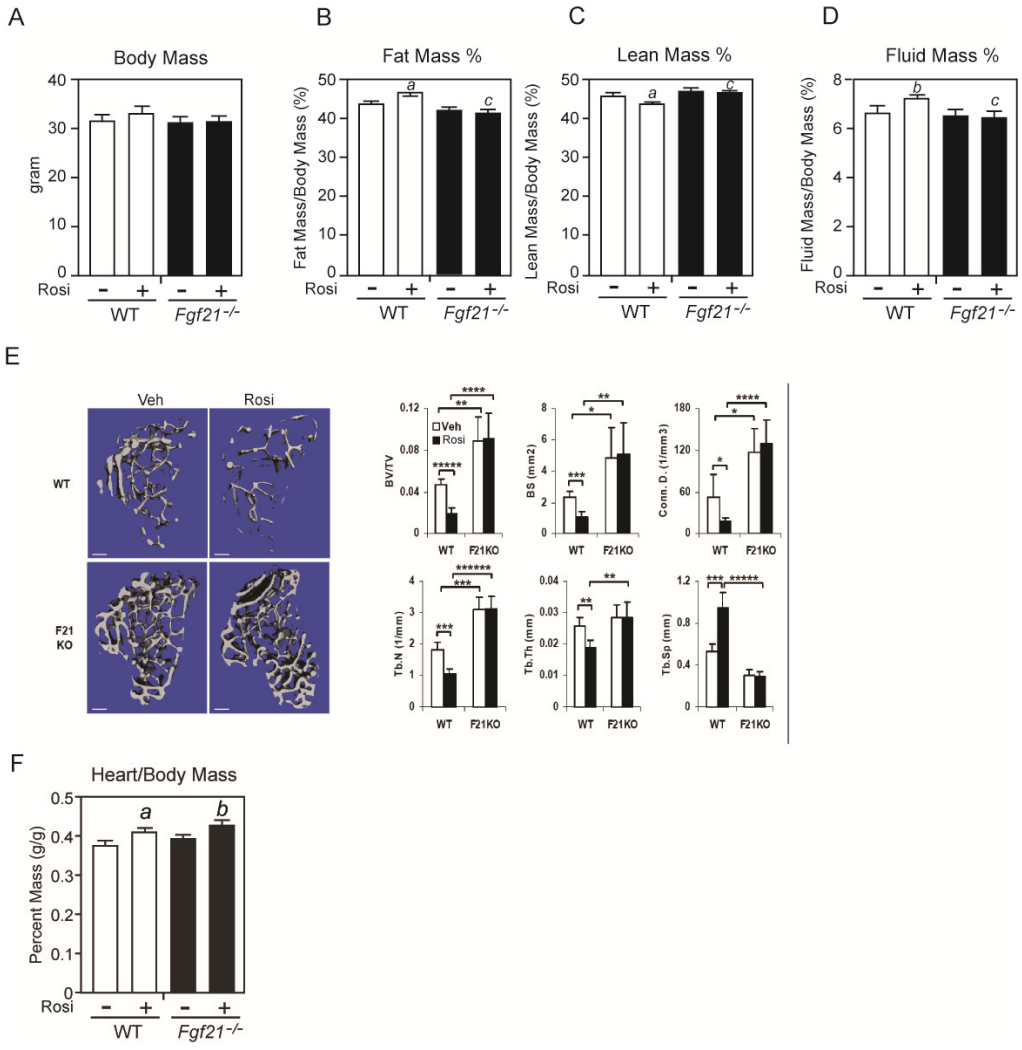

Figure 3.10 FGF21-Dependent Side Effects of TZDs.

Wild-type and *Fgf21*$^{-/-}$ mice were given a high fat diet for 10 weeks and treated with rosiglitazone (10mg/kg) or vehicle (1%methylcellulose) for the final 14 days. A-D) Body mass, fluid, fat and lean composition of 2-month WT and *Fgf21*$^{-/-}$ mice was measured using the Bruker Minispec mq10 NMR *a* $p \leq 0.05$, *b* $p < 0.01$ versus WT control; *c* $p < 0.01$ versus WT treated with rosiglitazone. E) Tibea from WT and *Fgf21*$^{-/-}$ mice were analyzed by a Scanco μCT instrument. Representative images of the entire proximal tibia (bottom, scale bar 1mm); quantification of trabecular bone volume and architecture (n=4). BV/TV, bone volume/tissue volume ratio; BS, bone surface; Conn. D., connectivity density; Tb.N, trabecular number; Tb.Th, trabecular thickness; Tb.Sp, trabecular separation. *, $p < 0.05$;**, $p < 0.01$;***, $p < 0.005$; ****, $p < 0.001$; *****, $p < 0.0005$; ******, $p < 0.0001$. F) The heart was removed and weighted to determine the heart to body mass ratio. *a* $p \leq 0.05$ versus WT control, *b* $p < 0.01$ versus *Fgf21*$^{-/-}$ control. (Bone Measurements performed in collaboration with Dr. Yihong Wan lab)

CHAPTER 4

MATERIALS AND METHODS

4.1 Animal Experiments

All experiments were performed using male mice. *Pparα*$^{-/-}$ mice on a pure 129S4/Sv background were purchased from the Jackson Laboratory; C57/Blk6 mice used in ligand screens were purchased from Jackson Laboratory; *Fgf21* transgenic and *Fgf21*$^{-/-}$ mice were generated in lab. To generate *Fgf21* transgenic mice, cDNA containing the mouse *Fgf21* coding region was inserted into the MluI and XhoI sites of pLiv7 (Miyake et al., 2001; Simonet et al., 1993). The 6.7kb SalI-SpeI fragment of pLiv7-FGF21 was injected into fertilized eggs as previously described (Shimano et al., 1996). Transgenic mice were generated and maintained on a C57BL/6J background. Two independent *Fgf21* transgenic mouse lines were established that had expressed hepatic *Fgf21* mRNA at ~50-fold and ~150-fold greater levels than fasted wild-type mice. The two lines were found to have similar fasting serum β-hydroxybutryate, triglycerides, total cholesterol, glucose and insulin; line 1 was used for all additional experiments. *Fgf21*$^{-/-}$ mice were created in our lab through targeting exons 1-3 with two *loxP* sites and breeding to the Meox-cre. Removal of the Meox-cre allele and deletion of the *Fgf21* gene were confirmed by PCR genotyping. Heterozygote breeding was performed and maintained by homozygous breeding. All

animal experiments were approved by the Institutional Animal Care and Use Committee of the University of Texas Southwestern Medical Center at Dallas.

All mice were maintained on standard chow (Harlan Teklad Global Diet #2916; 4% fat) ad libitum unless otherwise indicated. High fat diet D12492 (Research Diets Inc.) containing 60% kcal from fat was used to generate DIO mice. During high fat feeding, mice were individually caged; weight and food intake were measured weekly and insulin levels were monitored every second week from tail blood collected after a 4 hour fast. After 8 weeks on the high fat diet, mice were gavaged daily with 10mg/kg rosiglitazone (Cayman Chemical) or vehicle (1% methylcellulose; Sigma), as described in the figures legends.

Body temperature and locomotor activity measurements were made using the TAF2 telemetric temperature transmitters (Data Sciences International). The devices were implanted in the peritoneal cavity under general anesthesia (Avertin, Sigma). Mice were allowed to recover over 7 days before all experiments were performed. Mice were individually housed at 22˚C and data were collected using ART2.1 software (Data Sciences International). For recombinant leptin replacement studies, Alzet®osmotic pumps (Model# 1007D) were implanted to deliver a flow of 0.5 μL per hour of either saline (control) or recombinant leptin at 1μg/μL (National Hormone and Peptide Program, USA). Mice were allowed to recover for 3 days before 24 hr fasting experiments were performed.

One day PPAR ligand treatments were performed in lean C57Bl/6 mice. Mice were gavaged at 5PM and 8AM the next day with 10mg/kg of either GW7647 (GlaxoWellcome), rosiglitazone (Cayman Chemical) or vehicle (1% methylcellulose, Sigma). Tissues were harvested at 10AM, snap frozen in liquid nitrogen and stored at -80˚C until processed.

Circadian experiments were performed by reversing the 12-hour light-dark cycles and allowing the mice one week to acclimate before the start of the food entrainment. Mice were given chow for a 4 hour period beginning 4 hours after the onset of the dark cycle and were maintained on this feeding regime for two weeks before tissues were collected every 4 hours for 24 hours. All tissues were snap frozen in liquid nitrogen and stored at -80˚C until being processed.

4.2 FGF21, Insulin, Leptin and Adiponectin Elisa

FGF21 (Biovendor Cat# RD291108200R), insulin (Crystal Chem Inc.Cat#90080), leptin (Millipore Cat# EZML-82K) and adiponectin (Millipore Cat#EZMADP-60K) concentrations were measured as described in the kits manufacture using plasma collected in EDTA tubes. For ELISA measurements of FGF21 in white adipose tissue, fresh-frozen tissues were homogenized in buffer containing 150 mM NaCl, 10 mM HEPES (pH 7.4), and 0.5% Triton X-100 with anti-protease cocktail (Roche). Homogenates were snap frozen, thawed on ice and pre-cleared twice by centrifugation at 4ºC to remove lipid. The resulting protein

extract was analyzed with the FGF21 ELISA at a 1:2 dilution with the diluent buffer supplied by in the kit.

4.3 Metabolite Measurements

Plasma triglycerides, cholesterol and free fatty acids were measured from plasma using the L-type TG H Triglyceride kit, plasma Cholesterol E kit and NEFA C kit, respectively (Wako Chemicals Inc.). For liver measures, total lipids were extracted from ~50mg liver as previously described (Folch et al., 1957) and triglyceride and cholesterol content were measured as described above.

4.4 Body Composition Analysis

Body composition was determined using the Bruker Minispec mq10 NMR. Body fat mass, lean mass, and fluid mass were measured between 2PM and 3PM in live conscious mice with *ad libitum* access to food and water.

4.5 Morphometric Analysis of Adipose Tissue

Epididymal white adipose tissue was fixed in Bouin's fixative for 2 days and transferred to 70% ethanol. Sections were stained with hematoxylin and eosin and images were acquired using Nikon ACT-1 (Version 2.63) software on an Nikon

Eclipse TS100 microscope. Cell area was determined using ImageJ software package (Version 1.44p) with at least 150 adipocytes per group.

4.6 Perfused Liver Experiments

Livers from fed *Fgf21* transgenic mice or wild-type littermates were isolated and perfused for 60 min in a nonrecirculating fashion at 8 ml/min with a Krebs-Henseleit-based perfusion medium containing 1.5 mM lactate, 0.15 mM pyruvate, 0.25 mM glycerol, and 0.4 mM free fatty acid (algal mix bound to 3% albumin) as described (Burgess et al., 2004). Ketone production was determined by standard biochemical assays of the effluent perfusate.

4.7 Glucose Tolerance and Insulin Tolerance Tests

Oral glucose tolerance tests were performed on mice that were fasted for eight hours, beginning at 6AM, and given an oral glucose load of 2 mg/g body weight. Blood was collected by tail knick at the indicated time points and analyzed using the Autokit Glucose kit (Wako Chemicals Inc.). Insulin tolerance was performed in mice that were fasted for four hours, beginning at 10AM, and given an I.P. injection of 0.75U/kg insulin (Sigma). Tail blood was collected and assayed as described.

4.8 Human Hepatocytes

Human primary hepatocytes were obtained from the Liver Tissue Procurement and Distribution System as attached cells in six-well plates in human hepatocyte maintenance media containing 100 nM dexamethasone, 100 nM insulin, 100 U/ml penicillin G, and 100 mg/ml streptomycin medium (Cambrex Bio Science Walkersville Inc.). Media was changed to serum-free Williams' E medium and cells were treated with 1μM GW7647 or vehicle (0.1% DMSO) for twelve hours.

4.9 Chromatin Immunoprecipitation

Frozen adult mouse liver was crushed and DNA-protein crosslinking was performed with 1% formaldehyde in PBS containing 1 mM DTT and 1 mM PMSF for 10-15 minutes at room temperature. Crosslinking reactions were stopped by the addition of 0.125 M glycine. Liver nuclei were isolated with a Dounce homogenizer in hypotonic solution followed by centrifugation at 4000g for 1 minute. ChIP assays were performed with liver nuclei using the ChIP assy kit (Upstate Biotechnology) and anti-PPARα antibody (5μg, Affinity BioReagents) or control rabbit IgG (SantaCruz Biotechnology). The precipitated DNA was purified by spin column (QIAGEN) and eluted in 100μl water. DNA (1.25μL) was subjected to RT-qPCR analysis as described (Bookout and Mangelsdorf, 2003) using the following oligonucleotides:

Fgf21 -6533/-6470 forward, 50-TCAGCATGCCTCCAAAGC-30 , reverse, 5'-TCAGCCTTG AGGAAGAGTAGACA-3'; *Fgf21*-1119/-1044 forward, 5'-AGGGCCCGAATGCTAAGC-3' ; reverse, 5'-AGCCAAGCAGGTGGAAGTCT-3'.

4.10 Recombinant FGF21 Production

Recombinant mouse FGF21 comprising amino acids 33-209 was produced in *E.coli*, refolded in vitro, and purified to homogeneity by sequential affinity, ion exchange, and size exclusion chromatography as previously described (Plotnikov et al., 2000).

4.11 Adenovirus Infections of Mice

The *Fgf21* coding region was cloned into the pACCMVpLpA(-)loxP vector at BamHI and HindIII sites. Virus was generated as previously (Gerard and Meidell, 1995). Mice were infected with adenovirus by jugular vein injection using a 3/10cc syringe (Becton, Dickinson and Company). Each mouse received 7.5 X 10^9 particles/g body weight in 0.1 ml of saline. Four days after injection, mice were fed or fasted for 24 hours.

4.12 RT-qPCR Analysis

Primers were designed with Primer Express software (Applied Biosystems) based on GeneBank sequence data. Primers were selected to span exon junctions were possible. All tissue and cell culture RNA extraction protocols were performed with RNA Stat60 (Tel-Test, Inc.), except extraction from white adipose tissue where the RNeasy Lipid Tissue Mini Kit (Qiagen) was used according to manufacturer protocols. RNA extracts were subjected to DNase-treatment (Roche) and cDNA was synthesized from RNA (4µg) using the MultiScribe™ reverse transcriptase kit (Applied Biosystems). 10µL RT-qPCR reactions contained 25ng of cDNA, 50nM of each primer and 5µl of SYBR® GreenER™ (Invitrogen). All reactions were performed in triplicate on the Applied Biosystems Prism 7700HT system and relative mRNA levels were calculated by comparative threshold cycle method using U36B4 as an internal control (Bookout and Mangelsdorf, 2003).

Table 4.1 RT-qPCR Primer Sequences.

Gene Target	Orientation	Sequence
mouse *Fgf21*	forward	CCTCTAGGTTTCTTTGCCAACAG
	reverse	AAGCTGCAGGCCTCAGGAT
human *FGF21*	forward	ACCAGAGCCCCGAAAGTCT
	reverse	CTTGACTCCCAAGATTTGAATAACTC
mouse *Cpt1a*	forward	CAAAGATCAATCGGACCCTAGAC
	reverse	CGCCACTCACGATGTTCTTC

Gene Target	Orientation	Sequence
mouse *Hmgcs2*	forward	CCGTATGGGCTTCTGTTCAG
	reverse	AGCTTTGTGCGTTCCATCAG
mouse *Pnlip*	forward	ACAAACAGAAAAACCCGTATCATTAT
	reverse	TGCACATGTCAGATAGCCAGTT
mouse *Pnliprp2*	forward	CCCCTGTTCCTCCTATGAGAAG
	reverse	CCATTTTGGGACACCCTTGT
mouse *Cel*	forward	CTGGCCCAGCACAAAGC
	reverse	GGGAAAACAGGTAAGAATAGGTCTTG
mouse *Clps*	forward	ACCAACACCAACTATGGCATCT
	reverse	CCAGCTAACTGCGTGATCTCA
mouse *Hsl*	forward	GCTGGAGGAGTGTTTTTTTGC
	reverse	AGTTGAACCAAGCAGGTCACA
mouse atgl	forward	CTTGAGCAGCTAGAACAATG
	reverse	GGACACCTCAATAATGTTGGC
mouse βklotho	forward	GATGAAGAATTTCCTAAACCAGGTT
	reverse	AACCAAACACGCGGATTTC
mouse *Fgfr1-IIIc*	forward	GCCAGACAACTTGCCGTATG
	reverse	ATTTCCTTGTCGGTGGTATTAACTC
mouse *aP2*	forward	AGTGAAAACTTCGATGATTACATGAA
	reverse	GCCTGCCACTTTCCTTGTG
mouse *C/ebp*α	forward	GACATCAGCGCCTACATCGA
	reverse	TCGGCTGTGCTGGAAGAG
mouse *C*/ebpβ	forward	ATTTCTATGAGAAAAGAGGCGTATGT
	reverse	AAATGTCTTCACTTTAATGCTCGAA
mouse *C/ebpδ*	forward	TTCCAACCCCTTCCCTGAT
	reverse	CTGGAGGGTTTGTGTTTTCTGT
mouse *Ppar*γ	forward	CAAGAATACCAAAGTGCGATCAA
	reverse	GAGCTGGGTCTTTTCAGAATAATAAG
mouse *Slc25a1*	forward	GGCTGTCAGGTTGGGGATGT
	reverse	TGGGCATCCCGCATGT
mouse *Acly*	forward	GCCAGCGGGAGCACATC
	reverse	CTTTGCAGGTGCCACTTCATC
mouse *Me1*	forward	GCCGGCTCTATCCTCCTTTG
	reverse	TTTGTATGCATCTTGCACAATCTTT
mouse *Acc1*	forward	GGCAGCTCTGGAGGTGTATG
	reverse	TCCTTAAGCTGGCGGTGTT
mouse *Fas*	forward	GCTGCGGAAACTTCAGGAAAT
	reverse	AGAGACGTGTCACTCCTGGACTT

Gene Target	Orientation	Sequence
mouse *Dgat2*	forward	CCGCAAAGGCTTTGTGAAG
	reverse	GGAATAAGTGGGAACCAGATCA
mouse *Pepck*	forward	CACCATCACCTCCTGGAAGA
	reverse	GGGTGCAGAATCTCGAGTTG

4.13 Immunoprecipitation and Western Blotting

Frozen liver was crushed and 100mg was homogenized in 1 ml protein lysis buffer ((10 mM Tris-HCl [pH 7.4], 5 mM EDTA, 150 mM NaCl, 30 mM sodium phosphate, 10% glycerol, 0.5% NP40 containing complete protease inhibitor cocktail [Roche Diagnostics]) using a Polytron homogenizer. Samples were centrifuged at 16,000g for 15 min at 4˚C and supernatants were collected. Epididymal WAT was homogenized in protein lysis buffer consisting of 150 mM NaCl, 50 mM NaF, 100 μM Na_3VO_4, 50 mM $Na_4P_2O_7$, 10 mM $C_3H_7Na_2O_6P$, 5 mM EDTA, 5 mM EGTA, 0.5% Triton X-100 and supplemented with complete anti-protease cocktail (Roche), centrifuged at 16,000 g for 25 min at 4˚C, and supernatants were collected. Immunoblotting was performed using antibodies described in Table 4.2. β-Actin antibody (Sigma) was used as loading control for western analysis.

Fresh frozen adipose tissues were homogenized in WAT tissue lysis buffer described above supplemented with 10 mM N-ethylmaleimide (Sigma). Lysates were cleared by centrifugation 4ºC. The SUMO1 antibody (Cell Signaling Technology) or PPARγ antibody (Cell Signaling Technology) were used at 1:100 dilution with protein lysates for overnight pulldown at 4ºC. Immunoprecipitants were washed 1X

with lysis buffer, 2X with buffer A consisting of 50mM Tris-HCl (pH 7.4), 250 mM NaCl, 0.1% Triton-X100, 10 mM LiCl, and 10mM N-ethylmaleimide and once with buffer B consisting of 20 mM HEPES (pH 7.4), 2 mM EDTA, 10 mM $MgCl_2$, 0.1% Triton X-100 and 10 mM NEM.

Table 3.2: Lists of Antibodies, Dilutions for Western Blotting and Suppliers.

Primary Antibody	Application (Dillution)	Supplier
CPT1a	W.B. (1:1000)	(ESSER ET AL., 1993)
HMGCS2	W.B. (1:1000)	SantaCruz Biotechnology
ATGL	W.B. (1:1000)	Cell Signaling Technology
FASN	W.B. (1:1000)	Santa Cruz Biotechnology
HSL (Phospho-Ser660)	W.B. (1:500)	Cell Signaling Technology
HSL (Phospho-Ser565)	W.B. (1:500)	Cell Signaling Technology
HSL (Phospho-Ser563)	W.B. (1:500)	Cell Signaling Technology
HSL (H-300)	W.B. (1:1000)	SantaCruz Biotechnology
PPARγ (C26H12)	I.P./W.B. (1:100/1:1000)	Cell Signaling Technology
PPAR (81B8)	W.B. (1:1000)	Cell Signaling Technology
PPARγ (Phospho-Ser112)	W.B. (1:500)	Chemicon International
SUMO1 (C21A7)	W.B. (1:1000)	Cell Signaling Technology
SUMO1 (D-11)	I.P. (1:100)	SantaCruz Biotechnology
Anti-Rabbit IgG HRP	W.B (1:5000)	Cell Signaling Technology
Anti-Mouse IgG HRP	W.B. (1:5000)	GE Healthcare
Anti-HA HRP	W.B. (1:2000)	Sigma-Aldrich
Anti-FLAG M2 HRP	W.B. (1:2000)	Sigma-Aldrich
β-actin	W.B. (1:2000)	Sigma-Aldrich

4.14 3T3L1 Differentiation Assay

3T3L1 cells were differentiated into adipocytes using a standard differentiation protocol (Student et al., 1980). Briefly, 3T3L1 preadipocytes were

grown to confluency and incubated for 2 days in an induction cocktail comprised of high glucose DMEM without pyruvate, 10% FBS, 10 μg/ml insulin, 0.5 mM isobutylmethyxanthine and 0.25 μM dexamethasone. Cells were maintained in differentiation media comprised of high glucose DMEM with 10% FBS and 10 μg/ml insulin for 4 days. Cells were incubated for 2 additional days in high glucose DMEM with 10% FBS alone, before treatments.

4.15 Primary Adipocyte Differentiation Assay

Primary preadipocytes were isolated from P4 to P5 wild-type and *Fgf21*$^{-/-}$ mice. Briefly, pups were anesthetized on ice, decapitated, and inguinal adipose pads were isolated. Adipose pads were incubated with shaking at 37˚C in collagenase-buffer containing 12.5 mM HEPES (pH 7.4), 120 mM NaCl, 6 mM Na_2HPO_4, 2.5 mM D-glucose, 1.2 mM $MgSO_4$, 0.4 mM NaH_2PO_4, 2% bovine serum albumin, and 0.1% type 2 collagenase. Adipocytes were separated and removed from the stromal vascular layer, which contains the preadipocyte population, by centrifugation and aspiration. Cells were washed once in MEF media, to remove residual collagenase, containing 10% heat inactivated FBS, 20 mM HEPES (pH7.3), 1X non-essential amino acids, 1X glutamax, 0.1 mM β-mercaptoethanol and high glucose DMEM before plating in MEF media. Cells were grown to confluency and, after 2 days, differentiation was induced with an inducing cocktail comprised of high glucose DMEM, with 10% FBS, 10 μg/ml insulin, 0.5 mM isobutylmethyxanthine and 0.25

μM dexamethasone. Media was replaced every second day for 6 additional days with differentiation media comprised of high glucose DMEM with 10% FBS and 10 μg/ml insulin. Cell treatments were performed as described in the figure legends.

4.16 Plasmids and Transient Transfection Assays

Fgf21 promoter constructs were generated from -1497/+5, -977/+5 and -98/+5 using PCR from 129Sv mouse genomic DNA with oligonucleotide primers: -1497 forward, 5'-GACGGCAAGCTTGGCCTGAAGCCTCACCTTGAC-30 ; -977 forward, 5'-CCCAAGC TTCCAAAGCACCTTGTAGCTTAA-30 ; -98 forward, 5'-GACGGCAAGCTTGGTTCCTGC CAAGTGTGTC-30 ; +5 reverse, 5'-GACGGCCTCGAGTGTCTGGTGAACGCAGAATA CCC-3'. The PCR fragements were cloned into a luciferase reporeter construct using HindIII and XhoI sites. To generate the -66/+5 promoter fragment the following oligonucleotides were annealed, forward, 5'-AGCTTCAGGAGTGGGGAGGGCACGTGGGCGGGCC TGTCTGG GTATAAATTCTGGGTATTTCTGCGTTCACCAGACAC-3' ; reverse, 5'-TCGAGTGTCTGGTGAACGCAGAAATACCCAGAATTTATACCCAGACAG GCCCGCCCACGTGCCCTC CCACTCCTGA-3'. The annealed oligonucleotides were cloned into a luciferase reporter using HindIII and XhoI sites.

Fgf21 promoter assays were performed using transient transfection assays in CV-1 cells. Briefly, cells were maintained in 10% FBS supplemented with L-glutamine and antibiotics. Cells were plated in 96-well plates at a density of 10,000

cells per well. After 24 hr, cells were transfected by Lipofectamine 2000 (Invitrogen). Each well was transfected with 20ng of *FGF21* reporter gene, 5 ng CMX PPARα, and 20 ng CMV-β-galactosidase. pGEM was added to bring the total DNA to 110 ng/well. After overnight incubation, cells were treated with GW7647 or vechicle (0.1% DMSO) in delipidated medium for 24 hr before luciferase assays were performed. Light units were normalized to β-galactosidase activity.

*Ppar*γ2 was cloned using cDNA from adipose of C57/Blk6. *Ppar*γ2 was cloned using primers: forward 5'-TTGCGGCCGCTGGTGAAACTCTGGGAGATTCTC-4' and reverse 5'-TATCTAGAGTAATACAAGTCCTTGTAGAT-3'. PCR products and p3XFLAG-CMV™-10 were restricted with NotI and BamHI, purified and ligated with T4-DNA ligase. Primers containing mutational sites were created with PrimerX (http://www.bioinformatics.org/primerx/) and site directed mutagenesis of 3xFLAG-PPARγ2 was performed using QuikChange® Directed-Mutagenesis kit (Stratagene). The Lys107Arg mutation of PPARγ2 at was created using (+)strand primer 5'-CCAAAGTGCGATCAGAGTAGAACCTGCATC-3' and (–)strand primer: 5'-GATGCAGGTTCTACTCTGATCGCACTTTGG-3' and the K395R mutation of PPARγ2 was created using (+)strand primer 5'-GGTGACTTTATGGAGCCTAGGTTTGAGTTTGCTGTGAAG-3'and (-)strand primer 5'-CTTCACAGCAAACTCAAACCTAGGCTCC ATAAAGTCACC-3'.

4.17 Generation of Lentivirus Vectors

Generation of lentiviral vectors were made by subcloning the 3x-FLAG-tagged PPARγ2 coding region into pLVX-IRES-ZsGreen1 (Clonetech) and transfecting HEK293 cells with pVGVS, pΔ8.9 and the PPARγ2 expression vector in a 1:1:1 ratio with FugeneHD (Roche). After 48 hours media was collected and filtered through a 0.45μM filter, snap frozen in liquid nitrogen, and stored at -80˚C before use.

4.18 Gene Transfer into Primary Adipocytes

Primary preadipocytes were isolated as described previously. For transfection experiments one day after inducing cocktail was added to the stimulate differentiation, cells were transfected with 3X-Flag-tagged PPARγ (wild-type, Lys107Arg, Lys395Arg, or Lys107/395Arg), HA-SUMO1 and pCDNA4 empty vector using FugeneHD. The next day the inducing cocktail was replaced, and 2 days later the media was changed to differentiation media comprised of high glucose DMEM with 10% FBS and 10 μg/ml insulin for an additional 2 days. For FGF21 treatment experiments, media was replaces with high glucose DMEM with 10 μg./mL insulin and treated for 4 hours. Cells were harvested and lysates were subjected to immunoprecipitation and western blot analysis. For lentiviral infection experiments, 70%-confluent preadipocytes were infected with lentivirus expressing the 3X-Flag-tagged PPARγ2 (wild-type, Lys107Arg or Lys395Arg) or empty control in media

supplemented with 10μg/ml polybrene. Two days after reaching confluence, infected preadipocyte were induced to differentiate as previously described.

4.19 In Vitro Lipolysis Assay

3T3-L1 mouse fibroblasts were differentiated into adipocytes using a standard differentiation protocol (Student et al., 1980). Cells were maintained in differentiation media consisting of DMEM with 10% FBS and10 mg/ml insulin for 4 days, followed by a 2 day incubation in DMEM with 10% FBS alone. Glycerol release was measured using the adipolysis assay kit (Chemicon).

4.20 DNA Extraction from Adipose Tissue

Epididymal adipose pad was extracted from 2 month old mice. Briefly, DNA was extracted by mincing the tissue 5 mL of SNET buffer consisting of 10 mM Tris HCl (pH 8.0), 0.1 M EDTA, 0.5% SDS, 0.1 mg/mL Proteinase K, and 25 μg RNase. Tissues were incubated overnight at 55˚C with shaking and extracted with phenol-choloroform. DNA was precipitated with twice the volume of 95% ethanol and resuspended in water. UV absorption at 260 nm was used to determine DNA concentration.

4.21 Oil Red-O Staining

Staining of neutral lipid accumulation was performed as described in (Ramirez-Zacarias et al., 1992). Briefly, cells were washed with PBS, fixed for 15 min in 10% formalin (Sigma) and washed again with PBS. Oil Red-O stain was prepared by adding 0.5% (w/v) oil red-o in isopropanol to H_2O in a 3:2 ratio followed by filtration. Oil Red-O stain was added to cells and incubated for 1 hour. The stain was removed and cells were washed with PBS 3 times to remove residual stain and images were taken. Quantitation of lipid staining was performed by adding 100% isopropanol to the stained cells, and absorbance measurements were taken using the Molecular Devices SpectraMax 384 plate reader at 510 nm.

Chapter 5

Discussion

Over the past 20 years, it has become well established that PPARs are important regulators of metabolic homeostasis. The activation of PPARα in the liver during the starvation response is necessary for stimulating the transcription of genes involved in fatty acid oxidation and ketone body production (Kersten et al., 1999), whereas the activation of PPARγ is necessary and sufficient to stimulate adipocyte differentiation and lipid storage (Rosen et al., 1999; Tontonoz et al., 1994b). The work presented in this thesis expands our understanding of how PPARα and PPARγ regulate the expression of a common target gene, FGF21. As a consequence of this dual regulation, FGF21 has developed a unique ability to function as a metabolic regulator in both the fed and fasted state.

5.1 FGF21 and Ketogenesis.

During periods of extended energy deprivation, the activation of hepatic PPARα stimulates the production of FGF21 to stimulate ketone body production. Ketone body production is regulated by PPARα, which induces *HMGCS2, CPT1a,* and numerous other genes required for fatty acid oxidation and metabolism (Hashimoto et al., 2000; Kersten et al., 1999; Leone et al., 1999). However, FGF21 is not sufficient to induce ketone body production by increasing the mRNA expression

the genes involved in fatty acid oxidation, suggesting that FGF21 functions through a distinct mechanism from PPARα dependent effects on gene regulation. Notably, protein levels of HMGCS2 and CPT1a are significantly increased in the livers of *Fgf21* transgenic mice, suggesting a molecular basis for part of the effects of FGF21 on ketone body production. Recently, it was shown that FGF21 was not required for ketogenesis and triglyceride clearance in the liver (Hotta et al., 2009). In these experiments, Hotta *et al*., show that fasted $Fgf21^{-/-}$ mice produce more ketone bodies than wild-type. The reason of this discrepancy is not clear but may result from alternative fuel sources being used for the ketogenesis in the *Fgf21* transgenic or $Fgf21^{-/-}$ mice.

5.2 FGF21 and Lipolysis

Several lines of evidence indicated that FGF21 could increase ketogenesis by stimulating lipolysis in the adipose tissue to increase the supply of free fatty acids to the liver. First, *Fgf21* transgenic mice displayed smaller white adipocytes than their wild-type counterparts, indicating that the adipocytes were depleted of lipid. Secondly, both *Fgf21* transgenic mice and wild-type mice that were administered recombinant FGF21 had significantly increased serum free fatty acids, a major substrate for ketogenesis in the liver. Finally, FGF21 enhanced glycerol release in cultured 3T3-L1 adipocytes, suggesting that FGF21 acts directly on WAT to stimulate lipolysis. A potential mechanism to explain how FGF21 stimulates

lipolysis is the phosphorylation and activation of HSL, which was observed in cultured 3T3L1 adipocytes. Alternative physiological regulators of lipolysis were also examined in the *Fgf21* transgenic mice. Adrenaline and noradrenaline concentrations were reduced in the urine of transgenic mice, indicating that FGF21 does not stimulate catecholamine production to regulate lipolysis. In addition, the increase in HSL phosphorylation at Ser563 by FGF21 treatment in 3T3L1 adipocytes supports a role the activation of lipolysis. Phosphorylation at this residue is regulated by the cAMP-dependent protein kinase. Given the important role of cAMP in the differentiation process of adipocytes, the slight increase in the phosphorylation may be due to a subsequent increase in cellular cAMP levels as a result of enhanced differentiation (Madsen et al., 2008; Petersen et al., 2008). These data are in agreement with activation of lipolysis by FGF21 in the adipose tissue.

In contrast to these observations, the first described biological function of FGF21 was its ability to stimulate glucose uptake in the 3T3-L1 adipocytes (Kharitonenkov et al., 2005). Later publications demonstrated that FGF21 could enhance lipid deposition in cultured human adipocytes (Arner et al., 2008) and synergize with PPARγ to enhance the expression of GLUT1 and glucose uptake into the cell (Moyers et al., 2007). These data suggested an alternative model for the function of FGF21 in adipose tissue. As triglycerides are produced in the maturing adipocyte, glycerol must be available as a substrate for this reaction. Since FGF21 treatment stimulated only a very low level of glycerol release, it is possible that its source may have been leakage from the cell during glyceroneogenesis during the

formation of triglycerides. Moreover, the expression of the two key enzymes involved in glyceroneogenesis are induced in the adipose tissue in an FGF21 dependent manner, namely *Pck1* and pyruvate carboxylase (*PC*). Importantly, PPARγ is necessary for glyceroneogenesis in the adipose tissue, where knocking out the PPRE in the *Pck1* promoter abolished *Pck1* gene expression and prevents glyceroneogenesis, resulting in a lipodystrophic phenotype (Olswang et al., 2002). Therefore, the induction of *Pck1* by FGF21 in the adipose tissue could be explained by the requirement for glycerol-3-phosphate production for triglyceride biosynthesis in the fed-state, as well as enhanced glycerol mobilization during the fasted state.

The regulation of hepatic lipid metabolism by FGF21 is supported by our observations that *Fgf21* transgenic mice express elevated levels of mRNAs encoding the pancreatic lipases *Pnlip*, *Pnliprp2* and *Cel*. During fasting conditions, a substantial fraction of free fatty acids are taken up by the liver and re-esterfied to triglyceride (Baar, 2005). Thus, the induction of these lipases may provide a mechanism for the efficient hydrolysis of hepatic triglycerides, especially during long-term nutritional deficiencies and torpor (See Section 4.3). Consistent with this hypothesis FGF21 administration causes a significant reduction in hepatic triglycerides in the liver of fasted Pparα$^{-/-}$ mice. Based on these data, we propose that PPARα directly stimulates the expression of CPT1a, HMGCS2 and other genes involved in uptake and catabolism of fatty acids in the liver. In addition, PPARα induces hepatic expression of FGF21, which could act in an autocrine/paracrine manner to increase CPT1a, HMGCS2 and pancreatic lipase expression in the liver,

and in an endocrine manner to stimulate lipolysis in the WAT. The net result is the stimulation of ketogenesis by increasing both the supply of free fatty acids to the liver and the proteins required for ketone body production.

5.3 FGF21 and Torpor

Thermogenesis is an important mechanism by which metabolic fuel can be used to generate heat at the expense of stored energy. Our finding that FGF21 induces pancreatic lipase expression in the liver was interesting in light of a recent report that *Pnliprp2* and *Clps* were induced in the mouse liver during torpor, the murine equivalent of hibernation (Zhang, 2006). These data suggested that FGF21 might regulate torpor. Indeed, *Fgf21* transgenic mice entered torpor during fasting, whereas wild-type mice did not. Infection of mice with an FGF21 expressing adenovirus also sensitized mice to fasting-induced torpor. Thus, FGF21 regulates key aspects of the global torpor response including lipase expression, ketogenesis and body temperature.

The adipokine leptin has been reported to be an important regulator of body temperature during the fasting response (Freeman et al., 2004; Gavrilova et al., 1999; Swoap et al., 2006). Although the *Fgf21* transgenic mice express low leptin levels even during the fed state, exogenous leptin replacement into the *Fgf21* transgenic mice did not prevent the drop in body temperature during a fast. Interestingly, the

fed-state body temperature of *Fgf21* transgenic mice was slightly elevated by leptin treatment, but their body temperature dropped to a greater extent than vehicle counterparts during a 24 hour fast. These data suggest that low leptin in the *Fgf21* transgenic mice is not the stimulus for fasting induced torpor. An alternative explanation for the pronounced decrease in body temperature in the *Fgf21* transgenic mice is their relatively smaller size compared to wild-type mice.

The increase of pancreatic lipases in the liver of the fasted FGF21 transgenic mice could be explained by the biochemical properties of these lipases. For example, PNLIP is 10-fold more efficient than HSL at hydrolyzing triglycerides and retains full activity at temperatures as low as 0˚C (Andrews 1998, Frederikson 1981). Moreover, the activities of PNLIP and other pancreatic lipases are unaffected by catecholamine, which are ineffective at stimulating lipolysis at low temperatures (Dark 2003, Moreau-Hamsany, 1988). Thus, the extra-pancreatic induction of these lipases may ensure the continuous delivery of free fatty acids to tissues even under adverse environmental conditions when conventional lipase pathways are compromised.

5.4 Broader Implications of the PPARα-FGF21 Pathway during Fasting.

The studies presented in Chapter 2 focused on the role of the PPARα-FGF21 pathway in regulating fatty acid metabolism, ketogenesis and torpor. Similar effects of PPARα agonists and FGF21 on these parameters, together with the finding that FGF21 partially reverses the hypoketonemia and hypertriglyceridemia in *Pparα*$^{-/-}$

mice, suggest that FGF21 contributes to the pleiotropic actions of PPARα as a mediator of the fasted response. Both PPARα ligands and FGF21 lower LDL cholesterol, raise HDL cholesterol and improve insulin sensitivity in dyslipidemic rhesus monkeys (Kharitonenkov et al., 2007; Winegar et al., 2001). Furthermore, PPARα agonists and pharmacological doses of FGF21 also prevent diet-induced obesity and enhance insulin sensitivity in rodents (Chou et al., 2002; Kharitonenkov et al., 2005; Tsuchida et al., 2005). The finding that FGF21 is induced by PPARα in both mouse and human hepatocytes suggests that FGF21 contributes to the therapeutic actions of fibrate drugs.

5.5 FGF21 as a Fed-State Adipokine.

During the course of this thesis, FGF21 was shown to be differentially regulated in the adipose tissue from the liver. FGF21 was found to be induced by PPARγ agonists in WAT and synergize with rosiglitazone to promote glucose uptake and differentiation of 3T3L1 adipocytes (Moyers et al., 2007; Muise et al., 2008). However, the physiological regulation of FGF21 expression in the adipose tissue was overlooked, with numerous publications focusing on the regulation of hepatic FGF21 and its function during the fasted state. In addition, the contributions of FGF21 to the *in vivo* actions of PPARγ agonists were not explored.

My observation that *Fgf21* mRNA expression was robustly increased in the adipose tissue after feeding suggested that FGF21 production in the adipose was

unique from the liver. These data support my initial gene expression analysis in the FGF21 transgenic adipose tissue, which showed an upregulation of several genes involved with lipid synthesis and storage. In contrast, the adipose tissue gene expression of *Fgf21*$^{-/-}$ mice showed a significant impairment in these same lipogenic genes. Regarding the smaller adipocytes in the *Fgf21* transgenic mice, one explanation is that PPARγ inhibition by SUMOylation cannot occur due to the continual abundance of FGF21. This could elicit a similar phenotype as treatment with PPARγ ligands, which causes smaller more insulin-sensitive adipocytes (Okuno et al., 1998). In this regard, the data are consistent with our report that young FGF21 transgenic mice have a higher body fat content compared to wild-type mice (Inagaki et al., 2008). Collectively, these data suggest that FGF21 is a fed state autocrine/paracrine factor in the adipose tissue that regulates lipid biosynthesis. Therefore, FGF21 represents a unique metabolic regulator that is expressed in distinct tissue types by either fed or fasted conditions, contributing to different biological effects in these settings.

My *in vitro* adipocyte differentiation studies demonstrated that *Fgf21* and *Klb* gene expression are clearly induced 4 days after the initiation of differentiation, when lipid production and storage begin. Intriguingly, the expression of FGF21 was observed to be slightly elevated in the preadipocyte stage suggesting that paracrine signaling between the preadipocyte and maturing adipocyte populations may stimulate the mature adipocyte in the context of the whole tissue. These data suggest a role in late phase of adipocyte maturation and are consistent with the temporal and

quantitative impairment of lipogenic gene expression in the *Fgf21*$^{-/-}$ cells, but not the early phase differentiation markers. The inability of rosiglitazone to fully activate the expression of these genes in the *Fgf21*$^{-/-}$ cells supported the previous models that FGF21 acts synergistically with TZD (Moyers et al., 2007).

5.6 FGF21 Regulates PPARγ SUMOylation

Several lines of evidence indicate that the transcriptional activity of PPARγ is compromised in the *Fgf21*$^{-/-}$ WAT. We have shown the absence of FGF21 increases PPARγ SUMOylation, a post-translational modification that inhibits PPARγ transcriptional activation (Floyd and Stephens, 2004; Ohshima et al., 2004; Yamashita et al., 2004). Therefore, the actions of FGF21 and PPARγ in the adipose tissue are fundamentally intertwined through an autocrine-loop that regulates PPARγ post-translational modifications.

Although previous studies have shown that SUMOylation of PPARγ at Lys107 represses its transcriptional activity *in vitro*, the *in vivo* relevance of PPARγ SUMOylation at this site remained unclear. The increase in SUMOylated PPARγ corresponds to a decrease in PPARγ target genes. My *in vitro* studies with *Fgf21*$^{-/-}$ adipocytes show that PPARγ SUMOylation occurs at Lys-107 and that the effect of FGF21 deficiency on adipocyte differentiation can be overcome by expressing a PPARγ Lys107Arg mutant. These data strongly suggest that increased PPARγ SUMOylation contributes to the *Fgf21*$^{-/-}$ phenotype. Precisely how SUMOylation

blocks the transcriptional activity of PPARγ remains unclear, although in vitro studies suggest that it may involve the recruitment of corepressor proteins (Yamashita et al., 2004). Notably, SUMOylation of PPARγ has been shown to be reduced by mutating the adjacent phosphorylation site at Ser-112 (Yamashita et al., 2004), which also increases PPARγ transcriptional activity (Adams et al., 1997; Hu et al., 1996). However, we did not see changes in PPARγ phosphorylation in *Fgf21*$^{-/-}$ WAT, suggesting that that phosphorylation and SUMOylation are not coupled in this context. It may be possible that when PPARγ is SUMOylated at Lys107, the phosphorylation is also present at Ser112, but due to steric hinderance at the site, the monoclonal antibody to phospho-Ser112 is not able to detect in the higher molecular weight PPARγ protein band. The requirement of full PPARγ activation by TZD and FGF21 suggests a positive feedback look whereby two mechanisms regulate the activation capacity of a transcription factor, through ligand stimulation and post translational modification.

5.7 FGF21 Mediates the Insulin-Sensitizing Effect of TZDs

Proper expression of FGF21 is necessary for the insulin sensitizing effects of TZDs. Treatment of DIO *Fgf21*$^{-/-}$ mice with rosiglitazone over two weeks does not enhance glucose clearance, as determined by glucose tolerance tests, or insulin sensitivity, as determined by insulin tolerance tests. This effect is somewhat predictable as the adipose is a major tissue for the anti-diabetic effects of TZDs (Chao

et al., 2000). Therefore FGF21 must act within the adipose tissue to prevent the SUMOylation of PPARγ, permitting its full activation by TZD treatment. These data suggests that the insulin sensitizing effects of FGF21 primarily occur at the level of the adipose tissue.

5.8 Broader Implications of the PPARγ-FGF21 Pathway during Feeding.

The studies presented in Chapter 3, demonstrate the novel discovery that FGF21 is expressed in the adipose as part of the feeding response. The importance of FGF21 in feeding is justified by my observation that the adipose tissue of *Fgf21*$^{-/-}$ mice has reduced expression of lipogenic enzymes and mild lipodystrophy. In this respect, the phenotype of the *Fgf21*$^{-/-}$ mice is similar to several PPARγ mutant mice (Gray et al., 2005), suggesting that FGF21 functions as an autocrine/paracrine regulator of PPARγ activity. As triglycerides are continually being broken down and re-esterfied in the adipose tissue through the "triglyceride/fatty acid cycle", a process that is regulated by PPARγ (Guan et al., 2002), FGF21 could function to enhance the conversion of free fatty acids into triglycerides during the fed state.

CHAPTER 6

Perspectives and Future Directions

The work presented in this thesis shows the tissue dependent regulation and function of the metabolic regulator FGF21 in the fed and fasted state. Unfortunately, the complex nature of FGF21 regulation does not allow it to be studied using simple *in vivo* approaches, but will require the application of pharmacology, advanced molecular biology and the creation of new mouse models to fully illuminate its biological role. The results presented in this work highlight the importance of pursuing FGF21 regulated processes as therapeutic targets for metabolic disease.

Our understanding that FGF21 signal transduction requires the expression of βklotho and FGFR can be used to our advantage. By selectively knocking out the expression of βklotho or the FGF receptors from various tissues, including the brain, white adipose tissue, and brown adipose tissue, we will be able to determine the tissue specific contributions of FGF21 to the regulation of metabolism. One caveat to my studies is the use of whole-body FGF21 knockout mice. It is therefore possible that some of the *in vivo* effects FGF21 may occur outside of the adipose tissue, which was the focus of my studies. Particularly, recently published data suggest a role of FGF21 in the brain, where it can increase energy expenditure and increase insulin sensitivity in obese rats (Sarruf et al., 2010). This finding is intriguing, given the fact the FGF21 has been shown to be able to cross the brain-blood barrier (Hsuchou et al., 2007).

Therefore, specific deletions of the FGF signaling complexes will help to uncover its role in these tissues.

Using an alternative approach to dissect the effects of FGF21 function, we can specifically knock-out its expression in tissues where it is found to be expressed. This complementary approach will be useful to determine its role in physiological settings where its expression is specifically induced in one tissue over another. For instance, knocking out the expression of FGF21 in the liver will help to address its function as a fed state hepatokine, whereas knocking out its expression in the adipose tissue will address its *in vivo* role in as a fed-state adipokine. Although *in vitro* tissue culture of the *Fgf21*$^{-/-}$ adipocytes has yielded important findings, addressing these questions with an *in vivo* approach will be necessary.

The regulation of SUMOylation pathways by FGF21 will also be an important avenue for future discoveries. My data supports a role for a specific signal transduction pathway stemming from the FGFR to regulate the SUMOylation of PPARγ. Since I did not observe any specific changes in global SUMOylated proteins by FGF21 *in vitro*, the mechanism by which PPARγ is specifically regulated is important to define. Moreover, it will be necessary to examine if any additional proteins are deSUMOylated by FGF21 treatment. With advances in protein analysis methods, including mass spectrometry, discovering these targets could proceed quickly. Discovering new pathways that modulate PPARγ SUMOylation could represent an exciting new approach to sensitize the adipose tissue to lipid storage and

increase insulin-sensitization. Much work remains to characterize how SUMOylation is regulated at a cellular level. The discovery that FGF21 can influence the SUMOylation pathway has provided a new tool for future studies.

The role of PPARγ in adipose biology has clearly been established to be of importance. The creation of knock in mice has already been successful to show the importance of phosphorylation as a regulator of PPARγ function *in vivo* (Hu et al., 1996). Therefore, it would be useful to generate a specific knock-in at both SUMOylation sites in PPARγ to study their effects. Presumably, mutation at the C-terminal SUMO site (Ser 395 of PPARγ2) would impact macrophage function, whereas mutation at the N-terminal SUMO site would stimulate adipocyte differentiation and lipid storage. To this effect, using PPARγ knock-in mutant mice or using overexpression systems, progress can be made to characterize the mechanism of how SUMOylation effects PPARγ dependent gene transcription.

Finally, my discovery that rosiglitazone increases the heart to body mass ratio in an FGF21 independent manner indicates that PPARγ in the heart is an important consideration for future investigation. Recently, the therapeutic advantages to rosiglitazone treatment of type 2 diabetes have been overshadowed by the discovery that rosiglitazone can enhance the risk of death from heart disease. This raises the question as to what PPARγ is doing in the tissues of the heart. Is PPARγ differentially regulated in the heart than other tissues that express it? Future studies to address the

role of PPARγ in cardiac function would seem necessary if PPARγ is to remain a viable option as a treatment for disease.

The work presented in this thesis highlights my work over the last 5 years and describes FGF21 as an important metabolic regulator. It is my hope that metabolic research will remain on the forefront of biomedical science as metabolic diseases continue to affect the human population in a dreadful way. I look forward to the day when science will win this battle.

REFERENCES

Adams, A.C., Astapova, I., Fisher, F.M., Badman, M.K., Kurgansky, K.E., Flier, J.S., Hollenberg, A.N., and Maratos-Flier, E. (2010). Thyroid hormone regulates hepatic expression of fibroblast growth factor 21 in a PPARalpha-dependent manner. The Journal of biological chemistry *285*, 14078-14082.

Adams, M., Reginato, M.J., Shao, D., Lazar, M.A., and Chatterjee, V.K. (1997). Transcriptional activation by peroxisome proliferator-activated receptor gamma is inhibited by phosphorylation at a consensus mitogen-activated protein kinase site. The Journal of biological chemistry *272*, 5128-5132.

Andrews, M.T., Squire, T.L., Bowen, C.M., and Rollins, M.B. (1998). Low-temperature carbon utilization is regulated by novel gene activity in the heart of a hibernating mammal. Proceedings of the National Academy of Sciences of the United States of America *95*, 8392-8397.

Anghel, S.I., and Wahli, W. (2007). Fat poetry: a kingdom for PPAR gamma. Cell research *17*, 486-511.

Arner, P., Pettersson, A., Mitchell, P.J., Dunbar, J.D., Kharitonenkov, A., and Ryden, M. (2008). FGF21 attenuates lipolysis in human adipocytes - a possible link to improved insulin sensitivity. FEBS letters *582*, 1725-1730.

Badman, M.K., Pissios, P., Kennedy, A.R., Koukos, G., Flier, J.S., and Maratos-Flier, E. (2007). Hepatic fibroblast growth factor 21 is regulated by PPARalpha and is a key mediator of hepatic lipid metabolism in ketotic states. Cell metabolism *5*, 426-437.

Barger, P.M., Browning, A.C., Garner, A.N., and Kelly, D.P. (2001). p38 mitogen-activated protein kinase activates peroxisome proliferator-activated receptor alpha: a potential role in the cardiac metabolic stress response. The Journal of biological chemistry *276*, 44495-44501.

Beamer, B.A., Negri, C., Yen, C.J., Gavrilova, O., Rumberger, J.M., Durcan, M.J., Yarnall, D.P., Hawkins, A.L., Griffin, C.A., Burns, D.K*., et al.* (1997). Chromosomal localization and partial genomic structure of the human peroxisome proliferator activated receptor-gamma (hPPAR gamma) gene. Biochemical and biophysical research communications *233*, 756-759.

Beenken, A., and Mohammadi, M. (2009). The FGF family: biology, pathophysiology and therapy. Nat Rev Drug Discov *8*, 235-253.

Berg, A.H., Combs, T.P., Du, X., Brownlee, M., and Scherer, P.E. (2001). The adipocyte-secreted protein Acrp30 enhances hepatic insulin action. Nature medicine *7*, 947-953.

Blanquart, C., Mansouri, R., Paumelle, R., Fruchart, J.C., Staels, B., and Glineur, C. (2004). The protein kinase C signaling pathway regulates a molecular switch between transactivation and transrepression activity of the peroxisome proliferator-activated receptor alpha. Molecular endocrinology (Baltimore, Md *18*, 1906-1918.

Bookout, A.L., Jeong, Y., Downes, M., Yu, R.T., Evans, R.M., and Mangelsdorf, D.J. (2006). Anatomical profiling of nuclear receptor expression reveals a hierarchical transcriptional network. Cell *126*, 789-799.

Bookout, A.L., and Mangelsdorf, D.J. (2003). Quantitative real-time PCR protocol for analysis of nuclear receptor signaling pathways. Nuclear receptor signaling *1*, e012.

Brown, P.J., Stuart, L.W., Hurley, K.P., Lewis, M.C., Winegar, D.A., Wilson, J.G., Wilkison, W.O., Ittoop, O.R., and Willson, T.M. (2001). Identification of a subtype selective human PPARalpha agonist through parallel-array synthesis. Bioorganic & medicinal chemistry letters *11*, 1225-1227.

Burgess, S.C., Hausler, N., Merritt, M., Jeffrey, F.M., Storey, C., Milde, A., Koshy, S., Lindner, J., Magnuson, M.A., Malloy, C.R.*, et al.* (2004). Impaired tricarboxylic acid cycle activity in mouse livers lacking cytosolic phosphoenolpyruvate carboxykinase. The Journal of biological chemistry *279*, 48941-48949.

Cahill, G.F., Jr. (2006). Fuel metabolism in starvation. Annual review of nutrition *26*, 1-22.

Camp, H.S., Tafuri, S.R., and Leff, T. (1999). c-Jun N-terminal kinase phosphorylates peroxisome proliferator-activated receptor-gamma1 and negatively regulates its transcriptional activity. Endocrinology *140*, 392-397.

Catalioto, R.M., Gaillard, D., Maclouf, J., Ailhaud, G., and Negrel, R. (1991). Autocrine control of adipose cell differentiation by prostacyclin and PGF2 alpha. Biochimica et biophysica acta *1091*, 364-369.

Chao, L., Marcus-Samuels, B., Mason, M.M., Moitra, J., Vinson, C., Arioglu, E., Gavrilova, O., and Reitman, M.L. (2000). Adipose tissue is required for the antidiabetic, but not for the hypolipidemic, effect of thiazolidinediones. The Journal of clinical investigation *106*, 1221-1228.

Chawla, A., Repa, J.J., Evans, R.M., and Mangelsdorf, D.J. (2001). Nuclear receptors and lipid physiology: opening the X-files. Science (New York, NY *294*, 1866-1870.

Chehab, F.F. (2008). Obesity and lipodystrophy--where do the circles intersect? Endocrinology *149*, 925-934.

Chen, W.W., Li, L., Yang, G.Y., Li, K., Qi, X.Y., Zhu, W., Tang, Y., Liu, H., and Boden, G. (2008). Circulating FGF-21 levels in normal subjects and in newly diagnose patients with Type 2 diabetes mellitus. Exp Clin Endocrinol Diabetes *116*, 65-68.

Chou, C.J., Haluzik, M., Gregory, C., Dietz, K.R., Vinson, C., Gavrilova, O., and Reitman, M.L. (2002). WY14,643, a peroxisome proliferator-activated receptor alpha (PPARalpha) agonist, improves hepatic and muscle steatosis and reverses insulin resistance in lipoatrophic A-ZIP/F-1 mice. The Journal of biological chemistry *277*, 24484-24489.

Cornelius, P., MacDougald, O.A., and Lane, M.D. (1994). Regulation of adipocyte development. Annual review of nutrition *14*, 99-129.

Coskun, T., Bina, H.A., Schneider, M.A., Dunbar, J.D., Hu, C.C., Chen, Y., Moller, D.E., and Kharitonenkov, A. (2008). Fibroblast growth factor 21 corrects obesity in mice. Endocrinology *149*, 6018-6027.

Crockett, E.T., Spielman, W., Dowlatshahi, S., and He, J. (2006). Sex differences in inflammatory cytokine production in hepatic ischemia-reperfusion. Journal of inflammation (London, England) *3*, 16.

Deng, Y., and Scherer, P.E. (2010). Adipokines as novel biomarkers and regulators of the metabolic syndrome. Annals of the New York Academy of Sciences *1212*, E1-E19.

Dennis, G., Jr., Sherman, B.T., Hosack, D.A., Yang, J., Gao, W., Lane, H.C., and Lempicki, R.A. (2003). DAVID: Database for Annotation, Visualization, and Integrated Discovery. Genome biology *4*, P3.

Desvergne, B. (2007). PPARs special issue: anchoring the present to explore the future. Biochimica et biophysica acta *1771*, 913-914.

Desvergne, B., Michalik, L., and Wahli, W. (2006). Transcriptional regulation of metabolism. Physiological reviews *86*, 465-514.

Desvergne, B., and Wahli, W. (1999). Peroxisome proliferator-activated receptors: nuclear control of metabolism. Endocrine reviews *20*, 649-688.

Donnelly, K.L., Smith, C.I., Schwarzenberg, S.J., Jessurun, J., Boldt, M.D., and Parks, E.J. (2005). Sources of fatty acids stored in liver and secreted via lipoproteins in patients with nonalcoholic fatty liver disease. The Journal of clinical investigation *115*, 1343-1351.

Dostalova, I., Kavalkova, P., Haluzikova, D., Lacinova, Z., Mraz, M., Papezova, H., and Haluzik, M. (2008). Plasma concentrations of fibroblast growth factors 19 and 21 in patients with anorexia nervosa. The Journal of clinical endocrinology and metabolism *93*, 3627-3632.

Dreyer, C., Krey, G., Keller, H., Givel, F., Helftenbein, G., and Wahli, W. (1992). Control of the peroxisomal beta-oxidation pathway by a novel family of nuclear hormone receptors. Cell *68*, 879-887.

Elmquist, J.K., Ahima, R.S., Maratos-Flier, E., Flier, J.S., and Saper, C.B. (1997). Leptin activates neurons in ventrobasal hypothalamus and brainstem. Endocrinology *138*, 839-842.

Esser, V., Kuwajima, M., Britton, C.H., Krishnan, K., Foster, D.W., and McGarry, J.D. (1993). Inhibitors of mitochondrial carnitine palmitoyltransferase I limit the action of proteases on the enzyme. Isolation and partial amino acid analysis of a truncated form of the rat liver isozyme. The Journal of biological chemistry *268*, 5810-5816.

Eswarakumar, V.P., Lax, I., and Schlessinger, J. (2005). Cellular signaling by fibroblast growth factor receptors. Cytokine & growth factor reviews *16*, 139-149.

Evans, R.M., Barish, G.D., and Wang, Y.X. (2004). PPARs and the complex journey to obesity. Nature medicine *10*, 355-361.

Ferdinandusse, S., Denis, S., Dacremont, G., and Wanders, R.J. (2009). Toxicity of peroxisomal C27-bile acid intermediates. Molecular genetics and metabolism *96*, 121-128.

Floyd, Z.E., and Stephens, J.M. (2002). Interferon-gamma-mediated activation and ubiquitin-proteasome-dependent degradation of PPARgamma in adipocytes. The Journal of biological chemistry *277*, 4062-4068.

Floyd, Z.E., and Stephens, J.M. (2004). Control of peroxisome proliferator-activated receptor gamma2 stability and activity by SUMOylation. Obesity research *12*, 921-928.

Folch, J., Lees, M., and Sloane Stanley, G.H. (1957). A simple method for the isolation and purification of total lipides from animal tissues. The Journal of biological chemistry *226*, 497-509.

Fon Tacer, K., Bookout, A.L., Ding, X., Kurosu, H., John, G.B., Wang, L., Goetz, R., Mohammadi, M., Kuro-o, M., Mangelsdorf, D.J*., et al.* (2010). Research resource: Comprehensive expression atlas of the fibroblast growth factor system in adult mouse. Molecular endocrinology (Baltimore, Md *24*, 2050-2064.

Frederich, R.C., Lollmann, B., Hamann, A., Napolitano-Rosen, A., Kahn, B.B., Lowell, B.B., and Flier, J.S. (1995). Expression of ob mRNA and its encoded protein in rodents. Impact of nutrition and obesity. J Clin Invest *96*, 1658-1663.

Freeman, D.A., Lewis, D.A., Kauffman, A.S., Blum, R.M., and Dark, J. (2004). Reduced leptin concentrations are permissive for display of torpor in Siberian hamsters. Am J Physiol Regul Integr Comp Physiol *287*, R97-R103.

Gaillard, D., Negrel, R., Lagarde, M., and Ailhaud, G. (1989). Requirement and role of arachidonic acid in the differentiation of pre-adipose cells. The Biochemical journal *257*, 389-397.

Gaillard, D., Wabitsch, M., Pipy, B., and Negrel, R. (1991). Control of terminal differentiation of adipose precursor cells by glucocorticoids. Journal of lipid research *32*, 569-579.

Galman, C., Lundasen, T., Kharitonenkov, A., Bina, H.A., Eriksson, M., Hafstrom, I., Dahlin, M., Amark, P., Angelin, B., and Rudling, M. (2008). The circulating metabolic regulator FGF21 is induced by prolonged fasting and PPARalpha activation in man. Cell metabolism *8*, 169-174.

Gavrilova, O., Leon, L.R., Marcus-Samuels, B., Mason, M.M., Castle, A.L., Refetoff, S., Vinson, C., and Reitman, M.L. (1999). Torpor in mice is induced by both leptin-dependent and -independent mechanisms. Proceedings of the National Academy of Sciences of the United States of America *96*, 14623-14628.

Gerard, R.D., and Meidell, R.S. (1995). Adenovirus vectors. In DNA Cloning 4: A Practical Approach: Mammalian Systems. DM Glover and BD Hames, eds (Oxford:Oxford University Press), 285-307.

Glass, C.K., and Rosenfeld, M.G. (2000). The coregulator exchange in transcriptional functions of nuclear receptors. Genes & development *14*, 121-141.

Goetz, R., Beenken, A., Ibrahimi, O.A., Kalinina, J., Olsen, S.K., Eliseenkova, A.V., Xu, C., Neubert, T.A., Zhang, F., Linhardt, R.J*., et al.* (2007). Molecular insights into the klotho-dependent, endocrine mode of action of fibroblast growth factor 19 subfamily members. Molecular and cellular biology *27*, 3417-3428.

Goldfarb, M. (2005). Fibroblast growth factor homologous factors: evolution, structure, and function. Cytokine & growth factor reviews *16*, 215-220.

Goldfarb, M., Schoorlemmer, J., Williams, A., Diwakar, S., Wang, Q., Huang, X., Giza, J., Tchetchik, D., Kelley, K., Vega, A*., et al.* (2007). Fibroblast growth factor homologous factors control neuronal excitability through modulation of voltage-gated sodium channels. Neuron *55*, 449-463.

Gray, S.L., Dalla Nora, E., and Vidal-Puig, A.J. (2005). Mouse models of PPAR-gamma deficiency: dissecting PPAR-gamma's role in metabolic homoeostasis. Biochemical Society transactions *33*, 1053-1058.

Grohmann, M., Sabin, M., Holly, J., Shield, J., Crowne, E., and Stewart, C. (2005). Characterization of differentiated subcutaneous and visceral adipose tissue from children: the influences of TNF-alpha and IGF-I. Journal of lipid research *46*, 93-103.

Grundy, S.M. (2004). Obesity, metabolic syndrome, and cardiovascular disease. The Journal of clinical endocrinology and metabolism *89*, 2595-2600.

Guan, H.P., Ishizuka, T., Chui, P.C., Lehrke, M., and Lazar, M.A. (2005). Corepressors selectively control the transcriptional activity of PPARgamma in adipocytes. Genes & development *19*, 453-461.

Guan, H.P., Li, Y., Jensen, M.V., Newgard, C.B., Steppan, C.M., and Lazar, M.A. (2002). A futile metabolic cycle activated in adipocytes by antidiabetic agents. Nature medicine *8*, 1122-1128.

Hamm, J.K., el Jack, A.K., Pilch, P.F., and Farmer, S.R. (1999). Role of PPAR gamma in regulating adipocyte differentiation and insulin-responsive glucose uptake. Annals of the New York Academy of Sciences *892*, 134-145.

Harmer, N.J., Pellegrini, L., Chirgadze, D., Fernandez-Recio, J., and Blundell, T.L. (2004). The crystal structure of fibroblast growth factor (FGF) 19 reveals novel features of the FGF family and offers a structural basis for its unusual receptor affinity. Biochemistry *43*, 629-640.

Hart, A.W., Baeza, N., Apelqvist, A., and Edlund, H. (2000). Attenuation of FGF signalling in mouse beta-cells leads to diabetes. Nature *408*, 864-868.

Hashimoto, T., Cook, W.S., Qi, C., Yeldandi, A.V., Reddy, J.K., and Rao, M.S. (2000). Defect in peroxisome proliferator-activated receptor alpha-inducible fatty acid oxidation determines the severity of hepatic steatosis in response to fasting. The Journal of biological chemistry *275*, 28918-28928.

Hauser, S., Adelmant, G., Sarraf, P., Wright, H.M., Mueller, E., and Spiegelman, B.M. (2000). Degradation of the peroxisome proliferator-activated receptor gamma is linked to ligand-dependent activation. The Journal of biological chemistry *275*, 18527-18533.

Hays, T., Rusyn, I., Burns, A.M., Kennett, M.J., Ward, J.M., Gonzalez, F.J., and Peters, J.M. (2005). Role of peroxisome proliferator-activated receptor-alpha (PPARalpha) in bezafibrate-induced hepatocarcinogenesis and cholestasis. Carcinogenesis *26*, 219-227.

He, W., Barak, Y., Hevener, A., Olson, P., Liao, D., Le, J., Nelson, M., Ong, E., Olefsky, J.M., and Evans, R.M. (2003). Adipose-specific peroxisome proliferator-activated receptor gamma knockout causes insulin resistance in fat and liver but not in muscle. Proceedings of the National Academy of Sciences of the United States of America *100*, 15712-15717.

Heery, D.M., Kalkhoven, E., Hoare, S., and Parker, M.G. (1997). A signature motif in transcriptional co-activators mediates binding to nuclear receptors. Nature *387*, 733-736.

Heyman, R.A., Mangelsdorf, D.J., Dyck, J.A., Stein, R.B., Eichele, G., Evans, R.M., and Thaller, C. (1992). 9-cis retinoic acid is a high affinity ligand for the retinoid X receptor. Cell *68*, 397-406.

Hileman, S.M., Pierroz, D.D., Masuzaki, H., Bjorbaek, C., El-Haschimi, K., Banks, W.A., and Flier, J.S. (2002). Characterizaton of short isoforms of the leptin receptor in rat cerebral microvessels and of brain uptake of leptin in mouse models of obesity. Endocrinology *143*, 775-783.

Horton, J.D., Goldstein, J.L., and Brown, M.S. (2002). SREBPs: activators of the complete program of cholesterol and fatty acid synthesis in the liver. The Journal of clinical investigation *109*, 1125-1131.

Hosooka, T., Noguchi, T., Kotani, K., Nakamura, T., Sakaue, H., Inoue, H., Ogawa, W., Tobimatsu, K., Takazawa, K., Sakai, M.*, et al.* (2008). Dok1 mediates high-fat diet-induced adipocyte hypertrophy and obesity through modulation of PPAR-gamma phosphorylation. Nature medicine *14*, 188-193.

Hotta, Y., Nakamura, H., Konishi, M., Murata, Y., Takagi, H., Matsumura, S., Inoue, K., Fushiki, T., and Itoh, N. (2009). Fibroblast growth factor 21 regulates lipolysis in white adipose tissue but is not required for ketogenesis and triglyceride clearance in liver. Endocrinology *150*, 4625-4633.

Hsuchou, H., Pan, W., and Kastin, A.J. (2007). The fasting polypeptide FGF21 can enter brain from blood. Peptides *28*, 2382-2386.

Hu, E., Kim, J.B., Sarraf, P., and Spiegelman, B.M. (1996). Inhibition of adipogenesis through MAP kinase-mediated phosphorylation of PPARgamma. Science (New York, NY *274*, 2100-2103.

Huang da, W., Sherman, B.T., and Lempicki, R.A. (2009). Systematic and integrative analysis of large gene lists using DAVID bioinformatics resources. Nature protocols *4*, 44-57.

Hug, C., Wang, J., Ahmad, N.S., Bogan, J.S., Tsao, T.S., and Lodish, H.F. (2004). T-cadherin is a receptor for hexameric and high-molecular-weight forms of Acrp30/adiponectin. Proceedings of the National Academy of Sciences of the United States of America *101*, 10308-10313.

Hummasti, S., and Tontonoz, P. (2006). The peroxisome proliferator-activated receptor N-terminal domain controls isotype-selective gene expression and adipogenesis. Molecular endocrinology (Baltimore, Md *20*, 1261-1275.

Iizuka, K., Takeda, J., and Horikawa, Y. (2009). Glucose induces FGF21 mRNA expression through ChREBP activation in rat hepatocytes. FEBS letters *583*, 2882-2886.

Inagaki, T., Choi, M., Moschetta, A., Peng, L., Cummins, C.L., McDonald, J.G., Luo, G., Jones, S.A., Goodwin, B., Richardson, J.A*., et al.* (2005). Fibroblast growth factor 15 functions as an enterohepatic signal to regulate bile acid homeostasis. Cell metabolism *2*, 217-225.

Inagaki, T., Dutchak, P., Zhao, G., Ding, X., Gautron, L., Parameswara, V., Li, Y., Goetz, R., Mohammadi, M., Esser, V*., et al.* (2007). Endocrine regulation of the fasting response by PPARalpha-mediated induction of fibroblast growth factor 21. Cell metabolism *5*, 415-425.

Inagaki, T., Lin, V.Y., Goetz, R., Mohammadi, M., Mangelsdorf, D.J., and Kliewer, S.A. (2008). Inhibition of growth hormone signaling by the fasting-induced hormone FGF21. Cell metabolism *8*, 77-83.

Issemann, I., and Green, S. (1990). Activation of a member of the steroid hormone receptor superfamily by peroxisome proliferators. Nature *347*, 645-650.

Itoh, N. (2010). Hormone-like (endocrine) Fgfs: their evolutionary history and roles in development, metabolism, and disease. Cell and tissue research.

Itoh, N., and Ornitz, D.M. (2004). Evolution of the Fgf and Fgfr gene families. Trends Genet *20*, 563-569.

Itoh, N., and Ornitz, D.M. (2008). Functional evolutionary history of the mouse Fgf gene family. Dev Dyn *237*, 18-27.

Jia, Y., Qi, C., Zhang, Z., Hashimoto, T., Rao, M.S., Huyghe, S., Suzuki, Y., Van Veldhoven, P.P., Baes, M., and Reddy, J.K. (2003). Overexpression of peroxisome proliferator-activated receptor-alpha (PPARalpha)-regulated genes in liver in the absence of peroxisome proliferation in mice deficient in both L- and D-forms of enoyl-CoA hydratase/dehydrogenase enzymes of peroxisomal beta-oxidation system. The Journal of biological chemistry *278*, 47232-47239.

Juge-Aubry, C., Pernin, A., Favez, T., Burger, A.G., Wahli, W., Meier, C.A., and Desvergne, B. (1997). DNA binding properties of peroxisome proliferator-activated receptor subtypes on various natural peroxisome proliferator response elements. Importance of the 5'-flanking region. The Journal of biological chemistry *272*, 25252-25259.

Juge-Aubry, C.E., Hammar, E., Siegrist-Kaiser, C., Pernin, A., Takeshita, A., Chin, W.W., Burger, A.G., and Meier, C.A. (1999). Regulation of the transcriptional activity of the peroxisome proliferator-activated receptor alpha by phosphorylation of a ligand-independent trans-activating domain. The Journal of biological chemistry *274*, 10505-10510.

Kallen, C.B., and Lazar, M.A. (1996). Antidiabetic thiazolidinediones inhibit leptin (ob) gene expression in 3T3-L1 adipocytes. Proceedings of the National Academy of Sciences of the United States of America *93*, 5793-5796.

Kershaw, E.E., Schupp, M., Guan, H.P., Gardner, N.P., Lazar, M.A., and Flier, J.S. (2007). PPARgamma regulates adipose triglyceride lipase in adipocytes in vitro and in vivo. Am J Physiol Endocrinol Metab *293*, E1736-1745.

Kersten, S., Seydoux, J., Peters, J.M., Gonzalez, F.J., Desvergne, B., and Wahli, W. (1999). Peroxisome proliferator-activated receptor alpha mediates the adaptive response to fasting. The Journal of clinical investigation *103*, 1489-1498.

Kharitonenkov, A., Shiyanova, T.L., Koester, A., Ford, A.M., Micanovic, R., Galbreath, E.J., Sandusky, G.E., Hammond, L.J., Moyers, J.S., Owens, R.A*., et al.* (2005). FGF-21 as a novel metabolic regulator. The Journal of clinical investigation *115*, 1627-1635.

Kharitonenkov, A., Wroblewski, V.J., Koester, A., Chen, Y.F., Clutinger, C.K., Tigno, X.T., Hansen, B.C., Shanafelt, A.B., and Etgen, G.J. (2007). The metabolic state of diabetic monkeys is regulated by fibroblast growth factor-21. Endocrinology *148*, 774-781.

Kim, I., Moon, S., Yu, K., Kim, U., and Koh, G.Y. (2001). A novel fibroblast growth factor receptor-5 preferentially expressed in the pancreas(1). Biochimica et biophysica acta *1518*, 152-156.

Kliewer, S.A., Umesono, K., Noonan, D.J., Heyman, R.A., and Evans, R.M. (1992). Convergence of 9-cis retinoic acid and peroxisome proliferator signalling pathways through heterodimer formation of their receptors. Nature *358*, 771-774.

Kuro-o, M., Matsumura, Y., Aizawa, H., Kawaguchi, H., Suga, T., Utsugi, T., Ohyama, Y., Kurabayashi, M., Kaname, T., Kume, E*., et al.* (1997). Mutation of the mouse klotho gene leads to a syndrome resembling ageing. Nature *390*, 45-51.

Kurosu, H., Choi, M., Ogawa, Y., Dickson, A.S., Goetz, R., Eliseenkova, A.V., Mohammadi, M., Rosenblatt, K.P., Kliewer, S.A., and Kuro-o, M. (2007). Tissue-specific expression of betaKlotho and fibroblast growth factor (FGF) receptor isoforms determines metabolic activity of FGF19 and FGF21. The Journal of biological chemistry *282*, 26687-26695.

Kurosu, H., and Kuro-o, M. (2008). The Klotho gene family and the endocrine fibroblast growth factors. Current opinion in nephrology and hypertension *17*, 368-372.

Le Roith, D., Scavo, L., and Butler, A. (2001). What is the role of circulating IGF-I? Trends in endocrinology and metabolism: TEM *12*, 48-52.

Lee, S.S., Pineau, T., Drago, J., Lee, E.J., Owens, J.W., Kroetz, D.L., Fernandez-Salguero, P.M., Westphal, H., and Gonzalez, F.J. (1995). Targeted disruption of the alpha isoform of the peroxisome proliferator-activated receptor gene in mice results in abolishment of the pleiotropic effects of peroxisome proliferators. Molecular and cellular biology *15*, 3012-3022.

Lee, Y., Yu, X., Gonzales, F., Mangelsdorf, D.J., Wang, M.Y., Richardson, C., Witters, L.A., and Unger, R.H. (2002). PPAR alpha is necessary for the lipopenic action of hyperleptinemia on white adipose and liver tissue. Proceedings of the National Academy of Sciences of the United States of America *99*, 11848-11853.

Lehmann, J.M., Moore, L.B., Smith-Oliver, T.A., Wilkison, W.O., Willson, T.M., and Kliewer, S.A. (1995). An antidiabetic thiazolidinedione is a high affinity ligand for peroxisome proliferator-activated receptor gamma (PPAR gamma). The Journal of biological chemistry *270*, 12953-12956.

Leone, T.C., Weinheimer, C.J., and Kelly, D.P. (1999). A critical role for the peroxisome proliferator-activated receptor alpha (PPARalpha) in the cellular fasting response: the

PPARalpha-null mouse as a model of fatty acid oxidation disorders. Proceedings of the National Academy of Sciences of the United States of America *96*, 7473-7478.

Leuenberger, N., Pradervand, S., and Wahli, W. (2009). Sumoylated PPARalpha mediates sex-specific gene repression and protects the liver from estrogen-induced toxicity in mice. The Journal of clinical investigation *119*, 3138-3148.

Li, H., Fang, Q., Gao, F., Fan, J., Zhou, J., Wang, X., Zhang, H., Pan, X., Bao, Y., Xiang, K.*, et al.* (2010). Fibroblast growth factor 21 levels are increased in nonalcoholic fatty liver disease patients and are correlated with hepatic triglyceride. Journal of hepatology *53*, 934-940.

Li, L., Yang, G., Ning, H., Yang, M., Liu, H., and Chen, W. (2008). Plasma FGF-21 levels in type 2 diabetic patients with ketosis. Diabetes research and clinical practice *82*, 209-213.

MacFarlane, W.M., Read, M.L., Gilligan, M., Bujalska, I., and Docherty, K. (1994). Glucose modulates the binding activity of the beta-cell transcription factor IUF1 in a phosphorylation-dependent manner. The Biochemical journal *303 (Pt 2)*, 625-631.

Madsen, L., Pedersen, L.M., Liaset, B., Ma, T., Petersen, R.K., van den Berg, S., Pan, J., Muller-Decker, K., Dulsner, E.D., Kleemann, R.*, et al.* (2008). cAMP-dependent signaling regulates the adipogenic effect of n-6 polyunsaturated fatty acids. The Journal of biological chemistry *283*, 7196-7205.

Malhi, H., and Gores, G.J. (2008). Cellular and molecular mechanisms of liver injury. Gastroenterology *134*, 1641-1654.

Mangelsdorf, D.J., and Evans, R.M. (1995). The RXR heterodimers and orphan receptors. Cell *83*, 841-850.

Mangelsdorf, D.J., Ong, E.S., Dyck, J.A., and Evans, R.M. (1990). Nuclear receptor that identifies a novel retinoic acid response pathway. Nature *345*, 224-229.

McMillan, D.C., Sattar, N., and McArdle, C.S. (2006). ABC of obesity. Obesity and cancer. BMJ (Clinical research ed *333*, 1109-1111.

Micanovic, R., Raches, D.W., Dunbar, J.D., Driver, D.A., Bina, H.A., Dickinson, C.D., and Kharitonenkov, A. (2009). Different roles of N- and C- termini in the functional activity of FGF21. Journal of cellular physiology *219*, 227-234.

Miles, P.D., Barak, Y., and Evans, R.M. (1999). Metabolic characterization of mice heterozygous for PPARg deficiency. Diabetes *48*, Supp1. A68.

Miyake, J.H., Doung, X.D., Strauss, W., Moore, G.L., Castellani, L.W., Curtiss, L.K., Taylor, J.M., and Davis, R.A. (2001). Increased production of apolipoprotein B-containing lipoproteins in the absence of hyperlipidemia in transgenic mice expressing cholesterol 7alpha-hydroxylase. The Journal of biological chemistry *276*, 23304-23311.

Moyers, J.S., Shiyanova, T.L., Mehrbod, F., Dunbar, J.D., Noblitt, T.W., Otto, K.A., Reifel-Miller, A., and Kharitonenkov, A. (2007). Molecular determinants of FGF-21 activity-synergy and cross-talk with PPARgamma signaling. Journal of cellular physiology *210*, 1-6.

Muise, E.S., Azzolina, B., Kuo, D.W., El-Sherbeini, M., Tan, Y., Yuan, X., Mu, J., Thompson, J.R., Berger, J.P., and Wong, K.K. (2008). Adipose fibroblast growth factor 21 is up-regulated by peroxisome proliferator-activated receptor gamma and altered metabolic states. Molecular pharmacology *74*, 403-412.

Naar, A.M., Lemon, B.D., and Tjian, R. (2001). Transcriptional coactivator complexes. Annual review of biochemistry *70*, 475-501.

Naugler, W.E., Sakurai, T., Kim, S., Maeda, S., Kim, K., Elsharkawy, A.M., and Karin, M. (2007). Gender disparity in liver cancer due to sex differences in MyD88-dependent IL-6 production. Science (New York, NY *317*, 121-124.

Nawrocki, A.R., Rajala, M.W., Tomas, E., Pajvani, U.B., Saha, A.K., Trumbauer, M.E., Pang, Z., Chen, A.S., Ruderman, N.B., Chen, H*., et al.* (2006). Mice lacking adiponectin show decreased hepatic insulin sensitivity and reduced responsiveness to peroxisome proliferator-activated receptor gamma agonists. The Journal of biological chemistry *281*, 2654-2660.

Negrel, R., Gaillard, D., and Ailhaud, G. (1989). Prostacyclin as a potent effector of adipose-cell differentiation. The Biochemical journal *257*, 399-405.

Nishimura, T., Nakatake, Y., Konishi, M., and Itoh, N. (2000). Identification of a novel FGF, FGF-21, preferentially expressed in the liver. Biochimica et biophysica acta *1492*, 203-206.

Nixon, B.T., and Green, H. (1984). Growth hormone promotes the differentiation of myoblasts and preadipocytes generated by azacytidine treatment of 10T1/2 cells. Proceedings of the National Academy of Sciences of the United States of America *81*, 3429-3432.

Nolte, R.T., Wisely, G.B., Westin, S., Cobb, J.E., Lambert, M.H., Kurokawa, R., Rosenfeld, M.G., Willson, T.M., Glass, C.K., and Milburn, M.V. (1998). Ligand binding and co-activator assembly of the peroxisome proliferator-activated receptor-gamma. Nature *395*, 137-143.

Ogawa, Y., Kurosu, H., Yamamoto, M., Nandi, A., Rosenblatt, K.P., Goetz, R., Eliseenkova, A.V., Mohammadi, M., and Kuro-o, M. (2007). BetaKlotho is required for metabolic activity of fibroblast growth factor 21. Proceedings of the National Academy of Sciences of the United States of America *104*, 7432-7437.

Ohshima, T., Koga, H., and Shimotohno, K. (2004). Transcriptional activity of peroxisome proliferator-activated receptor gamma is modulated by SUMO-1 modification. The Journal of biological chemistry *279*, 29551-29557.

Okuno, A., Tamemoto, H., Tobe, K., Ueki, K., Mori, Y., Iwamoto, K., Umesono, K., Akanuma, Y., Fujiwara, T., Horikoshi, H*., et al.* (1998). Troglitazone increases the number of small adipocytes without the change of white adipose tissue mass in obese Zucker rats. The Journal of clinical investigation *101*, 1354-1361.

Olswang, Y., Cohen, H., Papo, O., Cassuto, H., Croniger, C.M., Hakimi, P., Tilghman, S.M., Hanson, R.W., and Reshef, L. (2002). A mutation in the peroxisome proliferator-activated receptor gamma-binding site in the gene for the cytosolic form of phosphoenolpyruvate carboxykinase reduces adipose tissue size and fat content in mice. Proceedings of the National Academy of Sciences of the United States of America *99*, 625-630.

Pajvani, U.B., Du, X., Combs, T.P., Berg, A.H., Rajala, M.W., Schulthess, T., Engel, J., Brownlee, M., and Scherer, P.E. (2003). Structure-function studies of the adipocyte-secreted hormone Acrp30/adiponectin. Implications fpr metabolic regulation and bioactivity. The Journal of biological chemistry *278*, 9073-9085.

Pajvani, U.B., Hawkins, M., Combs, T.P., Rajala, M.W., Doebber, T., Berger, J.P., Wagner, J.A., Wu, M., Knopps, A., Xiang, A.H*., et al.* (2004). Complex distribution, not absolute amount of adiponectin, correlates with thiazolidinedione-mediated improvement in insulin sensitivity. The Journal of biological chemistry *279*, 12152-12162.

Pascual, G., Fong, A.L., Ogawa, S., Gamliel, A., Li, A.C., Perissi, V., Rose, D.W., Willson, T.M., Rosenfeld, M.G., and Glass, C.K. (2005). A SUMOylation-dependent pathway mediates transrepression of inflammatory response genes by PPAR-gamma. Nature *437*, 759-763.

Perissi, V., and Rosenfeld, M.G. (2005). Controlling nuclear receptors: the circular logic of cofactor cycles. Nature reviews *6*, 542-554.

Petersen, R.K., Madsen, L., Pedersen, L.M., Hallenborg, P., Hagland, H., Viste, K., Doskeland, S.O., and Kristiansen, K. (2008). Cyclic AMP (cAMP)-mediated stimulation of adipocyte differentiation requires the synergistic action of Epac- and cAMP-dependent protein kinase-dependent processes. Molecular and cellular biology *28*, 3804-3816.

Pineda Torra, I., Jamshidi, Y., Flavell, D.M., Fruchart, J.C., and Staels, B. (2002). Characterization of the human PPARalpha promoter: identification of a functional nuclear receptor response element. Molecular endocrinology (Baltimore, Md *16*, 1013-1028.

Pires-daSilva, A., and Sommer, R.J. (2003). The evolution of signalling pathways in animal development. Nat Rev Genet *4*, 39-49.

Plotnikov, A.N., Hubbard, S.R., Schlessinger, J., and Mohammadi, M. (2000). Crystal structures of two FGF-FGFR complexes reveal the determinants of ligand-receptor specificity. Cell *101*, 413-424.

Potthoff, M.J., Inagaki, T., Satapati, S., Ding, X., He, T., Goetz, R., Mohammadi, M., Finck, B.N., Mangelsdorf, D.J., Kliewer, S.A*., et al.* (2009). FGF21 induces PGC-1alpha and regulates carbohydrate and fatty acid metabolism during the adaptive starvation response. Proceedings of the National Academy of Sciences of the United States of America *106*, 10853-10858.

Powers, C.J., McLeskey, S.W., and Wellstein, A. (2000). Fibroblast growth factors, their receptors and signaling. Endocrine-related cancer *7*, 165-197.

Rafiq, I., Kennedy, H.J., and Rutter, G.A. (1998). Glucose-dependent translocation of insulin promoter factor-1 (IPF-1) between the nuclear periphery and the nucleoplasm of single MIN6 beta-cells. The Journal of biological chemistry *273*, 23241-23247.

Rakhshandehroo, M., Sanderson, L.M., Matilainen, M., Stienstra, R., Carlberg, C., de Groot, P.J., Muller, M., and Kersten, S. (2007). Comprehensive analysis of PPARalpha-dependent regulation of hepatic lipid metabolism by expression profiling. PPAR research *2007*, 26839.

Ramirez-Zacarias, J.L., Castro-Munozledo, F., and Kuri-Harcuch, W. (1992). Quantitation of adipose conversion and triglycerides by staining intracytoplasmic lipids with Oil red O. Histochemistry *97*, 493-497.

Razzaque, M.S., Sitara, D., Taguchi, T., St-Arnaud, R., and Lanske, B. (2006). Premature aging-like phenotype in fibroblast growth factor 23 null mice is a vitamin D-mediated process. Faseb J *20*, 720-722.

Reddy, J.K., Azarnoff, D.L., and Hignite, C.E. (1980). Hypolipidaemic hepatic peroxisome proliferators form a novel class of chemical carcinogens. Nature *283*, 397-398.

Reddy, J.K., Goel, S.K., Nemali, M.R., Carrino, J.J., Laffler, T.G., Reddy, M.K., Sperbeck, S.J., Osumi, T., Hashimoto, T., Lalwani, N.D*., et al.* (1986). Transcription regulation of peroxisomal fatty acyl-CoA oxidase and enoyl-CoA hydratase/3-hydroxyacyl-CoA dehydrogenase in rat

liver by peroxisome proliferators. Proceedings of the National Academy of Sciences of the United States of America *83*, 1747-1751.

Reddy, J.K., and Hashimoto, T. (2001). Peroxisomal beta-oxidation and peroxisome proliferator-activated receptor alpha: an adaptive metabolic system. Annual review of nutrition *21*, 193-230.

Reddy, J.K., and Rao, M.S. (2006). Lipid metabolism and liver inflammation. II. Fatty liver disease and fatty acid oxidation. Am J Physiol Gastrointest Liver Physiol *290*, G852-858.

Reddy, J.K., Rao, S., and Moody, D.E. (1976). Hepatocellular carcinomas in acatalasemic mice treated with nafenopin, a hypolipidemic peroxisome proliferator. Cancer research *36*, 1211-1217.

Rentsch, J., and Chiesi, M. (1996). Regulation of ob gene mRNA levels in cultured adipocytes. FEBS letters *379*, 55-59.

Rhee, J., Inoue, Y., Yoon, J.C., Puigserver, P., Fan, M., Gonzalez, F.J., and Spiegelman, B.M. (2003). Regulation of hepatic fasting response by PPARgamma coactivator-1alpha (PGC-1): requirement for hepatocyte nuclear factor 4alpha in gluconeogenesis. Proceedings of the National Academy of Sciences of the United States of America *100*, 4012-4017.

Ristow, M., Muller-Wieland, D., Pfeiffer, A., Krone, W., and Kahn, C.R. (1998). Obesity associated with a mutation in a genetic regulator of adipocyte differentiation. The New England journal of medicine *339*, 953-959.

Rosen, E.D., Hsu, C.H., Wang, X., Sakai, S., Freeman, M.W., Gonzalez, F.J., and Spiegelman, B.M. (2002). C/EBPalpha induces adipogenesis through PPARgamma: a unified pathway. Genes & development *16*, 22-26.

Rosen, E.D., Sarraf, P., Troy, A.E., Bradwin, G., Moore, K., Milstone, D.S., Spiegelman, B.M., and Mortensen, R.M. (1999). PPAR gamma is required for the differentiation of adipose tissue in vivo and in vitro. Molecular cell *4*, 611-617.

Sanchez, J., Palou, A., and Pico, C. (2009). Response to carbohydrate and fat refeeding in the expression of genes involved in nutrient partitioning and metabolism: striking effects on fibroblast growth factor-21 induction. Endocrinology *150*, 5341-5350.

Sarruf, D.A., Thaler, J.P., Morton, G.J., German, J., Fischer, J.D., Ogimoto, K., and Schwartz, M.W. (2010). Fibroblast growth factor 21 action in the brain increases energy expenditure and insulin sensitivity in obese rats. Diabetes *59*, 1817-1824.

Scherer, P.E., Williams, S., Fogliano, M., Baldini, G., and Lodish, H.F. (1995). A novel serum protein similar to C1q, produced exclusively in adipocytes. The Journal of biological chemistry *270*, 26746-26749.

Schmidt, D.R., Holmstrom, S.R., Fon Tacer, K., Bookout, A.L., Kliewer, S.A., and Mangelsdorf, D.J. (2010). Regulation of bile acid synthesis by fat-soluble vitamins A and D. The Journal of biological chemistry *285*, 14486-14494.

Sher, T., Yi, H.F., McBride, O.W., and Gonzalez, F.J. (1993). cDNA cloning, chromosomal mapping, and functional characterization of the human peroxisome proliferator activated receptor. Biochemistry *32*, 5598-5604.

Shimada, T., Kakitani, M., Yamazaki, Y., Hasegawa, H., Takeuchi, Y., Fujita, T., Fukumoto, S., Tomizuka, K., and Yamashita, T. (2004). Targeted ablation of Fgf23 demonstrates an essential physiological role of FGF23 in phosphate and vitamin D metabolism. The Journal of clinical investigation *113*, 561-568.

Shimano, H., Horton, J.D., Hammer, R.E., Shimomura, I., Brown, M.S., and Goldstein, J.L. (1996). Overproduction of cholesterol and fatty acids causes massive liver enlargement in transgenic mice expressing truncated SREBP-1a. The Journal of clinical investigation *98*, 1575-1584.

Shulman, A.I., Larson, C., Mangelsdorf, D.J., and Ranganathan, R. (2004). Structural determinants of allosteric ligand activation in RXR heterodimers. Cell *116*, 417-429.

Simonet, W.S., Bucay, N., Lauer, S.J., and Taylor, J.M. (1993). A far-downstream hepatocyte-specific control region directs expression of the linked human apolipoprotein E and C-I genes in transgenic mice. The Journal of biological chemistry *268*, 8221-8229.

Sleeman, M., Fraser, J., McDonald, M., Yuan, S., White, D., Grandison, P., Kumble, K., Watson, J.D., and Murison, J.G. (2001). Identification of a new fibroblast growth factor receptor, FGFR5. Gene *271*, 171-182.

Smith, P.J., Wise, L.S., Berkowitz, R., Wan, C., and Rubin, C.S. (1988). Insulin-like growth factor-I is an essential regulator of the differentiation of 3T3-L1 adipocytes. The Journal of biological chemistry *263*, 9402-9408.

Stralfors, P., and Belfrage, P. (1983). Phosphorylation of hormone-sensitive lipase by cyclic AMP-dependent protein kinase. The Journal of biological chemistry *258*, 15146-15152.

Stratikopoulos, E., Szabolcs, M., Dragatsis, I., Klinakis, A., and Efstratiadis, A. (2008). The hormonal action of IGF1 in postnatal mouse growth. Proceedings of the National Academy of Sciences of the United States of America *105*, 19378-19383.

Student, A.K., Hsu, R.Y., and Lane, M.D. (1980). Induction of fatty acid synthetase synthesis in differentiating 3T3-L1 preadipocytes. The Journal of biological chemistry *255*, 4745-4750.

Swoap, S.J., Gutilla, M.J., Liles, L.C., Smith, R.O., and Weinshenker, D. (2006). The full expression of fasting-induced torpor requires beta 3-adrenergic receptor signaling. J Neurosci *26*, 241-245.

Tartaglia, L.A., Dembski, M., Weng, X., Deng, N., Culpepper, J., Devos, R., Richards, G.J., Campfield, L.A., Clark, F.T., Deeds, J*., et al.* (1995). Identification and expression cloning of a leptin receptor, OB-R. Cell *83*, 1263-1271.

Thissen, J.P., Ketelslegers, J.M., and Underwood, L.E. (1994). Nutritional regulation of the insulin-like growth factors. Endocrine reviews *15*, 80-101.

Tontonoz, P., Hu, E., Graves, R.A., Budavari, A.I., and Spiegelman, B.M. (1994a). mPPAR gamma 2: tissue-specific regulator of an adipocyte enhancer. Genes & development *8*, 1224-1234.

Tontonoz, P., Hu, E., and Spiegelman, B.M. (1994b). Stimulation of adipogenesis in fibroblasts by PPAR gamma 2, a lipid-activated transcription factor. Cell *79*, 1147-1156.

Tran, H., Brunet, A., Griffith, E.C., and Greenberg, M.E. (2003). The many forks in FOXO's road. Sci STKE *2003*, RE5.

Tsuchida, A., Yamauchi, T., Takekawa, S., Hada, Y., Ito, Y., Maki, T., and Kadowaki, T. (2005). Peroxisome proliferator-activated receptor (PPAR)alpha activation increases adiponectin receptors and reduces obesity-related inflammation in adipose tissue: comparison of activation of PPARalpha, PPARgamma, and their combination. Diabetes *54*, 3358-3370.

Turner, N., and Grose, R. (2010). Fibroblast growth factor signalling: from development to cancer. Nat Rev Cancer *10*, 116-129.

Urakawa, I., Yamazaki, Y., Shimada, T., Iijima, K., Hasegawa, H., Okawa, K., Fujita, T., Fukumoto, S., and Yamashita, T. (2006). Klotho converts canonical FGF receptor into a specific receptor for FGF23. Nature *444*, 770-774.

Vaisse, C., Halaas, J.L., Horvath, C.M., Darnell, J.E., Jr., Stoffel, M., and Friedman, J.M. (1996). Leptin activation of Stat3 in the hypothalamus of wild-type and ob/ob mice but not db/db mice. Nature genetics *14*, 95-97.

van Beekum, O., Fleskens, V., and Kalkhoven, E. (2009). Posttranslational modifications of PPAR-gamma: fine-tuning the metabolic master regulator. Obesity (Silver Spring, Md *17*, 213-219.

Vona-Davis, L., and Rose, D.P. (2007). Adipokines as endocrine, paracrine, and autocrine factors in breast cancer risk and progression. Endocrine-related cancer *14*, 189-206.

Wallenius, V., Wallenius, K., Ahren, B., Rudling, M., Carlsten, H., Dickson, S.L., Ohlsson, C., and Jansson, J.O. (2002). Interleukin-6-deficient mice develop mature-onset obesity. Nature medicine *8*, 75-79.

Wan, Y., Chong, L.W., and Evans, R.M. (2007). PPAR-gamma regulates osteoclastogenesis in mice. Nature medicine *13*, 1496-1503.

Wang, H., Qiang, L., and Farmer, S.R. (2008). Identification of a domain within peroxisome proliferator-activated receptor gamma regulating expression of a group of genes containing fibroblast growth factor 21 that are selectively repressed by SIRT1 in adipocytes. Molecular and cellular biology *28*, 188-200.

Wang, X., Sato, R., Brown, M.S., Hua, X., and Goldstein, J.L. (1994). SREBP-1, a membrane-bound transcription factor released by sterol-regulated proteolysis. Cell *77*, 53-62.

Wang, Y., Solt, L.A., and Burris, T.P. (2010). Regulation of FGF21 expression and secretion by retinoic acid receptor-related orphan receptor alpha. The Journal of biological chemistry *285*, 15668-15673.

Wente, W., Efanov, A.M., Brenner, M., Kharitonenkov, A., Koster, A., Sandusky, G.E., Sewing, S., Treinies, I., Zitzer, H., and Gromada, J. (2006). Fibroblast growth factor-21 improves pancreatic beta-cell function and survival by activation of extracellular signal-regulated kinase 1/2 and Akt signaling pathways. Diabetes *55*, 2470-2478.

Werman, A., Hollenberg, A., Solanes, G., Bjorbaek, C., Vidal-Puig, A.J., and Flier, J.S. (1997). Ligand-independent activation domain in the N terminus of peroxisome proliferator-activated receptor gamma (PPARgamma). Differential activity of PPARgamma1 and -2 isoforms and influence of insulin. The Journal of biological chemistry *272*, 20230-20235.

Weyer, C., Funahashi, T., Tanaka, S., Hotta, K., Matsuzawa, Y., Pratley, R.E., and Tataranni, P.A. (2001). Hypoadiponectinemia in obesity and type 2 diabetes: close association with

insulin resistance and hyperinsulinemia. The Journal of clinical endocrinology and metabolism *86*, 1930-1935.

Winegar, D.A., Brown, P.J., Wilkison, W.O., Lewis, M.C., Ott, R.J., Tong, W.Q., Brown, H.R., Lehmann, J.M., Kliewer, S.A., Plunket, K.D.*, et al.* (2001). Effects of fenofibrate on lipid parameters in obese rhesus monkeys. Journal of lipid research *42*, 1543-1551.

Wu, Z., Bucher, N.L., and Farmer, S.R. (1996). Induction of peroxisome proliferator-activated receptor gamma during the conversion of 3T3 fibroblasts into adipocytes is mediated by C/EBPbeta, C/EBPdelta, and glucocorticoids. Molecular and cellular biology *16*, 4128-4136.

Wu, Z., Rosen, E.D., Brun, R., Hauser, S., Adelmant, G., Troy, A.E., McKeon, C., Darlington, G.J., and Spiegelman, B.M. (1999). Cross-regulation of C/EBP alpha and PPAR gamma controls the transcriptional pathway of adipogenesis and insulin sensitivity. Molecular cell *3*, 151-158.

Xu, H.E., Lambert, M.H., Montana, V.G., Plunket, K.D., Moore, L.B., Collins, J.L., Oplinger, J.A., Kliewer, S.A., Gampe, R.T., Jr., McKee, D.D.*, et al.* (2001). Structural determinants of ligand binding selectivity between the peroxisome proliferator-activated receptors. Proceedings of the National Academy of Sciences of the United States of America *98*, 13919-13924.

Xu, J., Lloyd, D.J., Hale, C., Stanislaus, S., Chen, M., Sivits, G., Vonderfecht, S., Hecht, R., Li, Y.S., Lindberg, R.A.*, et al.* (2009). Fibroblast growth factor 21 reverses hepatic steatosis, increases energy expenditure, and improves insulin sensitivity in diet-induced obese mice. Diabetes *58*, 250-259.

Yamashita, D., Yamaguchi, T., Shimizu, M., Nakata, N., Hirose, F., and Osumi, T. (2004). The transactivating function of peroxisome proliferator-activated receptor gamma is negatively regulated by SUMO conjugation in the amino-terminal domain. Genes Cells *9*, 1017-1029.

Yamauchi, T., Kamon, J., Minokoshi, Y., Ito, Y., Waki, H., Uchida, S., Yamashita, S., Noda, M., Kita, S., Ueki, K.*, et al.* (2002). Adiponectin stimulates glucose utilization and fatty-acid oxidation by activating AMP-activated protein kinase. Nature medicine *8*, 1288-1295.

Yang, X.J., and Gregoire, S. (2006). A recurrent phospho-sumoyl switch in transcriptional repression and beyond. Molecular cell *23*, 779-786.

Yie, J., Hecht, R., Patel, J., Stevens, J., Wang, W., Hawkins, N., Steavenson, S., Smith, S., Winters, D., Fisher, S.*, et al.* (2009). FGF21 N- and C-termini play different roles in receptor interaction and activation. FEBS letters *583*, 19-24.

Yoon, J.C., Puigserver, P., Chen, G., Donovan, J., Wu, Z., Rhee, J., Adelmant, G., Stafford, J., Kahn, C.R., Granner, D.K.*, et al.* (2001). Control of hepatic gluconeogenesis through the transcriptional coactivator PGC-1. Nature *413*, 131-138.

Yu, J.G., Javorschi, S., Hevener, A.L., Kruszynska, Y.T., Norman, R.A., Sinha, M., and Olefsky, J.M. (2002). The effect of thiazolidinediones on plasma adiponectin levels in normal, obese, and type 2 diabetic subjects. Diabetes *51*, 2968-2974.

Zezulak, K.M., and Green, H. (1986). The generation of insulin-like growth factor-1--sensitive cells by growth hormone action. Science (New York, NY *233*, 551-553.

Zhang, J., Fu, M., Cui, T., Xiong, C., Xu, K., Zhong, W., Xiao, Y., Floyd, D., Liang, J., Li, E.*, et al.* (2004). Selective disruption of PPARgamma 2 impairs the development of adipose tissue and insulin sensitivity. Proceedings of the National Academy of Sciences of the United States of America *101*, 10703-10708.

Zhang, J., Kaasik, K., Blackburn, M.R., and Lee, C.C. (2006). Constant darkness is a circadian metabolic signal in mammals. Nature *439*, 340-343.

Zhang, X., Yeung, D.C., Karpisek, M., Stejskal, D., Zhou, Z.G., Liu, F., Wong, R.L., Chow, W.S., Tso, A.W., Lam, K.S.*, et al.* (2008). Serum FGF21 levels are increased in obesity and are independently associated with the metabolic syndrome in humans. Diabetes *57*, 1246-1253.

Zhang, Y., Proenca, R., Maffei, M., Barone, M., Leopold, L., and Friedman, J.M. (1994). Positional cloning of the mouse obese gene and its human homologue. Nature *372*, 425-432.

Zhu, Y., Qi, C., Korenberg, J.R., Chen, X.N., Noya, D., Rao, M.S., and Reddy, J.K. (1995). Structural organization of mouse peroxisome proliferator-activated receptor gamma (mPPAR gamma) gene: alternative promoter use and different splicing yield two mPPAR gamma isoforms. Proceedings of the National Academy of Sciences of the United States of America *92*, 7921-7925.